Apéndice A

Parámetros de Celda de Compuestos de la Familia $\mathbf{Li_2(MM')_x(A,A'O_4)_{1-x}}$

	T (K)	a(Å)	b(Å)	c(Å)	Autor	G. E.	β	Z	año
Na_2SO_4	302	9,8211(8)	12,3076(8)	5,8623(4)	McMurdie	Fddd		8	1986
Na_2SO_4	507	9,514	5,313	7,157	Eysel	Pna		4	1985
Na_2SO_4	543	5,42	5,42	7,24	Eysel	$P6_3mc$			1973
Na_2SO_4-I	543	5,3936(13)	9,34194(22)	7,2465(22)	Rasmussen	$P6_3/mmc$			1996
Na_2SO_4-II	493	5,3099(22)	9,46928(38)	7,1436(29)	Rasmussen	Pbnm			1996
Na_2SO_4-III	463	5,6304(21)	9,04343(34)	7,0377(24)	Rasmussen	Cmcm			1996
Na_2SO_4-V	293	5,8582(6)	12,2990(13)	9,8138(11)	Rasmussen	Fddd			1996
Na_2SO_4(III)	473	5,607(1)	8,955(2)	6,967(1)	Mehrotra	Cmcm		4	1981
Na_2SO_4(I)	533	5,408	5,408	7,216	Mehrotra			2	1973
Na_2SO_4(I)	693	5,444	5,444	7,347	Naruse				1987
Na_2SO_4(I)		5,326(2)	5,326(2)	7,126(3)	Eysel	$P6_3/mmc$		2	1985
Na_2SO_4(V)	575	5,863	12,304	9,821	Amirthalingam	Fddd			1977
Na_2SO_4(III)	298	5,592	8,926	6,953	Amirthalingam	Cmcm			1977
Na_2SO_4(I)	575	5,385	5,385	7,260	Amirthalingam				1977
Na_2SO_4(III)	293	5,607	8,955(2)	6,967(1)	Mehrotra	Cmcm		4	1981
Na_2SO_4(III)	293	5,592	8,926	6,953	Wyckoff				1960
Na_2SO_4(III)	498	5,610	9,160	7,000	Mehrotra	Cmcm		4	1981
Na_2SO_4(I)	543	9,39	5,42	7,24	Eysel	$P6_3mc$			1973
Na_2SO_4(II)	498	9,51	5,33	7,16	Eysel	Pnam			1973
Na_2SO_4(III)	293	8,946	5,608	6,963	Eysel	Ccmm			1973
Na_2SO_4(V)	293	5,861	9,815	12,307	Mehrotra	Fddd			1971
α-$NaHSO_4$		7,005	7,125	6,712	Sonneveld	P-1	95,94, 87,69, 104,48	4	1979
β-$NaHSO_4$					Sonneveld		95,94, 87,69, 104,48	4	1979
$Na_3H(SO_4)_2$		8,648	9,648	9,143	Catti	$P2_1/c$	β=108,77	4	1979

	T (K)	a(Å)	b(Å)	c(Å)	Autor	G. E.	β	Z	año
$KHSO_5 \cdot H_2O$	298	18,226	7,662	7,420	Schlemper	C2/c	β=90,83	8	
K_2SO_4	893	10,25	5,92	8,13	Eysel	P63mc			1973
K_2SO_4	293	10,073	5,771	7,471	Eysel	Pcmn			1973
β-K_2SO_4	832	5,927(4)	10,318(4)	7,882(4)	Arnold	Pmcn,	γ=119,87(3)	4	1981
α-K_2SO_4	847	5,886(4)	10,209(4)	8,118(4)	Arnold	$P6_3/mmc$	γ=119,97(3)	4	1981
α-K_2SO_4	913	5,917(4)	10,204(4)	8,182(4)	Arnold	$P6_3/mmc$	γ=120,02(3)	4	1981
α-K_2SO_4	1073	5,947(2)	5,947(2)	8,375(3)	Miyake	$P6_3/mmc$	γ=120,02(3)	2	1980
K_2SO_4	293	5,776(5)	10,08(1)	7,456(6)	Robinson		γ=119,81(10)		1958
K_2CrO_4	293	7,663(3)	10,388(4)	5,922(3)	McGinnety	Pnam	γ=119,78(3)	4	1972
K_2SO_4	293	5,763(2)	10,071(4)	7,476(3)	McGinnety	Pnam	γ=119,78(3)	4	1972
β-K_2SO_4	913	5,917(4)	5,917(4)	8,182(4)	Arnold	$P6_3/mmc$			1981
β-K_2SO_4	913	5,917(4)	5,917(4)	8,182(4)	Arnold	$P6_3/mmc$			1981

	T (K)	a(Å)	b(Å)	c(Å)	Autor	G. E.	β	Z	año
$LiNa_3(SO_4)_2 \cdot 6H_2O$	298	8,437(2)	8,437(2)	30,19(1)	Calvalca	R3c		6	1952
$LiNa_3(SO_4)_2 \cdot 6H_2O$	298	8,443(1)	8,443(1)	30,249(6)	Mendes-Filho	R3c		6	1999

$LiNaSO_4$	**T (K)**	**a(Å)**	**b(Å)**	**c(Å)**	**Autor**	**G. E.**	β	**Z**	**año**
β-$LiNaSO_4$	300	7.63071(5)	7.63071(5)	9.86196(9)	Granellí	P31c		6	1992
$LiNaSO_4$	6	7.60199	7.60199	9.82832	Graneli	P31c		6	1992
$LiNaSO_4$	298	7,613(4)	7,613(4)	9,80(3)	Cavalca	P31c		6	1948
$LiNaSO_4$	298	7,6270(7)	7,6270(7)	9,8579(10)	Morosin	P31c		6	1967
$LiNaSO_4$	298	7,6355	7,6355	9,861	Nat.Bur.Std.	P3/c		6	1968
$LiNaSO_4$	793	5,705	5,705	5,705	T.Hahn,	Fm3m		2	1978
$LiNaSO_4$	793	5,7481(10)	5,7481(10)	5,7481(10)	Solans	Fm3m		2	2002
$LiNaSO_4$	793	5,7215	5,7215	5,7215	Solans	Fm3m		2	2002
$LiNaSO_4$	823	5,7563(17)	5,7563(17)	5,7563(17)	Solans	Fm3m		2	2002
$LiNaSO_4$	823	5,7346	5,7346	5,7346	Solans	Fm3m		2	2002
$LiNaSO_4$	829	5,77	5,77	5,77	Forland	Fm3m		2	1958
$LiNaSO_4$	873	5,7508	5,7508	5,7508	Solans	Fm3m		2	2002
	T (K)	**a(Å)**	**b(Å)**	**c(Å)**	**Autor**	**G. E.**	β	**Z**	**año**
$LiNaSO_4$	298,15	7,631(0)/7,637(1)	7,631(0)/7,637(1)	9,860(0)/9,864(2)	Freiheit	P31c		6	1998
$LiNaSO_4$	328,15	7,634(1)	7,634(1)	9,864(2)	Freiheit	P31c		6	1998
$LiNaSO_4$	331,15	7,650(1)/7,647(1)	7,650(1)/7,647(1)	9,881(2)/9,876(2)	Freiheit	P31c		6	1998
$LiNaSO_4$	373,15	7,659(1)/7,657(1)	7,659(1)/7,657(1)	9,889(2)/9,885(2)	Freiheit	P31c		6	1998
$LiNaSO_4$	423,15	7,677(1)/7,674(1)	7,677(1)/7,674(1)	9,906(2)/9,901(2)	Freiheit	P31c		6	1998
$LiNaSO_4$	473,15	7,684(0)/7,687(1)	7,684(0)/7,687(1)	9,907(2)/9,912(2)	Freiheit	P31c		6	1998
$LiNaSO_4$	523,15	7,705(1)/7,703(1)	7,705(1)/7,703(1)	9,915(2)/9,915(2)	Freiheit	P31c		6	1998
$LiNaSO_4$	573,15	7,726(1)/7,729(1)	7,726(1)/7,729(1)	9,918(2)/9,925(2)	Freiheit	P31c		6	1998
$LiNaSO_4$	623,15	7,753(1)/7,755(2)	7,753(1)/7,755(2)	9,922(2)/9,927(3)	Freiheit	P31c		6	1998
$LiNaSO_4$	723,15	7,776(1)/7,785(1)	7,776(1)/7,785(1)	9,922(2)/9,931(2)	Freiheit	P31c		6	1998
$LiNaSO_4$	753,15	7,815(1)/7,808(1)	7,815(1)/7,808(1)	9,931(2)/9,928(2)	Freiheit	P31c		6	1998
$LiNaSO_4$	763,15	7,818(1)/7,817(1)	7,818(1)/7,817(1)	9,931(3)/9,932(2)	Freiheit	P31c		6	1998
$LiNaSO_4$	773,15	7,828(1)/7,826(1)	7,828(1)/7,826(1)	9,932(2)/9,930(2)	Freiheit	P31c		6	1998
$LiNaSO_4$	783,15	7,833(1)/7,837(1)	7,833(1)/7,837(1)	9,934(3)/9,934(3)	Freiheit	P31c		6	1998
	788 K								
$LiNaSO_4$	803,15	5,722(1)/5,720(2)	5,722(1)/5,720(2)	5,722(1)/5,720(2)	Freiheit	Fm3m			1998
$LiNaSO_4$	813,15	5,727(0)/5,726(1)	5,727(0)/5,726(1)	5,727(0)/5,726(1)	Freiheit	Fm3m			1998
$LiNaSO_4$	823,15	5,728(2)/5,732(1)	5,728(2)/5,732(1)	5,728(2)/5,732(1)	Freiheit	Fm3m			1998
$LiNaSO_4$	833,15	5,735(1)/5,735(1)	5,735(1)/5,735(1)	5,735(1)/5,735(1)	Freiheit	Fm3m			1998
$LiNaSO_4$	843,15	5,740(3)/5,742(3)	5,740(3)/5,742(3)	5,740(3)/5,742(3)	Freiheit	Fm3m			1998
$LiNaSO_4$	853,15	5,745(3)/5,748(2)	5,745(3)/5,748(2)	5,745(3)/5,748(2)	Freiheit	Fm3m			1998
$LiNaSO_4$	865,15	5,752(4)/5,752(4)	5,752(4)/5,752(4)	5,752(4)/5,752(4)	Freiheit	Fm3m			1998
$LiNaSO_4$	993,15	5,719(1)/5,718(2)	5,719(1)/5,718(2)	5,719(1)/5,718(2)	Freiheit	Fm3m			1998

	T (K)	**a(Å)**	**b(Å)**	**c(Å)**	**Autor**	**G. E.**	β	**Z**	**año**
$(NH_4)K_2SO_4$	231.5(5)	7.733(2)	10.588(3)	5.992(4)	González-Silgo	Pnam		4	1997
$(NH_4)_{10}K_{1.90}O_4$	298.3(1)	7.5000(9)	10.0755(14)	5.790(3)	González-Silgo	Pnam		4	1997
$(NH_4)_{10}K_{1.90}O_4$	234.6(5)	7.4835(10)	10.063(2)	5.778(3)	González-Silgo	Pnam		4	1997
$(NH_4)_{10}K_{1.90}O_4$	174.8(9)	7.4691(12)	10.028(2)	5.796(5)	González-Silgo	Pnam		4	1997
$(NH_4)_{1.80}K_{0.20}SO_4$	298.3(1)	7.747(2)	10.561(5)	5.9463(11)	González-Silgo	Pnam		4	1997
$(NH_4)_{1.80}K_{0.20}SO_4$	232.8(4)	7.7230(14)	10.542(6)	5.931(2)	González-Silgo	Pnam		4	1997
$(NH_4)_{1.80}K_{0.20}SO_4$	183.8(9)	5.9090(12)	10.514(5)	7.7834(13)	González-Silgo	$Pna2_1$		4	1997

	T (K)	a(Å)	b(Å)	c(Å)	Autor	G. E.	β	Z	año
Li_2SO_4	1073	7,123	7,123	7,123	Solans	Fm3m		2	2002
α-Li_2SO_4	908	7,07	7,07	7,07	Nilsson	Fm3m		4	1980
α-Li_2SO_4	908	7,07	7,07	7,07	Mellander	Fm3m		2	1985
Li_2SO_4	873	7,063	7.063	7,063	Nilsson	Fm3m		4	1985
Li_2SO_4	873	7,066	7,066	7,066	Solans	Fm3m		2	2002
Li_2SO_4	846	7,07	7,07	7,07	Forland	Fm3m		4	1957
Li_2SO_4	298	8,474(1)	4,9533(3)	8,2414(4)	Swanson	$P2_1/a$	107,98(5)	4	1968
α-Li_2SO_4	298	8,2390(8)	4,9536(7)	8,4737(9)	Nord	$P2_1/a$	107,98(2)	4	1973
Li_2SO_4	298	8,45(1)	4,95(1)	8,21(1)	Alcock	$P2_1/c$	107,5(2)	4	1972
Li_2SO_4	298	8,45	4,95	8,21	Albright	$P2_1/c$	107,5(2)	4	1932
$Li_2SO_4.H_2O$	298	5,4518	4,8707	8,175	Nat.Bur.Std.	P21	107,19.8	2	1965
Li_2SO_4	298	8,2414	4,9533	8,474	Nat.Bur.Std.	P21/a	107,58.8	4	1968
$Li_2SO_4 \cdot H_2O$	293	5.45	4.872	8.164	Lundgren	P1211	107.31	2	1984
$Li_2SO_4 \cdot H_2O$	293	5,450,	4,872	8,164	Lundgren	$P2_1$	β=107,31,	2	1984
$Li_2SO_4 \cdot H_2O$		5.44	4.84	8.16	Ziegler	P1211	107.58	2	1934
$Li_2SO_4 \cdot H_2O$		5.4553	4.869	8.1761	Karppinen	P1211	107.337	2	1986
Li_2SO_4		7.07	7.07	7.07	Forland	F4-3m		4	1957
$Li_2SO_4H_2O$		5.4537	4.857	8.1734	Smith	P1211	107.367	2	1968
Li_2SO_4		8.239	4.954	8.474	Nord	$P12_1/a1$	107.98	4	1976
Li_2SO_4		8.45	4.95	8.21	Alcock	$P12_1/c1$	107.5	4	1973
$Li_2SO_4 \cdot H_2O$		5.454	4.857	8.173	Larson	$P12_11$	107.37	2	1965
$Li_2SO_4H_2O$		5.43	4.83	8.14	Ozerov	$P12_11$	107.583	2	1963
$Li_2SO_4H_2O$		5.4518	4.8707	8.175	Rannev	$P12_11$	107.33	2	1965
Li_2SO_4		8.239	4.9536	8.4737	Nord	$P12_1/a1$	107.98	4	1973
$Li_2SO_4 \cdot H_2O$		5.43	4.836	8.14	Larson	$P12_11$	107.23	2	1954
Li_2SO_4		8.25	4.95	8.44	Albright	$P12_1/a1$	107.9	4	1932
$Li_2SO_4 \cdot H_2O$	80	5.449	4.832	8.141	Karppinen	$P12_11$	107.21	2	1986
$Li_2SO_4 \cdot H_2O$	80	5,449	4,832	8,141	Lundgren	$P2_1$	107,21	2	1984
$Li_2SO_4 \cdot H_2O$	80	5.449	4.832	8.141	Lundgren	P1211	107.21	2	1984
$Li_2SO_4 \cdot H_2O$	20	5.449	4.832	8.137	Lundgren	P1211	107.19	2	1984
$Li_2SO_4 \cdot H_2O$	20	5,449	4,832	8,137	Lundgren	$P2_1$	107,19	2	1984
H_2SO_4	113	8,14	4,70	8,54	P.Y. Yu	C2/c	β=111,42	4	1978
$NH_4(HSO_4)(H_2SO_4)$	298	7,5151(7)	12,5324(10)	7,7419(6)	Worzala	$P2_1/c$	92,767(7)	4	1997
$(NH_4)_4LiH_3(SO_4)_4$	298	7,633(1)	7,633(1)	29,496(2)	Prem	$P4_1$		4	1997
$N_2H_6SO_4$	298	8,2579(14)	9,178(2)	5,5386(11)	NBS	$P2_12_12_1$		4	1980

	T (K)	a(Å)	b(Å)	c(Å)	Autor	G. E.	β	Z	año
$Li_5Mn_4Mn(SeO_3)_8$	561.4	7.505	8.35	10.413	Wildner,	P1-	73.84 88.24 64.24	1	1993
$LiFe(Se_2O_5)_2$	416.66	5.987	6.76	10.295	Giester	Pnc2		2	1993
$Li_2Cu_3(SeO_3)_2(SeO_4)_2$	1175.47	16.293	5.007	14.448	Giester	I12/a1	94.21	4	1989
LiFe(SeO_3)2	1129.36	10.649	10.649	9.959	Giester	I4-2d		8	1994
$Li_{0.5}(Mg_{0.5}Al_{1.5})(SeO_4)_3$	1352.95	8.3722	8.3722	22.288	Slater	R3-h		6	1994
$Rb_2Li_4(SeO_4)_3(H_2O)_2$	726.65	5.256	5.178	26.739	Pietraszko	P121/c1	93.11	2	1999
$Li_2Co_3(SeO_3)_4$	523.94	8.095	9.236	7.781	Wildner	P121/c1	115.76	2	1999
$LiKSeO_4$	298	9,226	8,798	15,973	Glinnemann	$P2_1/n$	90,3	12	1977
$LiKSeO_4$	523	5,319	5,319	8,867	Glinnemann	$P6_3$		2	1977
$LiKSeO_4$	498	5,325	5,325	8,793	Glinnemann	$P6_3$		2	1978
NH_4KSO_4	298	5,806(1)	10.16(2)	7,491(1)	Srinivasa Rao				1995

	T (K)	a(Å)	b(Å)	c(Å)	Autor	G. E.	β	Z	año
$LiNaY_2(SO_4)_4$	298	14,150(3)	6,185(2)	6,181(2)	Korytnaya	Pcnm		2	1983
$KH_3(SO_4)_2{\cdot}H_2O$	298	7,2050 (9)	13,5936(23)	8,4424(10)	Worzala	$P2_1/c$	105,576(12)	4	1994
$Li_2NaK(SO_4)_2$	298	4,905(4)	7,753(6)	18,923(16)	Heeg Mary	$P2_12_12_1$		4	1987
γ-$Li_2NaK(SO_4)_2$	298	19,11	7,83	4,96	Liang	$P22_12_1$		4	1988
γ''-$Li_2NaK(SO_4)_2$	730	9,210(2)	8,4926(17)	5,0513(10)	Liang	Pmn2/Pmnm		2	1988
γ''-$Li_2NaK(SO_4)_2$	726	9,20	8,49	5,05	Liang	Pmn2/Pmnm		2	1988
$KNaSO_4$	298	5,6066(7)	5,6066(7)	7,177(1)	Okada K.	P3m1		2	1980
$K_3Na(SO_4)_2$	298	5,6801(6)	5,6801(6)	7,309(3)	Okada K.	P-3m1		1	1980
$(Na_{0.5}K_{0.5})_2SO_4$	293	9,711	5,607	7,177	Goldberg	P-3m1			1973
$(Na_{0.5}K_{0.5})_2SO_4$	413	9,86	5,69	7,42	Goldberg	P-3m1			1973
$(Na_{0.3}K_{0.7})_2SO_4$	293	9,809	5,663	7,298	Goldberg	P-3m1			1973
$(Na_{0.25}K_{0.75})_2SO_4$	293	10,163	5,868	7,932	Goldberg	P-3m1			1973
$(Na_{0.70}K_{0.30})_2SO_4$	293	9,923	5,729	7,214	Goldberg	P-3m1			1973
$(Na_{0.80}K_{0.20})_2SO_4$	293	9,938	5,635	7,164	Goldberg	C2/m	89,17º		1973
$(Na_{0.93}K_{0.07})_2SO_4$	413	9,53	5,35	7,11	Eysel	Pnam			1973
$Li_2SeO_4{\cdot}H_2O$	291	8,446	5,024	5,581	Pristorius	$P2_1$	107,64	2	1967
Li_2SeO_4	1387	13.931	13.931	9.304	Heeg	R3-h		18	1984
Li_2SeO_4		13.931	13.931	9.304	Hartmann	R3-h	120	18	1989
$LiHSeO_3$	295.43	5.0579	11.1868	5.2213	Chomnilpan	$P2_12_12_1$		4	1979
$LiH_3(SeO_3)_2$	258.4	6.2554	7.8823	5.4339	Chomnilpan	P1n1	105.325	2	1979
$LiH_3(SeO_3)_2$	258.34	6.2534	7.883	5.4335	Mohana-Rao	P1n1	105.31	2	1971
$LiH_3(SeO_3)_2$	298	6.258	7.886	5.433	Vedam,	P1n1	105.2	2	1960
$LiH_3(SeO_3)_2$	258.4	6.2554	7.8823	5.4339	Tellgren,	P1n1	105.325	2	1972
$LiD_3(SeO_3)_2$	259.78	6.2473	7.903	5.4471	Liminga	P1n1	104.995	2	1982
$LiNH_4SeO_4$	298	17,390	5,10	10,64	Brenner	Pnma		8	1969
$LiNH_4SeO_4$	298	17,424	5,123	10,567	Glinnemann	Pca		8	1987
$LiNH_4SeO_4$	298	10,567	5,123	17,424	Glinnemann	Pca		8	1977
$LiNH_4SeO_4$	468.38	17.346	5.278	5.116	Waskowska,	$Pbn2_1$		4	1982
$Li(HSeO_3)$	295.22	5.0551	11.1874	5.2202	Eichhorn	$P2_12_12_1$		4	1997
$Li_4(SeO_5)$	387.65	8.7329	5.7249	7.8357	Haas,	C12/c1	98.29	4	1999
$CsLiH_2(SeO_3)_2$	745.43	12.483	8.169	7.31	Vinogradova	$P2_12_12_1$		4	1989
$Li(H_2O)TiSe_2$	292.04	3.581	3.581	26.297	Patel	P3-m1		3	1985
$Li(H_2O)_2TiSe_2$	131.33	3.604	3.604	11.675	Patel	P3-m1		1	1985

	T (K)	a(Å)	b(Å)	c(Å)	Autor	G. E.	β	Z	año
$(NH_4)_2S_2O_3$	298	10,33	6,541	8,806	Elerman	C2, Cm	β=95,49	4	1978
$(NH_4)_2S_2O_3$	298	10,2233(15)	6,4956(9)	8,8074(10)	NBS	C2/m	94,66(1)	4	1980
$(NH_4)_2S_2O_8$	298	7,829(2)	8,0075(14)	6,1483(12)	NBS	$P2_1/n$	β=95,12(2)	2	1980
$(NH_4)HSO_4$	298	24,90	4,54	14,90	Pepinski	$B2_1/a$	β=90º18´	16	1958
$(NH_4)HSO_4$	298	14,51	4,54	14,90	Pepinski	$P2_1/c$	β=120º18´	8	1958
$(NH_4)HSO_4$	243	14,26	4,62	14,80	Pepinski	Pc	β=121º18´	8	1958
$(NH_4)HSO_4$	154	24,37	4,62	14,80	Pepinski	Ba	β=90º		1958
$(NH_4)HSO_4$	133	14,24	4,56	15,15	Pepinski	P1	β=123º24'		1958
$(NH_4)HSO_4$	133	24,43	4,56	15,15	Pepinski	B1	β=91,12		1958
$(NH_4)_2S_2O_6$	298	10,22	10,22	6,47	Larson	P321			1963
$(NH_4)_2SO_4$	183	7,890	10,563	5,954	Ahmed	Pnam			1987
$(NH_4)_2SO_4$	293	7,782	10,639	5,993	Ahmed	$Pna2_1$		4	1987
	232	7,733(2)	10,588(3)	5,992(4)	Gonzáles-Silgo	Pnam		4	1997
$(NH_4)_2SO_4$	298	7,782	10, 636	5,993	Schlemper	Pnam		4	1966
$(NH_4)_2SO_4$	183	7,837(7)	10,636(1)	5,967(6)	Schlemper	$Pna2_1$		4	1966

	T (K)	a(Å)	b(Å)	c(Å)	Autor	G. E.	β	Z	año
$LiNH_4SO_4$	950	5.277	8.984	8.656	Hasebe	P2111		4	1994
I-$LiNH_4SO_4$	523	5,292(9)	8,769(7)	9,198(3)	Solans	$P2_1nb$		4	1999
I-$LiNH_4SO_4$	523	8,7722	9,2304	5,3145	Tomaszewki	Pnam		4	1979
I´-$LiNH_4SO_4$	483	5,304(3)	8,774(2)	9,1661(11)	Solans	$P2_1nb$		4	1999
I- $LiNH_4SO_4$	483	8,757	9,199	5,310	Hildmann	$P2_1cn$		4	1978
I-$LiNH_4SO_4$	483	8,7605	9,2180	5,3112	Tomaszewki	Pnam		4	1979
β´´´-$LiNH_4SO_4$	483	9,199	5,311	8,757	Hildmann	Pcmn		4	1976
I-$LiNH_4SO_4$	478	5,299(2)	9,199(2)	8,741(1)	Itoh	Pmcn		4	1981
I-$LiNH_4SO_4$	463	8,7582	9,2091	5,3090	Tomaszewki	Pnam		4	1979
II-$LiNH_4SO_4$	453	8,7710	9,1850	5,3044	Tomaszewki	$Pna2_1$		4	1979
II-$LiNH_4SO_4$	453	8,74(2)	9,16(2)	5,13(2)	Yuzkav	$P2_1cn$		4	1974
II´-$LiNH_4SO_4$	423	5,304(4)	8,782(2)	9,1466(14)	Solans	$P2_1nb$		4	1999
II+II´-$LiNH_4SO_4$	383	5,302(6)	8,780(2)	9,140(2)	Solans	$P2_1nb$		4	1999
II-$LiNH_4SO_4$	373	8,7765	9,1450	5,2900	Tomaszewki	$Pna2_1$		4	1979
II+II´-$LiNH_4SO_4$	318	5,279(3)	8,775(3)	9,122(2)	Solans	$P2_1nb$		4	1999
II-$LiNH_4SO_4$	300	8,7747(2)	9,1262(2)	5,2783(1)	Tomaszewki	$Pna2_1$		4	1979
II-$LiNH_4SO_4$	298	5,282(1)	9,131(3)	8,780(2)	Mashiyama	$P2_1cn$		4	1993
$LiNH_4SO_4$	298	5,280(2)	9,140(7)	8,786(6)	Dollase	$P2_1cn$		4	1969
α-$LiNH_4SO_4$	298	10,196(2)	4,991(1)	17,100(3)	Pietraszko	$Pca2_1$		4	1992
α-$LiNH_4SO_4$	298	10,196	4,991	17,100	Lukaszewicz	$Pca2_1$		4	1992
β-$LiNH_4SO_4$	298	9,129	5,279	8,774	Lukaszewicz	$Pc2_1n$		4	1992
$LiNH_4SO_4$	298	9,123(3)	5,277(2)	8,776(2)	Martínez-Sarrión	$P2_1cn$		4	1998
$LiNH_4SO_4$	298	5,280(2)	9,140(7)	8,786(6)	Dollase	$P2_1cn$		4	1969
II-$LiNH_4SO_4$	298	5,276(2)	8,768(3)	9,122(2)	Solans	$P2_1nb$		4	1999
α-$LiNH_4SO_4$	295	17,06	5,102	9,985	Tomaszewski	$P12_1/a$		8	1992
α-$LiNH_4SO_4$	298	17,1053	4,9917	9,9824	Tomaszewski	$P2_1ca$		4	1992
$LiNH_4SO_4$		17.511	9.13	5.274	Kruglik	P1121/a		8	1978
β´´-$LiNH_4SO_4$	295	9,129	5,279	8,774	Hildmann	$Pc2_1n$		4	1976
$LiNH_4SO_4$	283	17,06	5,102	9,985	Hildmann	Pmca		8	1976
$LiNH_4SO_4$	213	17,511(6)	9,130(6),	6,274(2)	Kruglik	$P2_1/a$	γ=90.00(3)	8	1978
β´-$LiNH_4SO_4$	208	9,122	5,273	17,53	Hildmann	$P2_1/c$		8	1976
III-$LiNH_4SO_4$	190	5,283(2)	9,121(5)	17,444(7)	Mashiyama	$P2_1/c11$		8	1993
$LiHSO_4$		5.234	7.322	8.363	Kemnitz	P121/c1	90.02	4	1995
$LiHSO_4$	298	5,2461(7)	7,3314(10)	8,3619(10)	Worzala	$P2_1/c$	90,134(11)	4	1994
$Li(NH_2SO_3)$	298	5,059	16,265(2)	8,253(1)	Irran	$Pbc2_1$		8	1995
$LiNH_3OHSO_4$	298	7,274	6,713	18,449	Himmerich	Pbca		8	1976
$Li(N_2H_5)SO_4$	298	8,96(9)	9,91(3)	5,17(8)	Pepinski	$Pbn2_1$	β=90º18´	4	1958
$Li(N_2H_5)SO_4$	298	9,929	8,973	5,181	Anderson	$Pna2_1$		4	1974
$LiN_2H_5SO_4$	295	9.922	8.97	5.1728	Fukami,	Pna21		4	1998
$LiN_2H_5SO_4$	467	9.967	8.9772	5.2255	Fukami,	Pna21		4	1998
$LiND_4SO_4$	323	9.131	5.2786	8.771	Fischer,	Pc21n		4	1989
$Li_2(HSO_4)_2H_2SO_4$		17.645	5.378	10.667	Werner	Pccn	82.42 86.1 80.93	1	1995
$LiH(HSO_4)_2(H_2(SO_4))_2$	293.34	4.915	7.314	8.346	Werner	P1-			1996
$Li(NH_4)_{0.80}Rb_{0,20}SO_4$	295	9,121(3)	5,2826(14)	8,759(2)	Martinez-Sarrión	$Pc2_1n$		4	1998
$LiNH_4(SO_4)_{0,96}(SeO_4)_{0,04}$	295	9,120(7)	5,282(2)	8,774(2)	Martinez-Sarrión	$Pc2_1n$		4	1998
$Li(NH_4)_{0.50}Rb_{0,50}SO_4$	295	9,111(6)	5,286(4)	8,720(6)	Martinez-Sarrión	$Pc2_1n$		4	1998
$Li(NH_4)_{0.97}K_{0,03}SO_4$	295	9,095(3)	5,274(2)	8,7747(3)	Martinez-Sarrión	$Pc2_1n$		4	1998
$Li(NH_4)_{0.80}Rb_{0,20}SO_4$	295	9,121(3)	5,2826(14)	8,759(2)	Martinez-Sarrión	$Pc2_1n$		4	1998

	T (K)	a(Å)	b(Å)	c(Å)	Autor	G. E.	β	Z	año
$Lu_2(SO_4)_3$	293	6,418	6,418	6,418	Saito				1998
$Eu_2(SO_4)_3$	293	8397(15)	5,3495(9)	6,889(13)	Lin	Pnma			1998
$Gd_2(SO_4)_3$	293				Saito				1998
$Tb_2(SO_4)_3$	293				Saito				1998
$Tm_2(SO_4)_3$	293	6,455	6,455	6,455	Saito				1998
$Yb_2(SO_4)_3$	293	6,430	6,430	6,430	Saito				1998
$La_2(SO_4)_3$	293				Saito				1998
$Pr_2(SO_4)_3$	293				Saito				1998
$Nd_2(SO_4)_3$	293		39-301-311		Saito				1998
$Sm_2(SO_4)_3$	293				Saito				1988
$Fe_2(SO_4)_3$	293	8,2955	8,5332	11,6304	Holzer	$P2_1/n$	90,75	4	1991
$Tl_2(SO_4)_3$	293	8,606	9,006	12,173	Holzer	$P2_1/n$	90,87	4	1991
$In_2(SO_4)_3$	293	8,564	8,897	12,047	Holzer	$P2_1/n$	91,1	4	1991
$V_2(SO_4)_3$	293	8,293	8,540	11,634	Holzer	$P2_1/n$	90,6	4	1991
$Fe_2(SO_4)_3$	293	8,2362	8,2362	22,18	Holzer	R-3		6	1991
$Ti_2(SO_4)_3$	293	8,4400	8,4400	21,95	Holzer	R-3		6	1991
$V_2(SO_4)_3$	293	8,2300	8,2300	22,10	Holzer	R-3		6	1991
$Cr_2(SO_4)_3$	293	8,1320	8,1320	21,943	Holzer	R-3		6	1991
$Ga_2(SO_4)_3$	293	8,0650	8,0650	21,87	Holzer	R-3		6	1991
$Rh_2(SO_4)_3$	293	8,0620	8,0620	22,16	Holzer	R-3		6	1991
$Sc_2(SO_4)_3$	293	8,6700	8,6700	22,50	Holzer	R-3		6	1991
$Y_2(SO_4)_3$	293	9,1900	9,1900	22,87	Holzer	R-3		6	1991
$In_2(SO_4)_3$	293	8,4860	8,4860	22,85	Holzer	R-3		6	1991
β-$LiNd(SO_4)_2$	298	7,708(3)	7,708(3)	5,665(5)	Sirontinkin	Pnnm Pnn2			1978
$LiLa(SO_4)_2$	873	13,75	6,744	7,068	Chai	$P2_1/c$		4	1988
$NH_4In(SO_4)_2$	298	4,901	4,901	24,68	Pannetier	R32		3	1972
β-$Li_2Co(SO_4)_2$	298	8,104(1)	8,104(1)	14,916(4)	Touboul	Pbcn		6	1992
$Li_2Mg_2(SO_4)_3$	298	12.165	8.538	8.689	Touboul	Pbcn		4	1988
$Li_2Mg_2(SO_4)_3$	298	12,1098(11)	8,5056(7)	8,6660(9)	Touboul	Pbcn		4	1989
$Li_2Mn_2(SO_4)_3$	295	8,693(1)	8,799(1)	24,166(1)	Elfakir	Pbca		8	1998
$Li_2Ni(SO_4)_2$	295	9,008(1)	9,135(1)	13,544(1)	Elfakir	Pbca			1998
$Li_2Ni(SO_4)_2$	295				Touboul				1992
$Li_2V_2(SO_4)_3$		13.0582	8.6526	8.7247	Vaughan	$C12/c_1$	115.443	4	1999
$LiEr_2F_3(SO_4)_2$		14.791	6.336	8.1372	Wickleder	Pbcn		4	1999
$LiEu(SO_4)_2$		7.632	7.632	5.566	Sirotinkin	Pnn2		2	1977
$LiPr(SO_4)_2$		13.69	7.005	6.692	Sirotinkin	P1121/b	105.25	4	1978
$LiCsSO_3(H_2O)_2$		11.927	5.67	4.828	Archer	C1m1	109.26	2	1979
β-$LiLu(SO_4)_2$	298	12,575	9,051	9,138	Sirotinkin	Pbcn (60)		6	1978
$LiFSO_3$		8.54	7.62	4.98	Zak	C12/m1		4	1978
$LiN_2H_5SO_4$		9.929	8.973	5.181	Anderson	Pna21		4	1974
$LiNH_3OHSO_4$		18.46	7.28	6.712	Vilminot	Pbca		8	1973
$LiN_2H_5SO_4$		9.913	8.969	5.178	Padmanabhan	Pna21		4	1967
$LiAlCl_4(SO_2)_3$		9.516	13.271	10.174	Simon	Pnam		4	1980
$LiB(SO_3Cl)_4$		8.832	8.388	20.765	Mairesse	P121/c1	91.89	4	1980
$Li(N_2H_5)SO_4$		8.99	9.94	5.18	Brown	Pbn21		4	1964
$Li(N_2H_5)SO_4$		8.99	9.94	5.18	Van den Hende	Pbn21		4	1964

	T (K)	a(Å)	b(Å)	c(Å)	Autor	G. E.	β	Z	año
$Li_{0.25}(Mg_{0.25}Cr_{1.75})(SO_4)_3$		8.1467	8.1467	21.979	Slater	R3-h		6	1994
$Li_{0.5}(Mg_{0.5}Cr_{1.5})(SO_4)_3$		8.1681	8.1681	22.009	Slater	R3-h		6	1994
$Li_{0.5}(Zn_{0.5}Cr^{1.5})(SO_4)_3$		8.1462	8.1462	21.955	Slater	R3-h		6	1994
$Li_{0.4}(Ni_{0.4}Cr_{1.6})(SO_4)_3$		8.1534	8.1534	21.961	Slater	R3-h		6	1994
$Li_{0.5}(Mg_{0.5}Al_{1.5})(SO_4)_3$		8.1853	8.1853	21.201	Slater	R3-h		6	1994
$Li_{0.5}(Mg_{0.5}Cr_{1.5})(SO_4)_{1.7667}(SeO_4)_{1.2333}$		8.2711	8.2711	22.25	Slater	R3-h		6	1994
$Li_2S_2O_6(H_2O)_2$		6.01	10.44	10.151	Berthold	Pnma		4	1967
$Li_2(SO_4)(CO(NH_2)_2)_3$		17.078	9.292	7.978	Furmanova	C12/c1	112.17	4	1993
$Li_{3.17}Si_{0.7}S_{0.3}O_4$	298	6.1701	10.655	5.0175	Fitch	Pmnb		4	1984
$Li_{3.17}Si_{0.7}S_{0.3}O_4$	623	6.2217	10.7109	5.0571	Fitch	Pmnb		4	1984
$Li_{3.4}Si_{0.7}S_{0.3}O_4$	973	6.2859	10.7716	5.1059	Fitch	Pmnb		4	1984
$Li(H_2O)_2TiS_2$		3.425	3.425	25.41	Patel	P3-m1		3	1985
$Li(H_2O)_2TiS_2$		3.412	3.412	11.215	Patel	P3-m1		1	1985
$LiCe(SO_4)_2(H_2O)$		8.114	4.612	18.202	Iskhakova	P121/c1	96.89	4	1987
$LiCe(SO_4)_2(H_2O)$		8.114	4.612	18.202	Iskhakova	P121/c1	96.89	4	1987

	T (K)	a(Å)	b(Å)	c(Å)	Autor	G. E.	β	Z	año
$HgSO_4$	298	4,8150(2)	6,5752(3)	4,7810(2)	NBS	$P2_1mn$		2	1979
Hg_2SO_4	298	8,365(1)	4,4262(5)	6,2785(9)	NBS	P2/a		2	1979
$Fe_2(SO_4)_3$	773	8,236(1)	8,236(1)	22,166(6)	NBS	R-3		6	1979
γ-$CdSO_4$	1123	5.01	5,01	7,64	Spiess	P-3m1		2	1979
α-$CdSO_4$	598	8,901	8,901	4,836	Spiess	Pnma		4	1979
$CdSO_4$	298	4,7174	6,5590	4,7012	NBS	Pmmn		2	1963
$Cr_2(SO_4)_3$	298	8,132(1)	8,132(1)	21,943(6)	NBS	R-3		6	1979
$BeSO_4$	298	4,4927(4)	4,4927(4)	6,8937(8)	NBS	I-4		2	1978
$NiSO_4$	298	5,166	7,846	6,362	Wildner	Cmcm			1990
$PbSO_4$	1173	7,23	7,23	7,23	Spiess	F		4	1979
$SrSO_4$	298	6,906	7,150	6,613	Takahashi		β=102,68	4	1993
β-$CoSO_4$	298	6,522	6,522	5,198	NBS	Amam		4	1963
α-$CoSO_4$	298	8,6127(4)	6,7058(3)	4,7399(2)	Burns	Pnma		4	1993
$BaSO_4$	1438	7,39	7,39	7,39	Butler	F		4	1971
$BeSO_4$	298	4,4927(4)	4,4927(4)	6,8937(8)	NBS	I-4		2	1978
β-Tl_2SO_4	298	7,84(3)	10,75(3)	5,96(2)	Diot			4	1981
γ-Tl_2SO_4	298	7,89(6)	10,77(8)	5,96(5)	Diot		γ=90,7		1981
α-Tl_2SO_4	783	6,086	6.086	8,09	Pannetier	P-3m1		2	1966
α-Tl_2SO_4	781	6,16	6.16	8,28	Majumdar			2	1965
$Tl_2(SO_4)_3$	298	8,606	9,006	12,173	Holzer	$P2_1/n$	β=90,87	4	1991
Tl_2SO_4	783	7,84	10,75(3)	5,96(2)	Diot			4	1981
Tl_2SO_4	298				Diot				
α-Tl_2SO_4	783	6,086	6,086	8,09	Pennetier	P-3m1		2	1966
Tl_2SO_4	298	5,923	10,66	7,828	NBS	Pmcn		4	1956
$Tl_2Sr(SO_4)_2$	298	5,561	5,561	22,219	Scharz			3	1966
$Tl_2Sr(SeO_4)_2$	298	5,779	5,779	22,075	Scharz			3	1966
$LiPr(SO_4)_2$	298	13,69(9)	7,005(3)	6,692(3)	Sirontinkin	$P2_1/b$	β=105,25	4	1978
	T (K)	**a(Å)**	**b(Å)**	**c(Å)**	**Autor**	**G. E.**	β	**Z**	**año**
$LiAgSO_4$	813	5,77	5,77	5,77	Nilsson	I-43m			1989
$Li_{1.6}Ag_{0.4}SO_4$	838	7.14	7.14	7.14	Nilsson,	Fm3-m		4	1982
Ag_2SO_4	713	5,531(3)	5,531(3)	7,456(5)	Masciocchi			4	1990
Ag_2SO_4	693	5,54	5,54	7,44	Eysel	$P6_3mc$		2	1978
Ag_2SO_4	298	10,269(5)	12,706(7)	5,8181(3)	Natl.Bur.Stand	Fddd		8	1976
Ag_2SO_4	693	5,54	5,54	7,44	Illgut, Eysel	$P6_3mc$		2	1978

	T (K)	a(Å)	b(Å)	c(Å)	Autor	G. E.	β	Z	año
$(NH_4)_{1.82}Rb_{0.18}SO_4$	295	7.810(3)	10.616(4)	6.000(2)	Mestres	Pnam		4	1998
$(NH_4)_{1.73}Rb_{0.27}SO_4$	295	7.824(5)	10.591(6)	6.006(4)	Mestres	Pnam		4	1998
$(NH_4)_{1.64}Rb_{0.36}SO_4$	295	7.823(2)	10.592(2)	6.005(1)	Mestres	Pnam		4	1998
$(NH_4)_{1.34}Rb_{0.66}SO_4$	295	7.830(2)	10.517(2)	5,986(3)	Mestres	Pnam		4	1998
$(NH_4)RbSO_4$	295	7.826(1)	10.470(2)	5,982(2)	Mestres	Pnam		4	1998
$(NH_4)_{0.35}Rb_{1.65}SO_4$	295	7.820(1)	10.443(2)	5,977(2)	Mestres	Pnam		4	1998

	T (K)	a(Å)	b(Å)	c(Å)	Autor	G. E.	β	Z	año
$K_2Cu(SO_4)_2$									
$Rb_2Cu(SO_4)_2$									
$Na_2Cu(SO_4)_2$									
$Na_2Cu(SO_4)_2$									
$Tl_2Cu(SO_4)_2$									
$Rb_3In(SO_4)_3$	298	15,413	15,413	9,136	Tudo	R-3		6	1974
$K_3In(SO_4)_3$	298	14,862	14,862	8,96	Tudo	R-3		6	1974
$KIn(SO_4)_2$	298	8,463	4,874	8,477	Bernard			2	1970
$KIn(SO_4)_2$	298	4,875	4,875	23,91	Perret	R-3m		3	1972
$RbIn(SO_4)_2$	298	4,908	4,908	24,95	Perret	R-3m		3	1972
$Na_3In(SO_4)_3$	298	13,970	13,970	8,771	Tudo	R-3		6	1974
$NaMgCr(SO_4)_3$	298	8,341	8,341	22,111	Tudo	R-3		6	1974
$NaMgIn(SO_4)_3$	298	8,613	8,613	22,203	Tudo	R-3		6	1974
$TlIn(SO_4)_2$	298	4,919	4,919	24,95	Perret	R-3m		3	1972
$In_2(SO_4)_3$	298	8,486	8,486	22,845	Thrierr-Sorel				1968
$NH_4In(SO_4)_2$	298	4,902	4,902	24,69	Perret	R-3m		3	1972
$CsIn(SO_4)_2$	298	4,956	4,956	26,41	Perret	R-3m		3	1972
$CsAl(SO_4)_2$	623	4,75	4,75	8,81	Franke	P321		1	1965
$In_2(SO_4)_3$	298	12,047	8,897	8,564	Tudo	$P2_1/n$			1974
$Y_2(SO_4)_3$	298	9,190	9,190	22,87	Perret	R-3		6	1968
$Cs_3In(SO_4)_3$	298	16,068	16,068	9,211	Tudo	R-3		6	1974
$CsIn(SO_4)_2$	298	8,582	4,956	9,260	Bernard			2	1970
$NH_4In(SeO_4)_2$	298	5,053	5,053	25,35	Perret	R-3m		3	1972
$CsIn(SeO_4)_2$	298	5,091	5,091	27,07	Perret	R-3m		3	1972

	T (K)	a(Å)	b(Å)	c(Å)	Autor	G. E.	β	Z	año
$Li_{10}K_2Rb_2(SO_4)_7$	793				Lepeshkov		30-761		1972
$Li_{10}K_2Rb_2(SO_4)_7$	493				Lepeshkov		30-762		1972
$LiRb_{0.10}K_{0.90}(SO_4)_2$	298	5,135(2)	5,135(2)	8,635(3)	Righi	$P6_3$		2	1998
$LiRb_{0.50}K_{0.50}(SO_4)_2$	298	5,200(2)	5,200(2)	8,702(3)	Righi	P31c		2	1998
$Li_{10}Na_2Rb_2(SO_4)_7$	495				Kalinkin				
$Li_{18}Cs_4Na_6(SO_4)_{14}$	673				Kalinkin				1992
$LiN(CF_3SO_2)_2$		9.6351	5.4154	16.26389	Nowinski	Pnaa		4	1994
$LiCF_3SO_3$		10.2432	5.0591	9.5592	Tremayne,	$P12_1/c1$	90.319	4	1992
$Zn(HSO_4)_2{\cdot}(H_2SO_4)_2$	278	5,0470(5)	15,4312(19)	7,9539(10)	Schneider	$P2_1/c$	β=104,175(10)	2	1998
$ZnSO_4{\cdot}6\ H_2O$	278	9,981	7,250	24,280	Spiess	C_2/c	β=98,45	8	1979
$Zn_3O(SO_4)_2$	850	7,36	13,96	6,79	Spiess	$C222_1$		4	1979
$ZnSO_4$	973	7,18	7,18	7,18	Spiess	F-43m		4	1979
$ZnSO_4$	298	5,95	13,60	7,96	Pannetier	$P2_1/n$	90,18	4	1966
$ZnSO_4$	298	8,588	8,588	4,770	NBS	Pnma		4	1957

	T (K)	a(Å)	b(Å)	c(Å)	Autor	G. E.	β	Z	año
$BaSO_4$	298	7,1565	8,8811	5,4541	NBS	Pbnm		4	1972
γ-$Zr(SO_4)_2$	298	11,84	7,41	5,86	Bear			4	1967
Zr_9S_2	1448	9,752	9,752	19,216	Conard				1971
Zr_2S	1573	12,322	15,359	3,508	Conard				1971
β-$Zr(SO_4)_2{\cdot}H_2O$	298	7,86	5,34	8,97	Bear		α=91,0 β=100,7 γ=109,4	4	1970
α-$Zr(SO_4)_2{\cdot}H_2O$	298	7,32	8,54	11,82	Bear	P21/c	β=106	4	1970
γ-$Zr(SO_4)_2{\cdot}H_2O$	298	7,89	5,21	8,96	Bear	P-1	α=95,2 β=99,8 γ=109,2	2	1970
α-Rb_2SO_4	HT	6,139	6,139	8,510	Pannetier	P-3m		2	1966
Rb_2SO_4	298	7,8231(7)	5,9800(5)	10,4433(9)	Martin	Pnma		4	1991
$LiRbSeO_4$	298	5,408	5,408	9,162	Hahn	$P6_3$		2	1968
$LiRbSO_4$		5.288	9.105	8.731	Tanisaki	P1121/n	90.09	4	1980
$LiRbSO_4$	446	9.157	5.316	43.654	Steurer	P11n	89.97	2	1986
$LiRbSO_4$	421.78	9.118	5.294	8.738	Kruglik	P1121/n	89.53	4	1979
$LiRbSO_4$	240	9,244	5,345	8,743	Chung	$Pc2_1n$		4	1979
$LiRbSO_4$	298	9,118	5,294	8,738	Hahn	$P2_1/n$	90,12	4	1969
$LiRbSO_4$	298	9,118	5,294	8,738	Kruglik	$P2_1/n$	γ=89,53	4	1979
$LiRbSO_4$	298	9,120(3)	5,296(4)	8,723(3)	Martínez-Sarrión	$P2_1/n$		4	1998
$Li_3Rb(SO_4)_2{\cdot}H_2O$		5.1356	4.9853	8.2712	Pina	P1	90.032 105.729 90.004	1	1998
$LiRb_4H_3(SO_4)_4$		7.615	7.615	29.458	Zuniga	P41		4	1990
$LiCsSO_4$		8.36	9.223	5.306	Katkanant	Pnam		4	1992
$LiCsSO_4$	200	8.541	9.028	5.243	Katkanant	$P112_1/n$	89.767	4	1992
$LiCsSO_4$	253	5.443	9.441	8.786	Asahi	Pmcn		4	1988
$LiCsSO_4$	202	5.433	9.421	8.78	Asahi	$P112_1/n$	90.14	4	1988
$LiCsSO_4$	195	5.43	9.415	8.787	Asahi	$P112_1/n$	90.2	4	1988
$LiCsSO_4$	173	5.434	9.41	8.819	Asahi	$P112_1/n$	90.25	4	1988
$LiCsSO_4$	299	5.444	9.446	8.784	Niwata	Pmcn		4	1995
$LiCsSO_4$	205	5.444	9.446	8.784	Niwata	Pmcn		4	1995
$LiCsSO_4$	455.04	9.456	5.456	8.82	Kruglik	Pcmn		4	1979
$LiCsSO_4$	449.3	9.379	5.423	8.834	Kruglik	P1121/n	89.45	4	1979
$LiCsSO_4$	290	9.4444	5.4493	8.8085	Mestres	Pcmn		4	1999
$LiCsSO_4$	298	9,45	5,45	8,80	Delfino	Pcmn		2	1980
Cs_2SO_4	298	8,2436(6)	6,2620(4)	10,9474(6)	Martin	Pnma 62		4	1991
α-Cs_2SO_4	986	6,485	6,485	8,980	Tabrizi	P-3m1		4	1968
$LiKTb_2(SO_4)_4$		estable	530-730		Korytnaya				1983
$LiKY_2(SO_4)_4$		preparado	600 ºC		Korytnaya				1993
$LiKY_2(SO_4)_4$	293				Frech				
$Li_{1,5}K_{1,5}Nd_3(SO_4)_6$	293	17,46(1)	8,234(2)	6,911(3)	Korytnaya	B2/b	102,03	2	1984
$LiK(NH_2SO_3)_2$	298	5,196(1)	8,475(1)	8,868(1)	Meinhart	$P2_1$	105,05	2	1997
$LiNa(NH_2SO_3)_2$	298	8,631(1)	8,984(1)	17,386(1)	Meinhart	Pbca		8	1997
$LiTlSO_4$	295	8,388(1)	9,309(1)	5,3285(7)	Elfakir	$Pna2_1$		4	1998
$LiTlSO_4$	813	8,777(2)	5,350(1)	9,324(2)	Elfakir	Pnma		4	1998
α-$LiTlSO_4$	823	18,6699(8)	18,6699(8)	8,7015(6)	Elfakir	$Pnam/Pna2_1$		24	1998
β-$LiTlSO_4$	293	8,3815(4)	9,2914(4)	5,3175(3)	Elfakir	$P6_3$		4	1998
Li_2SeO_4	290	13,938	13,938	9,320	Pistorius	$P6_3$		18	1967
$Li_2SeO_4.H_2O$	291	8,446	5,024	5,581	Pistorius	$P2_1$	107,64	2	1967

	T (K)	a(Å)	b(Å)	c(Å)	Autor			G. E.	β	Z	año
$LiKSO_4$	973	5,2997(3)	5,2997(3)	8,8021(6)	Solans,	247,22	Hexagonal	$P6_3/mmc$		2	1999
$LiKSO_4$	973	5,31	5,31	8,82	Xie	248,69	Hexagonal	$P6_3/mmc$		2	1984
$LiKSO_4$	803	5.270(2)	9.193(2)	8.751(2)	Pinheiro	423,96	Rómbico	Pmcn		4	2000
$LiKSO_4$	773	5,2150(3)	9,1321	8,6652(4)	Solans,	412,67	Rómbica	$P2_1cn$		4	1999
$LiKSO_4$	723	5.264(4)	9.148(2)	8.668(4)	Pinheiro	417,41	Rómbico	Pmcn		4	2000
$LiKSO_4$	713	8,665(14)	5,229(8)	9,081(14)	Sankaran	411,45	Rómbico	Pnma		4	1988
$LiKSO_4$	712	17,33	10,458	9,081(14)	Li	1645,81	Rómbico	Pnma		8	1988
$LiKSO_4$	712	8,665(14)	5,229(8)	9,081(14)	Li	411,45	Rómbico	Pnma		8	1984
$LiKSO_4$	708	5.27	5.27	8.655	Fischmeister			$P6_3/mmc$		2	1962
$LiKSO_4$	573	5.202(1)	5.202(1)	8.647(2)	Pinheiro	233,99	Hexagonal	$P6_3$		2	2000
$LiKSO_4$	568	5.19	5.19	8.637	Furmanova			$P6_3$		2	1985
$LiKSO_4$	568	5,190(3)	5,190(3)	8,637(4)	Schulz,	232,65	Hexagonal	$P6_3$		2	1985
$LiKSO_4$	398	5,160(3)	5,160(3)	8,634(4)	Schulz,	229,89	Hexagonal	$P6_3$		2	1985
$LiKSO_4$	313	5,15	5,15	8,63	Delfino	228,89	Hexagonal	$P6_3$		2	1980
$LiKSO_4$	302	5,146(1)	5,146(1)	8,636(2)	Bhakay-Tamhane	228,69	Hexagonal	$P6_3$	90,83	2	1984
$LiKSO_4$	302	5,146(2)	5,144(2)	8,635	Bhakay-Tamhane	228,58	Monoclínico	$P2_1$	119.98	4	1984
$LiKSO_4$	299	5,1457	5,1457	8,6298	Nat.Bur.Std.	228,50	Hexagonal	$P6_3$		2	1964
$LiKSO_4$	299	5,143(1)	5,143(1)	8,628(2)	Martínez-Sarrión	228,21	Hexagonal	$P6_3$		2	1998
$LiKSO_4$	298(1)	5,1421(11)	5,1421(11)	8,634(2)	Solans,	228,29	Hexagonal	$P6_3$		2	1999
$LiKSO_4$	298	5,147	5,147	8,633	Lim,	228,70	Hexagonal	$P6_3$		2	2001
$LiKSO_4$	298	5,147	5,147	8,633	Pimienta	228,70	Hexagonal	$P6_3$		2	1989
$LiKSO_4$	298	5,147	5,147	8,633	Shin,	228,70	Hexagonal	$P6_3$		2	1991
$LiKSO_4$	298	5,147	5,147	8,633	Cummins	228,70	Hexagonal	$P6_3$		2	1990
$LiKSO_4$	298	5,1452(2)	5,1452(2)	8,6343(6)	Karppinen	228,58	Hexagonal	$P6_3$		2	1983
$LiKSO_4$	298	5.142	5.142	8.632	Sandomirskii			$P6_3$		2	1983
$LiKSO_4$	298	5,151	5,151	8,639	Yan.	229,22	Hexagonal	$P6_3$		2	1984
$LiKSO_4$	293	5,146(1)	5,146(1)	8,638(2)	Bhakay-Tamhane	228,75	Hexagonal	$P6_3$		2	1991
$LiKSO_4$	293	5,147(3)	5,147(3)	8,633(4)	Schulz,	228,70	Hexagonal	$P6_3$		2	1985
$LiKSO_4$	293	5,15	5,15	8,63	Bradley	228,89	Hexagonal	$P6_3$		2	1925
$LiKSO_4$	293	5,143(4)	5,143(4)	8,641(4)	Rajagopal	228,56	Hexagonal	P63		2	1991
$LiKSO_4$	293	5,147	5,147	8,633Å	Sandomirski	228,70	Hexagonal	$P6_3$		2	1983
$LiKSO_4$		5.154	5.154	8.648	Gu			$P6_3$		2	1983
$LiKSO_4$		5.142	5.142	8.632	Balagurov			$P6_3$		2	1984
$LiKSO_4$		5.151	5.151	8.639	Yan, Q.-W.			$P6_3$	89.1	2	1984
$LiKSO_4$	260(1)	5,123(2)	5,123(2)	8,639(3)	Solans,	226,73	Hexagonal	$P6_3mc$		2	1999
$LiKSO_4$	233(1)	5,1341(12)	5,1341(11)	8,638(4)	Solans,	227,69	Hexagonal	$P6_3$		2	1999
$LiKSO_4$	205	5,139(3)	5,139(3)	8,677(3)	Rajagopal	229,15	trigonal	P31c		2	1991
$LiKSO_4$	200	5,154(3)	8,800(3),	8,628(3)	Tomaszewski	391,32	Rómbico	$Cmc2_1$		4	1983
$LiKSO_4$	200	5,1290	5,1290	8,6390	Zhang	227,26	Trigonal	P31c		2	1988
$LiKSO_4$	200	5.129	5.129	8.639	Zhang			P31c		2	1988
$LiKSO_4$	200	5.129	5.129	8.639	Zhang			P31c		2	1988
$LiKSO_4$	200	5.129	5.129	8.639	Zhang			P31c		2	1988
$LiKSO_4$	190-210	5,138(3)	5,138(3)	8,655(9)	Bhakay-Tamhane		Trigonal	P31c		2	1991
$LiKSO_4$	190	5,138(3)	5,138(3)	8,655(9)	Bhakay-Tamhane		Trigonal	P31c		2	1991
$LiKSO_4$	190	5,142	5,142	8,632	Balagurov	228,23	Hexagonal	$P6_3$		2	1984
$LiKSO_4$	189(1)	5,117(2)	5,117(2)	8,638(6)	Solans,	226,17	Trigonal	P31c		2	1999

	T (K)	a(Å)	b(Å)	c(Å)	Autor			G. E.	β	Z	año
$LiKSO_4$	182	5,101(2)	8,959(5)	8,653(3)	Rajagopal	395,44	Monoclínico	Cc	β= 90.1	4	1991
$LiKSO_4$	180	5,138(3)	5,138(3)	8,655(9)	Bhakay-Tamhane	228,48	Trigonal	P31c		2	1991
$LiKSO_4$	179-150	5,154	5,154	8,628	Bhakay-Tamhane	229,19	Monoclínico	Cc	γ=119.3	4	1987
$LiKSO_4$	T>180	5,154(3)	8,800(3)	8,628(3)	Tomaszewski.		Rómbica	$Cmc2_1$		4	1983
$LiKSO_4$	170	5,202	8,701	8,619	Tomaszewski.	390,12	Rómbica	$Cmc2_1$		4	1982
$LiKSO_4$	150	5,096	5,181	8,611	Desert	227,35	Monoclínico	Cc	β=119,63	2	1995
$LiKSO_4$	123(1)	5,114(2)	8,857(3)	8,630(2)	Solans,	390,89	Rómbica	$Cmc2_1$		4	1999
$LiKSO_4$	100	5.072	8.955	8.655	Rajagopal			C1c1		4	1991
$LiKSO_4$	100	5,072(4)	8,955(7)	8,655(7)	Rajagopal	393,06	Monoclínico	Cc	β= 89.1	4	1991
$LiKSO_4$	1,65Gpa	7,993	9,493	9,679	Shen	734,42	Rómbico	Pnc		8	1987

	T K	*a*	*b*	*c*	*AUTOR*	*G.E.*		Z	año
$Li_2NH_4K(SO_4)_2$	298	18.2140(11)	18.2140(11)	8.6094(8)	Mata	$P6_3$		2	2000
$Li_2NH_4K(SO_4)_2$	483	10.5569(6)	10.5569(6)	8.7128(7)	Mata	$P6_3/mmc$		2	2000
$LiK(NH_2SO_3)_2$	298	5,196 (1)	8,475(1)	8,868(1)	Meinhart	$P2_1$	β=105,05(1)	2	1998
$LiNa(NH_2SO_3)_2$	298	8,631 (1)	8,984(1)	17,386(1)	Meinhart	Pbca		8	1998
$LiK(NH_2SO_3)_2$	293	5,196(1)	8,475(1)	8,868(1)	Meinhart	$P2_1$	β=105,05(1)	2	2001
$LiRb(NH_2SO_3)_2$	293	7,844(1)	9,804(1)	10,825(1)	Meinhart	P-1	α=108,77(1) β=93,29(1) γ=98,64(1)	4	2001
$LiCs(NH_2SO_3)_2$	200	5,535(1)	7,877(1)	9,857(1)	Meinhart	P-1	α=74,07(1), β=76,33(1), γ=87,07(1)	2	2001

	T (K)	a	b	c	Autor	G.E		Z	Año
$Li_6(Mn_3(H_2O)_{12}V_{18}O_{42}(V_{0.5}S_{0.5}O_4))(H_2O)_{24}$	183	15.5378	15.5378	15.5378	Khan	Im3-m		2	1999
$Li_4Rh(SO_3)_3(OH_2)_3OH$		8.077	8.077	13.381	Maeurer	R3h		3	1993
$Na_4Li_4A_{16}Si_6S_{2.05}O_{24}(H_2O)_{.85}$		8.68	8.68	8.68	Podschus	P4-3n		1	1936

Journal of Solid State Chemistry **148,** 316–324 (1999)
Article ID jssc.1999.8453, available online at http://www.idealibrary.com on IDEAL®

Thermal Analysis and X-Ray Diffraction Study on $LiKSO_4$: A New Phase Transition

Xavier Solans,* M. Teresa Calvet,* M. Luisa Martínez-Sarrión,† Lourdes Mestres,† Aniss Bakkali,† Eduardo Bocanegra,‡ Jorge Mata,* and Marta Herraiz†

*Departamento de Cristal.lografia, Mineralogia, i Dipòsits Minerals, Universitat de Barcelona, E-08028-Barcelona, Spain; †Departmento de Química Inorgànica, Universitat de Barcelona, E-08028-Barcelona, Spain; and ‡Departamento de Física Aplicada II, Universidad del Pais Vasco, E-48080-Bilbao, Spain

Received April 19, 1999; in revised form July 13, 1999; accepted July 22, 1999

Results of a detailed X-ray diffraction and thermal analysis study of the structural phase transitions in $LiKSO_4$ carried out in the temperature range 123–1000 K are presented. The study indicates five phase transitions in the temperature range studied at 937, 707, 226 (268), 200 (251), and 186 (190) K (values in parentheses are for a warming process). The transition at 226 (268) K is reported for the first time. The different phases (from high to low temperature) show the space groups $P6_3/mmc$, $P2_1cn$, $P6_3$, $P6_3mc$, $P3_1c$, and $Cmc2_1$. The working conditions allowed us to obtain the different phases without twin crystals and without mixtures of several phases. We were thus able to determine the crystal structures of the different phases with more accuracy. The transitions at high temperature produce large variations in the crystal structure and the enthalpy of process is high, while at low temperature, as the structure is more compact, an activation energy is necessary, and the transitions show a thermal hysteresis, while the structural variation is as small as the enthalpy of the process. © 1999 Academic Press

INTRODUCTION

In recent years, a great number of studies have been reported on the physical properties of, and the phase transitions in, lithium potassium sulfate, $LiKSO_4$. The interest of this compound is due to its pyroelectric, superionic conductivity, ferroelastic and ferroelectric properties, and the discovery of several phase transitions in the temperature range 10 to 950 K. These phase transitions have been studied using a variety of techniques: thermal expansion (1), thermal analysis (2, 3), laser–Raman spectroscopy (4–7), NMR (8), ESR (9–14), electrical and optical studies (15–23), and diffraction (24–31). In general, the conclusions drawn by various authors are contradictory. The phase transitions of $LiKSO_4$ in the range 150 to 1000 K are summarized in Table 1.

In our literature revision, we have observed that some authors worked with twinned crystals, while other authors did not test the quality of crystal and the heating and cooling rates and the sample masses were not specified by them. In order to elucidate and to characterize the phase transition of the title compound, a thermal and X-ray diffraction study has been carried out.

EXPERIMENTAL SECTION

Synthesis

The lithium potassium sulfate was obtained via the reaction of K_2SO_4 with $Li_2SO_4H_2O$ in aqueous solution. The molar ratio between the potassium and lithium sulfates was 1:1.5. The obtained compound was analyzed by ICP (induced condensed plasma) with a Jobin–Yvon analyzer. Crystals were obtained by slow evaporation at 313 K.

Thermal Analysis

The thermal analysis for the temperature range 298–975 K was carried out in a differential thermal analysis (DTA) and thermogravimetry (TG) Netzsch 409. The warming rate was 10 K/min., the weight of the sample, was 101.5 mg, and the reference material was alumina. The sample did not lose weight throughout the process.

The thermal analysis for the temperature range 103–473 K was carried out in a differential scanning calorimeter (DSC) Perkin–Elmer DSC7. The weight of sample was 38.9 mg. The experiment was a cooling process followed by a warming process between the mentioned temperatures with the same cooling and warming rate (10 K/min). The phase transitions and enthalpies of the process are given in Table 2. As a new phase transition was observed at 250 K (Fig. 1), a warming process for the temperature range 200–293 K was carried out at different warming rates (5 and 2 K/min).

0022-4596/99 $30.00

TABLE 1
Phase Transitions of $LiKSO_4$ in the Range 150–1000 K, According to the References

Phase I:	Space groups: $Cmc2_1$, $P6_3$, Cc, $P6_3mc$	
	Physical prop.: ferroelastic, ferroelectric	
Transition I:	Temperature: 178–203 K	Thermal hysteresis: 0–32 K
Phase II:	Space groups: Incomensurate, $P3_1c$, $P6_3mc$	
	Physical prop.: ferroelectric, paraelastic	
Transition II:	Temperature: 200–210 K (cooling) 248–265 (heating)	Thermal hysteresis: 35–55 K
Phase IV:	Space groups: $P6_3$, $P2_1$	
	Physical prop.: paraelectric	
Transition IV:	Temperature: 708 K	Thermal hysteresis: 0 K
Phase V:	Space groups: $P2_1cn$, Incomensurate	
Transition V:	Temperature 941 K	Thermal hysteresis: 0 K
Phase VI:	Space groups: $P6_3mc$, $P6_3/mmc$	
(989 K pass to melt)		

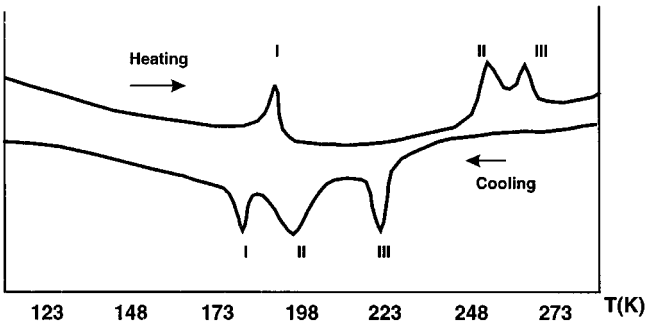

FIG. 1. The thermal analysis data of the low temperature phase transitions for the warming and cooling process.

X-Ray Powder Diffraction

Powder diffraction data in the range 298–968 K were collected using the Bragg–Brentano geometry with a Siemens D500 automated diffractometer, using Cu$K\alpha$ radiation and a secondary monochromator. The experiment was a warming process from 298 to 968 K, followed by a cooling process between the same temperatures with the same sample. The cooling and warming rates were 10 K/min, and the sample was left for 10 min at the measuring temperature in order to stabilize the equipment and the sample. Measurements were taken at 298, 473, 673–718 (every 5 K), 873, and 923–953 K (every 5 K) and at the same temperatures in the cooling process. The step size was 0.025°, the time of step 10 sec, and the 2θ range was 16–120°.

Powder diffraction data in the 163–298 K range were collected using Debye–Sherrer geometry, a 120° arch detector INEL, and the sample in a rotating capillary to diminish preferred orientation. The radiation was Cu$K\alpha$, using a primary planar quartz monochromator. The time of exposure was defined giving a minimum count for the highest reflection (about 1 h). All processes were followed with the same sample, first a cooling process with a cooling rate of 10 K/min, after which the sample was left for 10 min at the measuring temperature in order to stabilize the sample and the equipment, and a warming process at the same conditions and temperatures. The measurements were taken at 163–208 (every 5 K), 223, and 243–298 (every 5 K). Cell parameters (Fig. 2) from powder diffraction were determined using the TREOR (32) computer program and refined with the CELREF computer program (33).

TABLE 2
Onset Temperatures (K) and Enthalpies of the Phase Transitions Obtained from Thermal Analysis

Phase transition	T (H)	T (C)	ΔH
I	190	186	46 J mol^{-1}
II	251	200	33 J mol^{-1}
III	268	226	9 J mol^{-1}
IV	707	707	5 kJ mol^{-1}
V	937	937	1 kJ mol^{-1}

Note. H, heating, C, cooling.

X-Ray Structure Determination

A similar method was followed in all single-crystal structure determinations, using the same crystal. The intensities were measured at 298, 233, 189, 123, and 260 K. All phases were measured after cooling, with the exception of phase III (the new phase) which was measured after warming. Diffraction data were collected on an Enraf–Nonius CAD4 automated diffractometer equipped with a graphite monochromator. The ω–θ scan technique was used to record the intensities. Scan widths were calculated as $A + B \tan\theta$, where A is estimated from the mosaicity of the crystal and B allows for the increase in peak width due to Mo$K\alpha_1$–$K\alpha_2$ splitting.

Details of the structure determination are listed in Table 3. The unit-cell parameters were obtained by a least-squares fit to the automatically centered settings from 25 reflections ($12° < 2\theta < 21°$). The intensities from three control reflections for each measurement showed no significant fluctuation during the data collection.

The structures were solved by Patterson synthesis, using SHELXS-86 computer program (34) and refined by the full-matrix least-squares method, using the SHELXL-93 computer program (35). The function minimized was $w||F_o|^2-|F_c|^2|^2$, where the weighting scheme was $w = [\sigma^2(I) + (k_1P)^2 + k_2P]^{-1}$ and $P = (|F_o|^2 + 2\ |F_c|^2)/3$. The

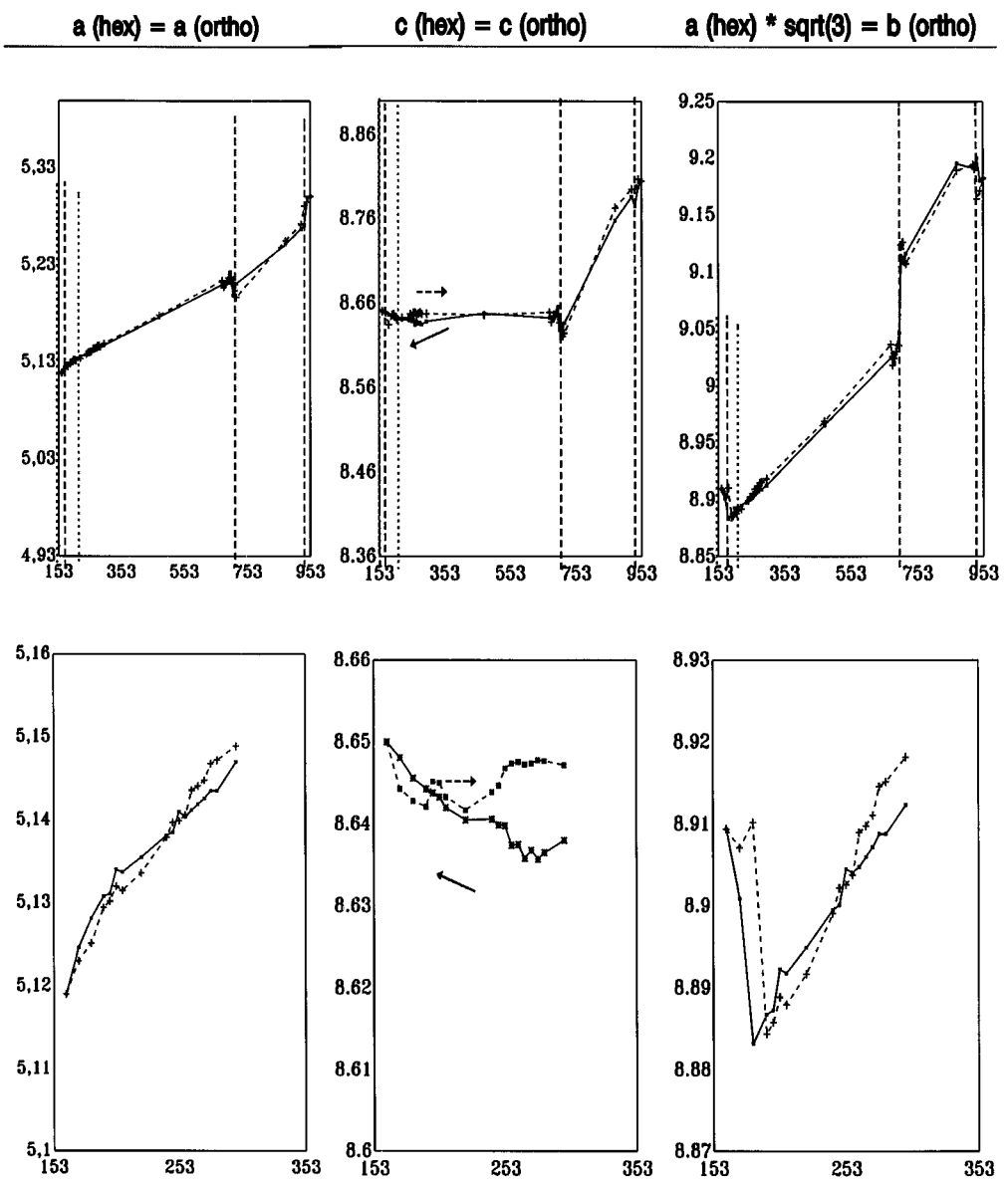

FIG. 2. Cell-parameters versus temperature, obtained from X-ray diffraction on powder samples. In the bottom the sector at low temperature is shown with a more appropriate scale.

values of k_1 and k_2 were also refined. The chirality of the structure was defined from the Flack coefficient (36).

Structures at 773 and 973 K were determined from a powder sample. Diffraction data were recorded with the Siemens D-500 diffractometer. The step of scan was 0.025° and the time of the step was 10 s. The structures were solved by direct methods using the SIRPOW computer program (37) and refined using the FULLPROF computer program (38). The Li position in both structures was constrained to be in the center of its tetrahedron, O positions in the structure at 773 K were constrained to have the same S–O bond length. The intensity statistic at 773 K shows that the space group is $P2_1cn$, while that at 973 K is $P6_3/mmc$, which was confirmed with the refinement. Details of the refinement are given in Table 4. The chirality of structure at 773 K was defined from the results at low temperature. Final atomic coordinates are given in Table 5. Figures 3 and 4 shows two projections of the cell content.

RESULTS AND DISCUSSION

The results of DTA, DSC, and TG analyses (Table 2) show that the $LiKSO_4$ underwent five phase transitions in the temperature range studied (103–975 K). Four of them

TABLE 3
Crystal Data and Structure Refinement for Structure Determined by Single-Crystal Diffractometry

	For all structures				
Empirical formula	$KLiSO_4$				
Formula weight	142.10				
Wavelength (Å)	0.71069				
Crystal size (mm)	$0.3 \times 0.2 \times 0.2$				
Theta range for data collection	4.58 to 29.89°				
Refinement method	Full-matrix least-squares on F^2				
Temperature (K)	298(1)	233(1)	189(1)	260(1)	123(1)
Crystal system	Hexagonal	Hexagonal	Trigonal	Hexagonal	Orthorhombic
Space group	$P6_3$	$P6_3$	$P3_1c$	$P6_3mc$	$Cmc2_1$
a (Å)	5.1421(11)	5.1341(12)	5.117(2)	5.123(2)	5.114(2)
b (Å)	5.1421(11)	5.1341(12)	5.117(2)	5.123(2)	8.857(3)
c (Å)	8.634((2)	8.638(3)	8.638(6)	8.639(3)	8.630(3)
Volume (Å^3)	197.71(8)	197.18(9)	195.9(2)	196.38(11)	390.9(2)
Z	2	2	2	2	4
Dx (Mg/m^3)	2.387	2.393	2.409	2.403	2.415
μ (mm^{-1})	1.734	1.739	1.750	1.746	1.754
$F(000)$	140	140	140	140	280
Index ranges	$-6 \le h \le 7$ $-6 \le k \le 7$ $0 \le l \le 12$	$-6 \le h \le 7$ $-6 \le k \le 7$ $0 \le l \le 12$	$-6 \le h \le 7$ $-6 \le k \le 7$ $0 \le l \le 12$	$-6 \le h \le 7$ $-6 \le k \le 7$ $0 \le l \le 12$	$0 \le h \le 7$ $0 \le k \le 12$ $0 \le l \le 12$
Reflections collected	660	660	660	660	310
Independent refl.	205	206	205	136	310
R (int)	0.012	0.010	0.045	0.034	–
Data/parameters	200/23	199/23	203/23	133/23	310/53
S (F^2)	0.862	0.971	1.040	1.034	1.149
Final $R(F)$	0.029	0.025	0.073	0.051	0.054
Final w$R(F^2)$	0.071	0.079	0.188	0.135	0.128
Flack parameter	0.2(2)	0.10(11)	0.9(4)	0.2(4)	0.1(3)
Extinction coeff.	3.4(2)	0.69(3)	0.00(5)	0.56(12)	0.00(1)
Largest diff. syn. peak (e.Å^{-3})	0.323	0.309	0.509	0.518	0.497
hole (e.Å^{-3})	−0.433	−0.345	−0.577	−0.331	−0.419

had been described previously. The transitions at 226 (in the cooling process) and 268 K (in the warming process) are reported for the first time. The results obtained for transitions II and III at different warming rates are: rate 10 K/min, transition temperatures 251 and 268 K; 5 K/min, 250 and 267 K; and 2 K/min, 251 and 267 K. This shows that the thermal effect is independent of kinetics, as is the existence of the phase transition. The ΔH of the IV phase transition is close to the value obtained for the transition of K_2BeF_4 (39) at 913 K (5 kJ mol^{-1}) and higher than those obtained for $(NH_4)_2SO_4$ (40) at 223 K (3.9 kJ mol^{-1}). The ΔH of the V transition is close to the value obtained (1.3 kJ/mol) for the transition of $(NH_4)_2BeF_4$ at 176 K (40). The ΔH of the transitions at low temperature are higher than those obtained for the transition at 93 K of K_2SeO_4 (41) (2 J/mol). The transitions at low temperature show thermal hysteresis.

Cell parameters were refined using all identified maxima in the powder patterns. Peaks of two phases are observed from 928 to 948 K. The space groups of different phases according to systematic absences are $Cmc2_1$ for phase I, $P3_1c$ for phase II, $P6_3mc$ or $P6_3/mmc$ for phase III, $P6_3$ for phase IV, $P2_1cn$ for phase V, and $P6_3mc$ or $P6_3mmc$ for phase VI. Phase transition III is not clear from powder diffraction, but an anomalous behavior in the cell parameters (Fig. 2) and the modification of the intensity of some reflections were observed. The highest variation in cell parameters was observed in transitions I and IV with a major increase of the b_{ortho} cell parameter.

We have solved the crystal structures at 298, 260, 233, 189, and 123 K without using a twin crystal. This has not been made and reported previously. The crystal structure at 189 K was poorly resolved, which may be because the measuring temperature is close to a transition temperature in this crystal. This was not due to the quality of the crystal, because in the following measurements the results were correct. The space groups of the $LiKSO_4$ phases are $P3_1c$ for phase II, $P6_3mc$ for phase III, and $P6_3$ for phase IV.

The crystal structure at 973 K (phase VI) can be described as a hexagonal close packing of sulfate tetrahedra, with the

TABLE 4
Crystal Data and Structure Refinement for Structures Determined by Powder Diffractometry

Empirical formula	$LiKSO_4$	$LiKSO_4$
Formula weight	142.10	142.10
Temperature (K)	773	973
Crystal system	orthorhombic	hexagonal
Space group	$P2_1cn$	$P6_3/mmc$
a (Å)	5.2150(3)	5.2997(3)
b (Å)	9.1321	5.2997(3)
c (Å)	8.6652(4)	8.8021(6)
Volume (Å^3)	412.7(2)	214.10(4)
Z	4	2
ρ(calculated) (Mg/m^3)	2.286	2.204
μ (mm^{-1})	1.624	1.565
$F(000)$	280	140
θ range (•)	15–100	15–100
No. of data	3401	3389
Refl. collected	484	116
Refined parameters	30	20
R_{wp}	7.4	6.11
R_B	12.9	9.1
S	5.3	8.47
DWD	1.91	1.90

Note. $R_{wp} = 100 \times \{\sum w_i(y_i - y_{0i})^2/\sum w_i y_i^2\}^{1/2}$. $R_B = 100 \sum \bullet I_o - I_c \bullet / \sum I_o$. S = Goodness of fit = $R_{wp}/R_{expected}$. DWD = weighted Durbin–Watson statistic D.

K ions occupying the octahedral sites (every K ion is surrounded by six sulfate ions) and the Li ions occupying the tetrahedral sites. This produces a framework of corner-shared LiO_4 and SO_4 tetrahedra with K filling the cavities within the framework. The K ion displays a tricapped trigonal prism coordination with respect to oxygen atoms.

The shrinking of the K^+ cavity produces phase V. The sulfate ion rotates 20° around the c-axis and 25° around an axis perpendicular to it, which leads to the structure at 773 K. These rotations produce a large cavity for the Li^+ ion. This fact was suggested by Pimenta *et al.* (19) from infrared reflectivity. The sulfate ion rotates $-38°$ around the c-axis and $-25°$ around an axis perpendicular to it, which leads to the structure at 298 K (phase IV). In this structure the S and Li tetrahedra are distorted in such a way that the O(2)–X–O(2) angle is larger than the O(2)–X–O(1) angle.

Phase IV was measured at two different temperatures (298 and 233 K). The differences between these two structures are the rotation of $-2°$ of the sulfate ion when the temperature falls and the shortening of K–O(2) length (from 2.836(3) to 2.826(2) Å). The structure at 189 K (phase II) is a reorganization of the tetrahedral framework of the structure at 298 K. The sulfate ion rotates 56° around the c-axis, which reduces the K–O(2) stress. The structure at 260 K (phase III) is intermediate between those of phases II and IV and it is the typical twin phase shown by compounds with a high number of phase transitions. This suggests that phase III would not be detected if the conditions of analysis were more extreme than those reported here. The last phase, at 123 K, is a new disordered structure, where the sulfate ion rotates 4° or $-57°$ around the c-axis, depending of the assumed disorder position.

We have studied the stability of the structure from the bond-valence model and the distortion theorem described by Brown (42). At 973 K the K^+ ion occupies a large cavity which produces the instability of the structure. At 773 K the

TABLE 5
Atomic Coordinates ($\times 10^4$ .S,O, and Li atoms at 973 and 773 K$\times 10^3$)

		x	y	z
973 K	S	667	333	250
	K	0	0	0
	Li	667	333	615(8)
	O(1)	667	333	82(4)
	O(2)	515(8)	1030(8)	305(4)
773 K	S	707(6)	80(2)	777(1)
	K	2357	2031(8)	4956(10)
	Li	707(31)	387(10)	679(8)
	O(1)	435(7)	52(4)	745(4)
	O(2)	849(8)	−58(3)	773(4)
	O(3)	734(8)	147(2)	930(2)
	O(4)	810(7)	179(4)	660(3)
298 K	S	3333	6667	9007(2)
	K	10000	10000	11938(1)
	Li	3333	6667	5134(12)
	O(1)	3333	6667	7310(7)
	O(2)	5979(5)	9425(5)	9538(4)
233 K	S	3333	6667	9003(1)
	K	10000	10000	11939(1)
	Li	3333	6667	5134(9)
	O(1)	3333	6667	7321(4)
	O(2)	5991(4)	9422(4)	9546(3)
189 K	S	3333	6667	8863(3)
	K	10000	0	11831(3)
	Li	3333	6667	5113(26)
	O(1)	3333	6667	7300(36)
	O(2)	3567(26)	9495(48)	9246(14)
260 K	S	3333	6667	8873(3)
	K	10000	0	11815(3)
	Li	3333	6667	5008(27)
	O(1)	3333	6667	7167(14)
	O(2)	6014(21)	9447(20)	9419(10)
123 K	S	0	1667(2)	2375(3)
	K	0	4994(2)	315(2)
	O(1)	0	1579(11)	674(11)
	O(2)	−2838(26)	1726(11)	2897(16)
	O(3)	1476(30)	3064(13)	2848(18)
	O(4)	−1307(21)	332(10)	2982(13)
	Li	0	1870(23)	−1484(24)

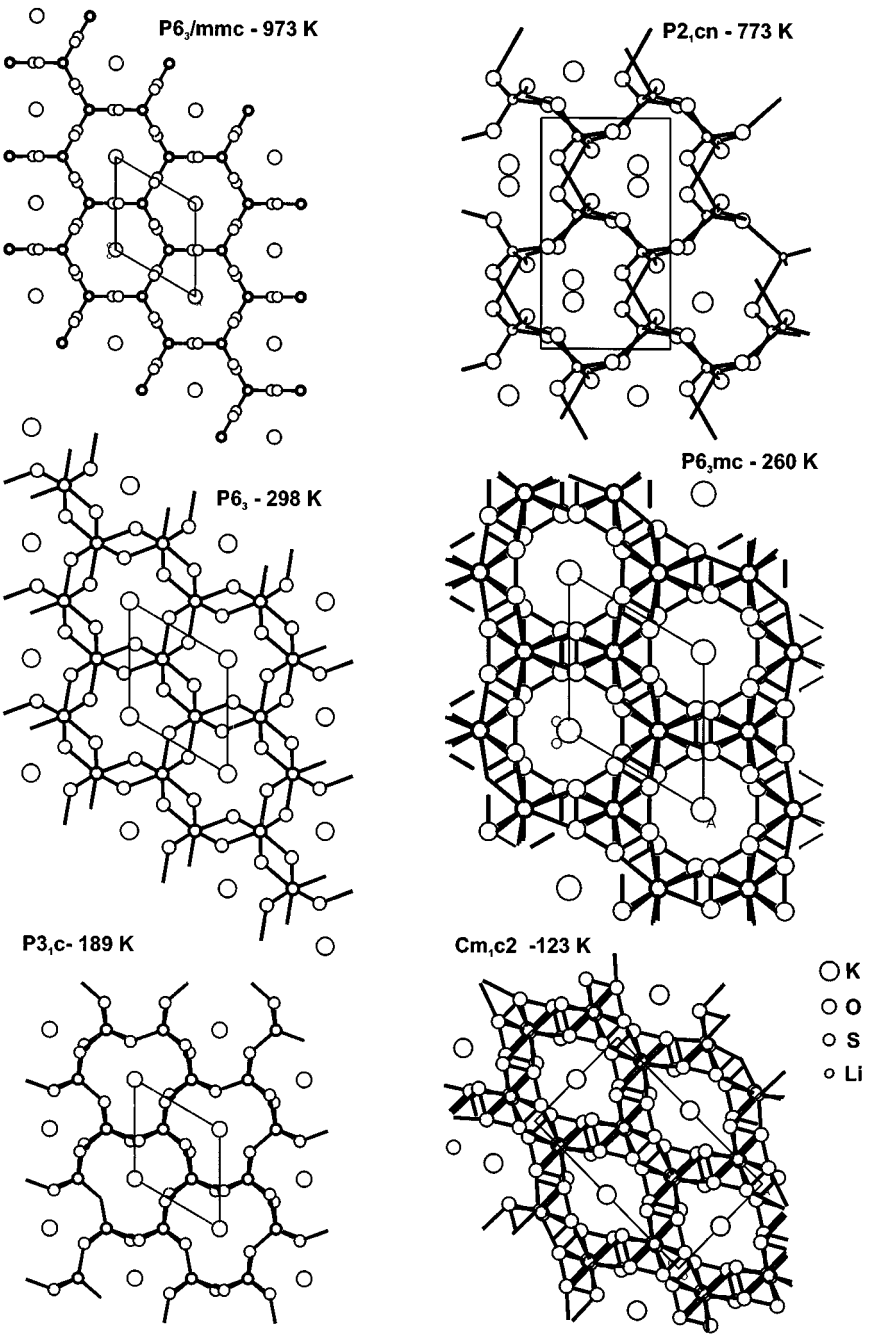

FIG. 3. Unit cell content of the different phases of $LiKSO_4$ viewed down the *c*-axis.

stress of the structure is in the K–O(4) bond, while the Li^+ ion occupies a larger cavity (sum of the bond valence 1.02 for K and 0.86 for Li ions). From 298 to 123 K the site driving the instability is the K ion which occupies the more asymmetric cavity (see Table 6).

It is important to note that the two disordered structures (phases III and I) have an average symmetry $P6_3mc$ and $Cmc2_1$. The local symmetry of these two phase is $P6_3$ and Cc, respectively, which may explain why the first was not observed and why the second gives conflicting results when the spectroscopic technique was used.

CONCLUSIONS

We have structurally characterized the six phases of $LiKSO_4$ in the temperature range 150–1000 K. The

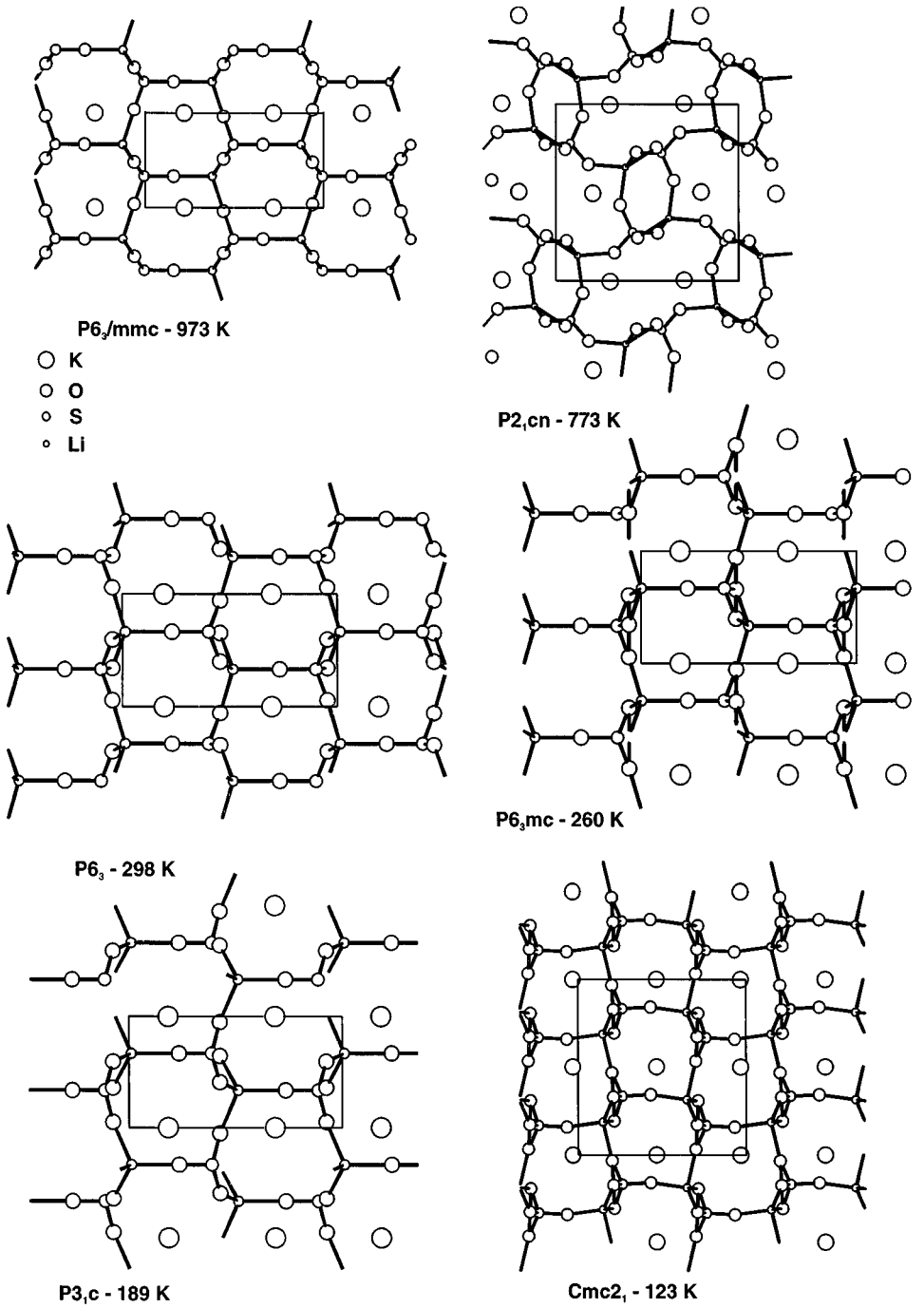

FIG. 4. Unit cell content of the different phases viewed parallel to the (010) plane.

working conditions allowed us to obtain the different phases without twin crystals and without mixtures of several phases; this has led to determination of the crystal structures of the different phases with greater accuracy. The framework of corner-shared LiO_4 and SO_4 tetrahedra is relatively flexible, shown by the large number of phases. The transition between phases, V and VI is order–disorder or displacive if phase VI is assumed to be multiple domains of $P6_3mc$ symmetry, giving an average structure of $P6_3/mmc$ symmetry. The second explanation would be to agree with those authors who assigned this space group to phase VI. The remaining transitions are displacive, except those to

TABLE 6
Bond Lengths [Å] and Angles [•]

	973 K	773 K	298 K	233 K	189 K	260 K	123 K
S–O	1.47(4) × 4	1.46(4) 1.46(4) 1.47(5) 1.47(2)	1.464(3) × 3 1.465(6) × 1	1.467(2) × 3 1.453(4) × 1	1.43(2) × 3 1.35(3) × 1	1.477(9) × 3 1.474(13) × 1	1.521(14) 1.470(10) 1.456(8) 1.506(14)
K–O	3.144(8) × 3 3.16(4) × 6	2.65(3) 2.74(3) 2.74(4) 2.99(4) 3.01(4) 3.02(3) 3.29(4) 3.32(4) 3.50(4)	2.836(3) × 3 2.965(3) × 3 2.9861(9) × 3	2.826(2) × 3 2.964(2) × 3 2.9824(8) × 3	2.867(14) × 3 2.976(12) × 3 2.982(5) × 3	2.821(8) × 3 2.955(9) × 3 2.974(2) × 3	2.923(12) × 1 2.810(12) × 1 2.934(5) × 1 2.776(10) × 2 2.839(14) × 2 2.876(14) × 2
Li–O	1.84(4) × 1 1.77(5) × 3	1.98(10) 1.99(16) 2.02(12) 2.18(17)	1.878(10) × 1 1.928(4) × 3	1.889(7) × 1 1.927(3) × 3	1.89(4) × 1 1.95(2) × 3	1.86(2) × 1 1.915(10) × 3	1.88(2) 1.75(2) 1.89(2) 2.11(2)
O–S–O	109.2(14) × 3 109.7(14) × 3	109(2) 109(3) 109(2) 110(2) 110(2) 110(3)	110.6(2) × 3 108.3(2) × 3	110.28(9) × 3 108.65(9) × 3	103.4(5) × 3 114.8(4) × 3	110.3(3) × 3 108.6(4) × 3	108.4(6) 109.9(7) 108.3(7) 111.0(6) 107.3(5) 111.7(8)

pass to phases III and I, where we did not elucidate the domain of each disordered site. However, the disordered phases are at low temperature, so thermodynamic reasons suggest that these phases have multiple domains of $P6_3$ and Cc symmetry and the phase transitions are also displacive. The conclusion of multiple domains for phase I agrees with the crystal optical studies of Kleemann, Schäfer, and Chaves (21) who observed the formation of domains for this phase.

The phase transitions at high temperature produce large variations in the crystal structure; the enthalpy of the process is high and the transitions do not shown thermal hysteresis. A hysteresis of 3 K was only observed at the phase transition IV by electrical conductivity measurements (19), but it is not observed by IR reflection spectra. Brillouin scattering (19), powder diffraction, thermal analysis (this work), or linear bi-refrigence (21). At low temperature, as the structure is more compact (the c-parameter remains practically constant, Fig. 2), an activation energy is necessary and the transitions show thermal hysteresis, while the structural variation is as small as the enthalpy of the process.

REFERENCES

1. D. P. Sharma, *Pramana*, **13,** 223 (1979).
2. I. M. Iskornev, I. N. Flerov, M. V. Gorev, L. A. Kot, and V. A. Grankina, *Soviet Phys.: Solid State* **26,** 1926 (1984).
3. L. Abello, K. Chhor, and C. Pommier, *J. Chem. Thermodynam.* **17,** 1023 (1985).
4. M. L. Bansal, S. K. Deb, A. P. Roy, and V. C. Sahni, *Solid State Commun.* **36,** 1047 (1980).
5. J. Mendes-Filho, J. E. Moreira, F. E. A. Melo, F. A. Germano, and A. S. B. Sombra, *Solid State Commun.* **60,** 189 (1986).
6. A. J. Oliveira, F. A. Germano, J. Mendes-Filho, F. E. A. Melo, and J. E. Moreira, *Phys. Rev. B* **38,** 12633 (1988).
7. F. Ganot, B. Kihal, R. Farhi, and P. Moch, *Jap. J. Appl. Phys.* **24,** 491 (1985).
8. B. Topic, U. Haeberlen and R. Blinc, *J. Phys. B-Condens. Matter* **70,** 95 (1988).
9. F. Holuj and M. Drozdowski, *Ferroelectrics* **36,** 379 (1981).
10. T. Shibata, R. Abe, and M. Fukui, *J. Phys. Soc. Japan* **55,** 2088 (1986).
11. J. T. Yu and S. Y. Chou, *J. Phys. Chem. Solids* **47,** 1171 (1986).
12. J. T. Yu, J. M. Kou, S. J. Huang, and L. S. Co, *J. Phys. Chem. Solids* **47,** 121 (1986).
13. K. Murthy, U. Ramesh, and S. V. Bhat, *J. Phys. Chem. Solids* **47,** 927 (1986).
14. K. Maezawa, T. Takeuchi, and K. Ohi, *J. Phys. Soc. Japan* **54,** 3106 (1985).
15. S. Fujimoto, N. Yasuda, H. Hibino, and P. S. Narayanan, *J. Phys. D: Appl. Phys.* **17,** L35 (1984).
16. B. Mroz, T. Krajewski, T. Breczewski, W. Chomka, and D. Sematowicz, *Ferroelectrics* **42,** 71 (1982).
17. T. Krajewski, T. Breczewski, M. Kassem, and B. Mroz, *Ferroelectrics* **55,** 143 (1984).
18. G. Sorge and H. Hempel, *Phys. Stat. Solidi A* **97,** 431 (1986).
19. M. A. Pimenta, P. Echegut, Y. Luspin, G. Hauret, F. Gervais, and P. Abèlard, *Phys. Rev. B* **39,** 3361 (1989).

20. T. Breczewski, T. Krajewski, and B. Mroz, *Ferroelectrics* **33,** 9 (1981).
21. W. Kleemann, F. J. Schäfer, and A. S. Chaves, *Solid State Commun.* **64,** 1001 (1987).
22. J. Ortega, T. Eyxebarría, and T. Breczewski, *J. Appl. Cryst*. **26,** 549 (1993).
23. K. Staduicka, A. M. Glazer, and S. Arzt, *J. Appl. Cryst*. **26,** 555 (1993).
24. P. E. Tomaszewski and K. Lukaszewicz, *Phase Transitions* **4,** 37 (1983).
25. R. H. Chen and R. T. Wu, *J. Phys. Condens. Matter* **1,** 6913 (1989).
26. S. Bhakay-Tamhane, A. Sequeira, and R. Chidambaram, *Acta Cryst*. *C* **40,** 1648 (1984).
27. S. Bhakay-Tamhane and A. Sequeira, *Ferroelectrics* **69,** 241 (1986).
28. A. M. Balagurov, B. Mroz, N. C. Popa, and B. N. Savenko, *Phys. Stat*. *Sol*., *A* **96,** 25 (1986).
29. S. Bhakay-Tamhane, A. Sequeira, and R. Chidambram, *Phase Transition* **35,** 75 (1991).
30. Y. Y. Li, *Solid State Commun.* **51,** 355 (1984).
31. H. Schulz, U. Zucker, and R. Frech, *Acta Cryst*., *B* **41,** 21 (1985).
32. P. E. Werner, "TREOR, Trial and error program for indexin of unknown powder patterns," University of Stockholm, Sweden, 1984.
33. J. Laugier and A. Filhol, "Programme CELREF, ILL," Grenoble, France, 1978.
34. G. M. Sheldrick, *Acta Cryst*. *A* **46,** 467 (1990).
35. G. M. Sheldrick, "SHELXL, A computer program for crystal structure determination." Univ. Göttingen, Germany, 1993.
36. H. D. Flack, *Acta Cryst*. *A* **39,** 867 (1983).
37. A. Altomare, G. Cascarano, C. Giacovazzo, A. Guagliardi, M. C. Burla, G. Polidori, and M. Camalli, "SIRPOW, Instituto di Ricerca per lo Svilupp di Metodologie Cristallografiche," Universita di Bari, Italy, 1992.
38. J. Rodríguez-Carvajal, "FULLPROF," Version 3.1c. Laboratoire Leon Brillouin, Paris, France, 1996.
39. X. Solans, C. González-Silgo, M. T. Calvet, C. Ruiz-Pérez, M. L. Martínez-Sarrión, and L. Mestres, *Phys. Rev. B* **57,** 5122 (1998).
40. S. Hoshino, K. Vedam, Y. Okaya, and R. Pepinsky, *Phys. Rev*. **112,** 405 (1958).
41. K. Aiki, K. Hukuda, H. Kaga, and T. Kobayashi, *J. Phys. Soc. Jpn.* **28,** 389 (1970).
42. I. D. Brown, *Acta Cryst*., *B* **48,** 553 (1992).

J. Phys.: Condens. Matter **11** (1999) 8995–9007. Printed in the UK PII: S0953-8984(99)03914-4

X-ray structural characterization, Raman and thermal analysis of $LiNH_4SO_4$ above room temperature

Xavier Solans, Jorge Mata, M Teresa Calvet and Mercè Font-Bardia

Departament Cristallografia, Mineralogia i Dipòsits Minerals, Universitat de Barcelona, E-08028-Barcelona, Spain

Received 4 May 1999, in final form 8 September 1999

Abstract. Results are presented of a detailed x-ray diffraction, Raman and thermal analysis study of the structural phase transitions in $LiNH_4SO_4$ carried out in the temperature range 298–600 K. Either two or just one phase transition was recorded in the temperature range between 335 and 461 K, depending on the warming process rate. Crystal structures at 298, 318, 383, 423 and 483 K during a slow warming process and at 298 and 523 K during a fast warming process were solved. The transition at 335 K is reported for the first time and consists of a rotation by 41° of the sulphate ion around an S–O bond. The new obtained phase above 335 K is close to the enantiomeric phase at room temperature. The high temperature phase crystallized in the non-polar $P2_1nb$ space group, but the crystal structure obtained removed the spontaneous polarization, according to the calculations made using an ionic model, and agrees with the experimental results.

1. Introduction

The phase transition sequence displayed by $LiNH_4SO_4$ (LAS) above room temperature has been extensively studied in recent years but a definitive picture has yet to be obtained. Interest in this compound is derived from its ferroelastic and ferroelectric properties and the identification of several phase transitions in the temperature range 10 to 615 K. According to the literature [1–3] the paraelectric phase at high temperature (phase I) undergoes a phase transition at 460 K to the ferroelectric phase II which in turn undergoes a transition to ferroelastic phase III at 285 K. Dollase [4] determined the structure at room temperature as being orthorhombic, with the space group $P2_1nb$ and four formulae in the unit cell. This structure was subsequently refined by Mashiyama and Kasano [5]. Itoh *et al* [2] solved the structure of the paraelectric phase at 478 K. It is also orthorhombic, with the space group *Pmnb*. Polomska *et al* [6] observed a DTA maximum at about 350 K, which was related to an irreversible transformation from phase I to phase II. Torgashev *et al* [7] observed an anomalous behaviour of Raman spectra at high temperatures (above 460 K) when the space group was assigned as *Pmnb* and they accounted for this by indicating the presence of orientational disorder in the *Pmnb* phase. Here, in order to elucidate and to characterize the phase transition of LAS, a thermal, Raman and x-ray diffraction study was carried out.

0953-8984/99/468995+13$30.00

Table 1. Crystal data and structure refinement for $LiNH_4SO_4$ at different temperatures.

Data for all structures						
Empirical formula	$LiNH_4SO_4$					
Formula weight	121.04					
Wavelength (Å)	0.710 69					
Crystal system, space group	orthorhombic, $P2_1nb$					
Z	4					
$F(000)$	248					
Crystal size (mm)	$0.2 \times 0.2 \times 0.4$					
θ range (°) for data collection	3.22 to 29.96					
Index ranges	$0 \leqslant h \leqslant 7, 0 \leqslant k \leqslant 12, 0 \leqslant l \leqslant 12$					
	Phase II	Phase II + II′	Phase II + II′	Phase II′	Phase I′	Phase I
Temperature (K)	298.0(2)	318.0(2)	383.0(2)	423.0(2)	483.0(2)	523.0(2)
a (Å)	5.276(4)	5.279(3)	5.302(6)	5.304(4)	5.304(3)	5.292(9)
b (Å)	8.768(3)	8.775(3)	8.780(2)	8.782(2)	8.774(2)	8.769(7)
c (Å)	9.122(2)	9.122(2)	9.140(2)	9.1466(14)	9.1661(11)	9.198(3)
Volume (Å^3)	422.0(4)	422.6(3)	425.5(5)	426.0(3)	426.6(3)	426.8(8)
ρ (Mg m^{-3})	1.905	1.903	1.890	1.887	1.885	1.884
μ (mm^{-1})	0.651	0.650	0.645	0.644	0.644	0.643
Reflec. collected/unique	654/654	1296/669	698/651	668/668	668/662	659/659
Completeness to 2θ	96.7%	98.7%	95.4%	97.4%	96.6%	96.1%
Data/parameters	654/77	660/78	651/82	668/80	662/80	659/77
S	1.122	1.078	1.142	1.188	1.095	1.101
R_1 index (all data)	0.0376	0.0364	0.0439	0.0494	0.0500	0.0783
wR_2 index (all data)	0.1144	0.1008	0.1046	0.1166	0.1225	0.2172
Flack parameter	0.1(3)	0.0(2)	0.0(5)	0.0(3)	−0.3(4)	0.6(6)
Phase II/(Phase II + II′) rate	1.00	0.874	0.118	0.00	—	—
Extinction coefficient	0.002(9)	0.04(8)	0.99(9)	0.61(7)	0.45(5)	0.14(4)
Largest diff. peak (e Å^{-3})	0.613	0.451	0.455	0.672	0.844	1.220

2. Experimental section

2.1. Synthesis and crystallization

The LAS was obtained via the reaction of $(NH_4)_2SO_4$ with $Li_2SO_4.H_2O$ in aqueous solution at 333 K. The molar ratio between the ammonium and lithium sulphates was 1:1, 1.5:1 and 2:1. Crystals were grown by slow evaporation at 333 K. An increase in the ammonium ratio decreased the growth velocity. The best phase II crystals were obtained with the ratio 1.5:1. The compound obtained was analysed by ICP (induced condensed plasma) with a Jobin–Yvon analyser and x-ray powder diffraction.

2.2. Thermal analysis

The thermal analysis for the temperature range 293–600 K was carried out in a differential scanning calorimeter (DSC) Perkin–Elmer DSC-7. The warming rate was 5 K min^{-1} and 20 K min^{-1} and the sample weight was 12.66 mg.

2.3. X-ray structure determination

A similar method was followed in all single-crystal structure determinations, where the same crystal was used in all measurements. The intensities were measured at the constant temperatures of 298, 318, 383, 423 and 483 K, applying a warming rate of 5 K min^{-1}. The crystal was cooled to 298 K and intensity data were recorded. Subsequently, the crystal was warmed at a faster rate (20 K min^{-1} rate) at and the intensity data were recorded at 523 K. Diffraction data were collected on an Enraf–Nonius CAD4 automated diffractometer equipped with a graphite monochromator. The ω–2θ scan technique was used to record the intensities. Scan widths were calculated as $A + B\tan\theta$, where A is estimated from the mosaicity of the crystal and B allows for the increase in peak width due to Mo Kα_1–Kα_2 splitting.

Table 2. Equivalent isotropic displacement parameters (Å$^2 \times 10^3$) at different temperatures, which are compared with the values at 478 K obtained by Itoh *et al* [2] (* = atoms with an occupancy factor equal to 0.5). U(eq) is defined as one third of the trace of the orthogonalized U_{ij} tensor.

	$T = 298.0$ K	$T = 318.0$ K	$T = 383.0$ K	$T = 423.0$ K	$T = 483.0$ K	$T = 523.0$ K	$T = 478.0$ K
S	22(1)	17(1)	20(1)	22(1)	25(1)	34(1)	34(1)
O(1)	41(1)	63(1)	73(1)	80(2)	97(2)	114(4)	126 (3)*
O(2)	39(1)	47(1)	57(1)	63(1)	76(1)	98(3)	76(1)*
O(3)	33(1)	37(1)	40(1)	44(1)	51(1)	82(3)	111(2)*
O(4)	31(1)	33(1)	45(1)	49(1)	59(1)	71(2)	67(1)*
N	26(1)	29(1)	35(1)	38(1)	43(1)	52(1)	54(1)
Li	18(1)	23(1)	27(1)	30(1)	33(1)	42(2)	44(1)

Details of structure determination are listed in table 1. The unit-cell parameters were obtained by a least-squares fit to the automatically centred settings from 25 reflections ($12^\circ < 2\theta < 21^\circ$). The intensities from three control reflections for each measurement showed no significant fluctuation during data collection.

The structures were solved by direct methods, using the SHELXS-97 computer program [8] and refined by the full-matrix least-squares method, using the SHELXL-97 computer program [9]. The function minimized was $w||F_0|^2 - |F_c|^2|^2$, where the weighting scheme was $w = [\sigma^2(I) + (k_1P)^2 + k_2P]^{-1}$ and $P = (|F_0|^2 + 2|F_c|^2)/3$. The values of k_1 and k_2 were also refined. The chirality of the structure was defined from the Flack coefficient [10].

Refinements assuming the possible mixture of different phases were carried out on all intensity data collected. The crystal structures at 483 and 523 K were solved by direct methods in both space groups $P2_1nb$ and *Pmnb*. The positions of all non-hydrogen atoms were obtained using the $P2_1nb$ space group, though the structure was not solved when the *Pmnb* space group was used. Refinements were made to these structures in both space groups, using the average positions obtained in the non-centrosymmetric group for the centrosymmetric space group and assuming the oxygen and hydrogen atoms to lie in disorder sites. The results obtained with the *Pmnb* group were in agreement with those obtained by Itoh *et al* [2], with larger equivalent isotropic thermal parameters for disorder atoms with an occupancy factor equal to 0.5 (table 2). Refinements assuming the contribution to intensity as coming partially from the non-centrosymmetric coordinates and partially from those equivalent by a mirror plane to the previous values (as if the crystal were a twin crystal) did not converge at 523 K and gave a contribution equal to 100% for the assumed enantiomer at 483 K. The lower R value, lower density in the maximum peak in the final difference map and the lower Flack parameter indicate that the correct solution at 483 and 523 K is obtained by using the non-polar group. The poorer results obtained at 523 K can be explained by defective growth produced by the dilatation and

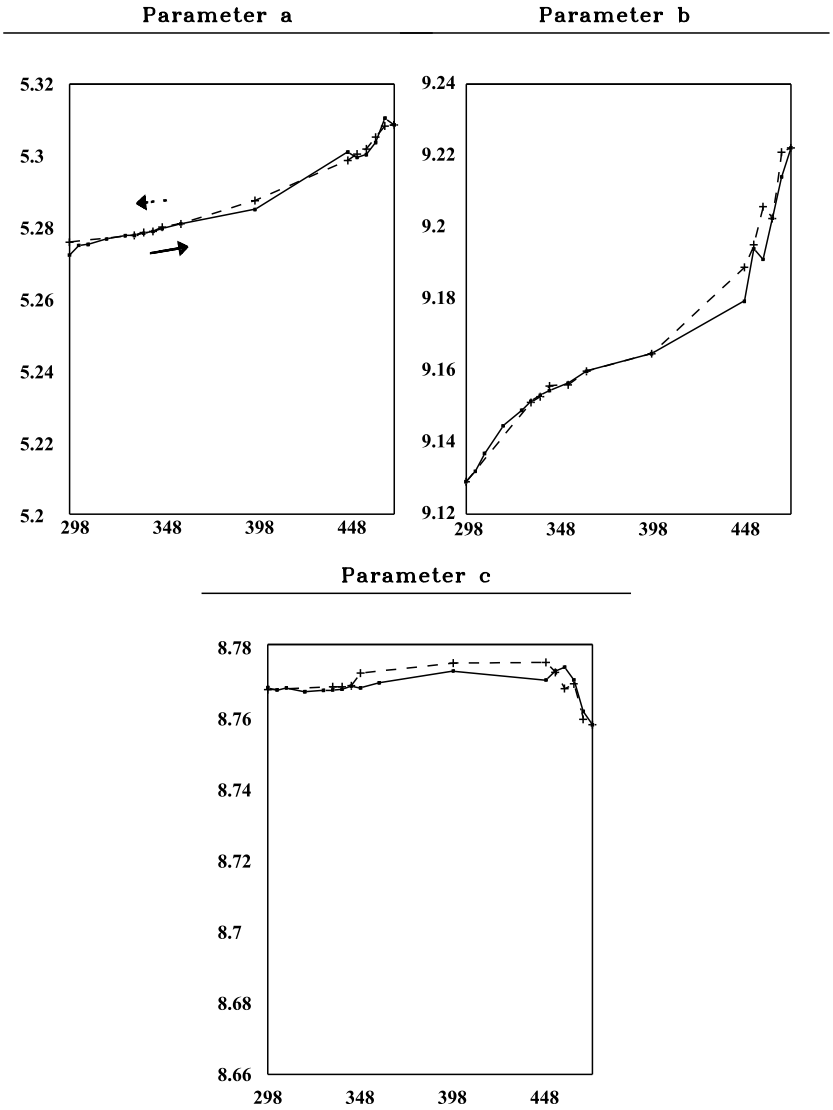

Figure 1. Variation of the cell parameters versus the temperature for $LiNH_4SO_4$.

contraction of crystal after undergoing the two warming and the cooling processes, in particular the fast warming process.

Hydrogen atoms were located in all crystal structure determinations from a difference map, and were refined with the N–H bond length constrained to 0.95 Å.

2.4. X-ray powder diffraction

Powder-diffraction data were collected with a Siemens D500 at different temperature, using Cu Kα radiation and a secondary monochromator. The experiment was a warming process from 298 to 500 K followed by a cooling process between the same temperatures. The cooling and warming rates were 5 K min^{-1} and the sample was left for 10 min. At measuring temperature

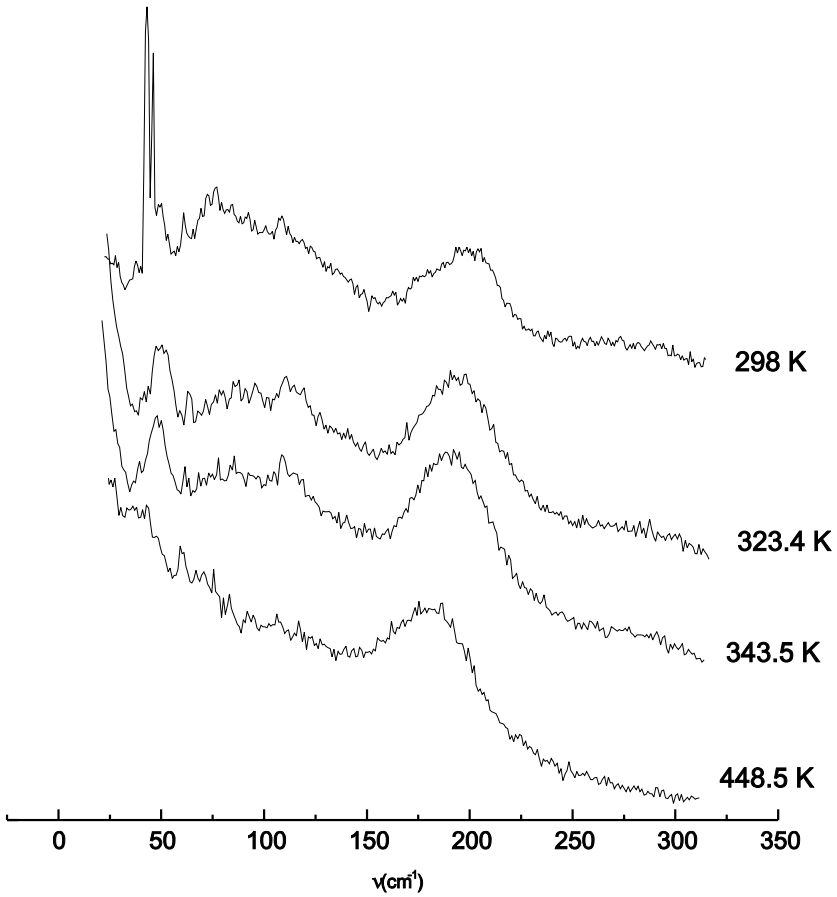

Figure 2. External modes of Raman spectra of LAS at different temperatures.

in order to stabilize the equipment and the sample. The step size was 0.025°, the time of each step 10 s, and the 2θ range was 10–80°. Cell parameters (figure 1) from powder diffraction were refined with the FULLPROF computer program [11].

2.5. Raman scattering

Polarized Raman spectra were excited on the powder sample using a Jobin–Yvon T64000 spectrometer, and an argon-ion laser excitation. The detector used was a Control Data CDC. The spectra were recorded with three monochromator gratings and the 514.5 nm line was used with a light power equals to 1.05 W. All spectra were calibrated against selected neon lines. A Mettler FP84 sample warming cell was used in order to measure the spectra at different temperatures. The position, half width and relative intensity of each peak (table 3) was determined, assuming it to be a Lorentzian function (the Gaussian contribution is negligible).

3. Results and discussion

The DSC revealed two maxima at 335 and 461 K when the warming rate was 5 K min^{-1}. Thus, the maximum described by Polomska *et al* [6] was observed, but the 335 K maximum was not

Table 3. Frequencies (in cm^{-1}), half-width and integrated area of phonon modes in LAS at different temperatures.

	$T = 298$ K	$T = 323.4$ K	$T = 343.5$ K	$T = 448.5$ K
t^{SO_4}	41.14(7)	43.2(4)	44.2(4)	31.7(6)
	3.4(2)	37(2)	31(2)	66(4)
	172	1085	959	406
t^{SO_4}	76.5(18)	78.9(12)	76.1(13)	71.7(6)
	107(5)	25(7)	31(8)	26(4)
	3385	213	355	263
L^{SO_4}	118.3(17)	108(2)	108(2)	110.9(11)
	21(9)	70(5)	73(6)	102(6)
	117	1818	1912	2890
t^{NH_4}	195.2(6)	190.4(4)	190.2(5)	183.1(2)
	39(3)	48.7(16)	59.9(19)	56.2(11)
	761	1480	1907	2026
t^{Li}	366(2)	362(3)	367(3)	
	44(23)	18(21)	32(31)	
	169	20	65	
t^{Li}	394.6(8)	394.4(11)	391.6(10)	
	16(5)	19(8)	18(6)	
	77	85	94	
$\nu_2^{SO_4}$	463.9(7)	463.8(5)	469.35(19)	465.13(7)
	27.2(8)	23.2(8)	30.8(6)	25.5(2)
	4748	2415	6145	5161
$\nu_2^{SO_4}$	475.1(7)	474.71(15)		
	11(3)	14.7(5)		
	497	2143		
$\nu_4^{SO_4}$	633.2(12)	632.93(12)	634.6(3)	634.01(12)
	27(1)	16.5(3)	22.2(8)	23.0(4)
	2252	2764	2468	2581
$\nu_4^{SO_4}$	642.3(6)	645.80(17)		
	9(3)	9.3(6)		
	421	445		
$\nu_1^{SO_4}$	1007.83(3)	1008.67(1)	1008.78(2)	1006.978(13)
	6.93(8)	8.19(3)	8.43(5)	12.43(4)
	5493	5743	5301	5440
$\nu_3^{SO_4}$	1086.6(3)	1090.4(3)	1090.8(3)	
	16.8(10)	11.6(15)	10.3(13)	
	374	208	153	
$\nu_3^{SO_4}$	1104.86(8)	1105.6(4)	1105.3(3)	1103(4)
	14.2(4)	27.8(10)	27.7(7)	47.1(10)
	1217	1393	1320	2216
$\nu_3^{SO_4}$	1121.6(3)			
	14.6(12)			
	327			

Table 3. (Continued)

	$T = 298$ K	$T = 323.4$ K	$T = 343.5$ K	$T = 448.5$ K
$\nu_3^{SO_4}$	1149.9(4)	1148.20(19)	1148.13(17)	1145.0(4)
	29.3(14)	24.4(8)	25.2(7)	30.9(19)
	677	1155	1068	1114
$\nu_3^{SO_4}$	1175.0(5)	1174.8(4)	1180.5(9)	
	20.2(22)	19.1(17)	54(2)	
	440	385	1502(79)	
$\nu_3^{SO_4}$	1192.7(2)	1191.9(3)	1191.8(2)	
	15.9(6)	16.0(9)	14.7(7)	
	419	524	386	
$\nu_4^{NH_4}$	1408.70(8)	1412.4(8)		
	25.2(3)	31(2)		
	641	371		
$\nu_4^{NH_4}$	1441.5(8)	1438.5(7)	1431.2(5)	1435.1(9)
	55.4(16)	37.0(16)	69(2)	98(3)
	382	647	1438	1410
$\nu_2^{NH_4}$	1646(2)	1645(4)		
	60(5)	71(7)		
	618	548		
$\nu_2^{NH_4}$	1680.55(17)	1680.9(2)	1678.4(2)	1674.6(5)
	28.3(7)	31.4(10)	50.4(8)	86.8(16)
	1590	1336	1967	1951
$\nu_1^{NH_4}$	2855.9(9)	2855(3)	2848(2)	2848(6)
	80(3)	72(9)	125(6)	293(13)
	1275	1168	2123	3405
$\nu_1^{NH_4}$	3051.6(4)	3044.8(13)	3048(1)	3058(2)
	123.0(16)	121(5)	145(4)	162(9)
	7925	8099	8457	6783
$\nu_3^{NH_4}$	3186.0(9)	3176(2)	3181.9(11)	3185.4(13)
	185(2)	153(5)	160(3)	154(3)
	10000	10000	10000	10000

observed when the warming rate was 20 K min^{-1}. This suggests that LAS might undergo two phase transitions in the temperature range studied (293–600 K). The ΔH (J mol^{-1}) were 119 and 610 for the transitions at 335 and 461 K, respectively and the ΔT (difference between the initial and final onset temperatures) were 17.7 and 6.2 K, respectively. The melting point was 601 K.

5 K min^{-1}

$$\text{Phase II} \xrightarrow{335\ \text{K}} \text{Phase II}' \xrightarrow{461\ \text{K}} \text{Phase I}' \xrightarrow{601\ \text{K}} \text{Melt}$$

20 K min^{-1}

$$\text{Phase II} \xrightarrow{461\ \text{K}} \text{Phase I} \xrightarrow{601\ \text{K}} \text{Melt}.$$

The two transitions were confirmed by x-ray powder diffraction. At 461 K the transition is observed by means of an abrupt change in the values of *b* and *c* parameters (figure 1). The *a*

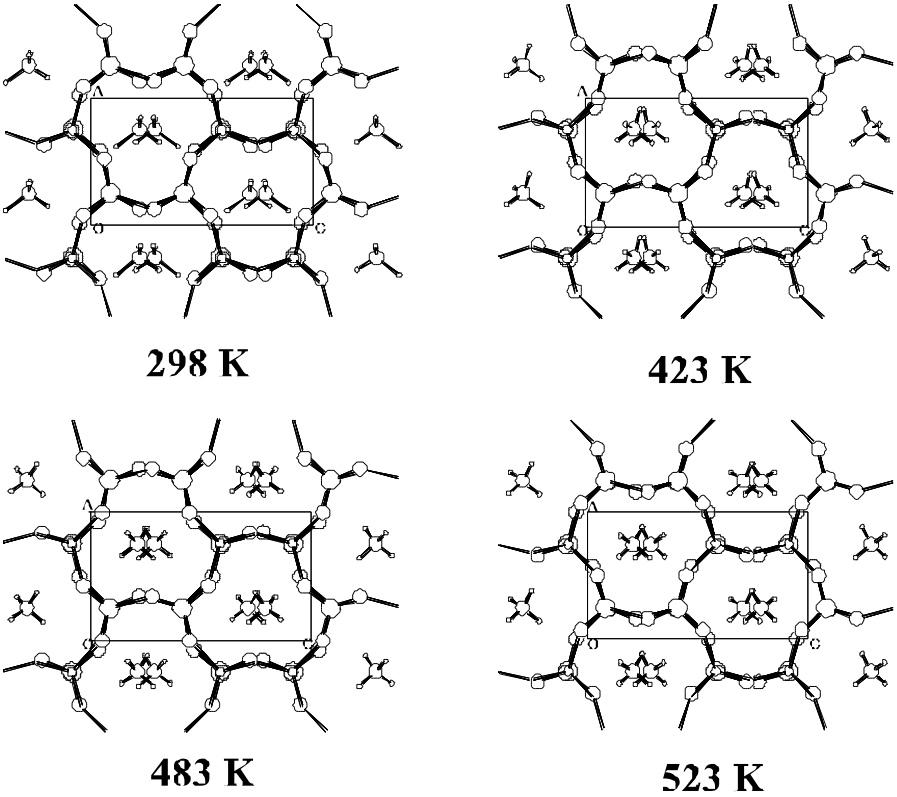

Figure 3. Unit-cell content of $LiNH_4SO_4$ at 298, 423, 483 and 523 K viewed down the *c*-axis.

and *c* parameters practically do not change during the transition at 335 K, but the variation of the slope of the $b(T)$ curve at this temperature suggests the transition.

The transitions are also observed in the Raman spectra. (The heat produced by the laser decreases the transition temperatures in this process). The frequencies of t^{SO_4}, L^{SO_4} and t^{NH_4} in the phase at room temperature change at 323.4 K and these drops when the compound passes to the high-temperature phase (figure 2).

Atomic coordinates of structures at 298, 318, 383, 423 and 483 K, bond lengths and angles and hydrogen bond lengths are listed in tables 4, 5 and 6, respectively. Figure 3 shows a cell projection down the *b*-axis for the structures at 298, 423, 483 and 523 K. The two crystal structures solved here at 298 K are similar to those obtained by Dollase [4]. The main differences are a result of the different number of reflections used in the refinement. Our structures and those described by Dollase have the opposite chirality to those obtained by Mashiyama and Kasano [5], where a chirality test was not carried out.

The crystal structures obtained during the slow warming process show that LAS undergo two phase transitions. We shall give the name phase II to the structure at 298 K, phase II′ at 423 K and phase I′ at 483 K. Phase II′ is produced from phase II by a rotation of the sulphate ion of about 41° around the S–O1 bond and by the displacement of NH_4 ion, practically, along the *a*-axis. This new phase is near to the enantiomeric phase of II. The mixture rate obtained in the refinement of crystal structures at 318 and 383 K shows that the transition was occurred in domains. Phase I′ is produced from phase II′ by a rotation of $-1°$ around the S–O1 bond

Table 4. Atomic coordinates ($\times 10^4$) at different temperatures.

	x	*y*	*z*
298.0 K			
S	2500	2037(1)	4169(1)
O(1)	2422(15)	364(3)	4107(3)
O(2)	1281(7)	2736(3)	2834(4)
O(3)	825(7)	2554(3)	5352(3)
O(4)	5186(7)	2587(3)	4451(3)
N	2492(12)	−33(3)	7847(3)
Li	7430(3)	1768(5)	5881(4)
318.0 K			
S	2500	2031(1)	4164(1)
O(1)	2490(12)	387(2)	4037(3)
O(2)	1568(5)	2714(3)	2813(2)
O(3)	844(5)	2502(3)	5374(2)
O(4)	5094(4)	2566(3)	4457(2)
N	2437(9)	2(2)	7856(2)
Li	7463(19)	1782(4)	5868(3)
383.0 K			
S	2500(7)	2033(1)	4160(1)
O(1)	2536(2)	391(3)	4038(4)
O(2)	3456(9)	2697(4)	2800(3)
O(3)	−62(6)	2572(4)	4473(3)
O(4)	4181(7)	2505(4)	5356(3)
N	2518(13)	5(2)	7868(3)
Li	24 760(4)	−1766(6)	4134(4)
423.0 K			
S	2500	2034(1)	4157(1)
O(1)	2510(3)	395(3)	4037(5)
O(2)	3443(10)	2698(5)	2795(3)
O(3)	−44(8)	2577(4)	4478(4)
O(4)	4206(9)	2510(4)	5343(4)
N	2526(16)	3(3)	7874(3)
Li	2480(4)	−1760(7)	4140(5)
483.0 K			
S	2500	2039(1)	4150(1)
O(1)	2480(3)	408(3)	4039(6)
O(2)	3400(12)	2701(7)	2793(4)
O(3)	−49(9)	2575(5)	4483(5)
O(4)	4215(10)	2514(5)	5317(4)
N	2519(17)	1(3)	7888(3)
Li	2540(4)	−1749(7)	4142(5)
523.0 K			
S	2500	2046(1)	4142(1)
O(1)	2360(4)	428(6)	4030(12)
O(2)	1660(2)	2705(12)	2778(8)
O(3)	740(2)	2527(12)	5259(11)
O(4)	5041(17)	2576(11)	4508(10)
N	2510(3)	−4(5)	7908(6)
Li	2520(6)	−1735(13)	4156(8)

and by the displacement of Li ion. The coordinates obtained for the crystal structure at 298 K, measured after the slow warming process, indicate that the transition at 335 K is reversible.

Table 5. Bond lengths (Å) and angles (°).

	$T = 298.0$ K	$T = 318.0$ K	$T = 383.0$ K	$T = 423.0$ K	$T = 483.0$ K	$T = 523.0$ K
S–O(1)	1.468(3)	1.4471(18)	1.446(2)	1.444(3)	1.434(3)	1.424(6)
S–O(2)	1.507(3)	1.456(2)	1.464(3)	1.461(4)	1.454(3)	1.452(6)
S–O(3)	1.467(3)	1.468(2)	1.467(6)	1.463(3)	1.464(4)	1.449(8)
S–O(4)	1.519(4)	1.472(2)	1.471(4)	1.473(3)	1.465(4)	1.463(8)
O(1)–Li	1.870(6)	1.906(4)	1.896(6)	1.895(6)	1.895(7)	1.902(13)
O(2)–Li [1]	1.932(6)	1.888(4)	1.902(7)	1.903(8)	1.894(8)	1.901(12)
O(3)–Li [2]	1.979(13)	1.946(9)	1.956(14)	1.960(16)	1.936(16)	1.92(3)
O(4)–Li [3]	1.903(10)	1.922(8)	1.921(18)	1.92(2)	1.95(2)	1.94(2)
O(1)–S–O(2)	111.3(2)	109.98(19)	109.1(3)	109.3(3)	109.9(4)	108.6(7)
O(1)–S–O(3)	108.7(2)	109.78(19)	110.5(6)	110.2(6)	109.2(6)	108.0(8)
O(2)–S–O(3)	102.2(2)	108.63(17)	111.0(3)	110.9(2)	110.7(3)	107.4(7)
O(1)–S–O(4)	110.5(3)	109.6(3)	109.3(4)	109.6(4)	109.9(5)	112.3(10)
O(2)–S–O(4)	113.94(17)	109.69(14)	108.0(4)	107.7(3)	107.9(4)	110.8(5)
O(3)–S–O(4)	109.84(17)	109.12(13)	109.0(2)	109.1(2)	109.3(3)	109.5(6)
S–O(1)–Li	176.9(5)	172.8(2)	172.7(4)	172.8(4)	172.9(5)	170.7(12)
S–O(2)–Li [1]	134.6(4)	143.8(3)	142.5(7)	143.0(7)	145.5(8)	146.8(12)
S–O(3)–Li [2]	128.1(2)	129.01(17)	128.9(4)	129.1(4)	128.7(4)	131.6(6)
S–O(4)–Li [3]	125.2(3)	127.8(2)	129.5(3)	129.9(3)	130.5(3)	130.2(8)
O(1)–Li–O(2) [4]	102.7(3)	101.1(2)	01.5(4)	101.6(4)	102.2(4)	101.0(8)
O(1)–Li–O(4) [2]	112.3(5)	113.1(3)	111.4(9)	111.4(10)	109.9(11)	112.8(14)
O(2) [4]–Li–O(4) [2]	110.6(6)	112.5(5)	113.0(6)	112.8(7)	111.6(7)	109.4(12)
O(1)–Li–O(3) [3]	110.6(6)	109.1(5)	112.3(7)	113.0(8)	114.7(8)	114.6(14)
O(2) [4]–Li–O(3) [3]	115.5(4)	111.8(3)	109.4(8)	109.1(9)	110.8(10)	112.5(12)
O(4) [2]–Li–O(3) [3]	105.3(3)	109.00(19)	109.1(3)	108.8(3)	107.6(3)	106.6(7)

Symmetry code: [1] $= x, y + 1/2, -z + 1/2$; [2] $= x - 1/2, -y, -z + 1$; [3] $= x + 1/2, -y, -z + 1$; [4] $= x, y - 1/2, -z + 1/2$.

The crystal structure obtained after the fast warming process shows that LAS underwent only one phase transition. The metastability of phase II in the fast warming process suggests that the transition between phase II and phase II′ is of the first order. We shall give the name phase I to the structure solved at 523 K. Phase I has the same enantiomeric form as phase II, and is produced from phase II by a rotation of 9° around the S–O1 bond and by the displacement of NH_4 and Li ions.

The assignment of non-polar $P2_1nb$ space group in the phases I and I′ is corroborated by the Raman spectra. The main differences between the Raman of the three phases II, II′ and I′ are in the external modes and $\nu_2^{SO_4}$, $\nu_3^{SO_4}$ and $\nu_4^{SO_4}$ modes. The *Pmnb* structure for phase I′, as described by Itoh *et al* [2], consists of a mixture of two enantiomer, one similar to those found for phase II and the second to phase II′, so the $\nu_n^{SO_4}$ frequencies for phase I′ should be a mixture of those observed in the Raman spectra for II and II′, which is not observed in figure 4 and table 3. This is consistent with the assumption of non-disorder structure in the high-temperature phase.

The SO_4 ion was rotated 26.8° (at 298 K) around the S–O1 bond in order to show an hypothetical ordered centrosymmetric structure with space group *Pmnb*. This angle was 17.4° in phase I at 523 K and −19.3° in phase I′ at 483 K. Thus, the angle decreased as temperature increased, suggesting that the ferroelectric–paralectric transition is a displacive transition.

The SO_4 ion has C_{2h} symmetry at 298 K, with two short and two long S–O bonds, while it shows a C_{3h} symmetry in phases II′, I′ and I. This is also observed in the stretching $\nu_n(SO_4)$ modes (figure 4 and table 3). The shortest S–O bond length corresponded to the O atom

Table 6. Hydrogen bond lengths (Å) at different temperatures.

298 K		423 K	
N–H1. . .O2 [2]	3.162(6)	N–H1. . .O4 [4]	2.872(6)
N–H2. . .O3 [3]	2.819(5)	N–H2. . .O2 [3]	2.962(8)
N–H2. . .O4 [4]	2.867(5)	N–H2. . .O3 [5]	2.886(6)
N–H3. . .O1 [1]	3.227(9)	N–H3. . .O1 [1]	3.202(15)
N–H3. . .O4 [1]	3.300(5)	N–H4. . .O1 [2]	3.188(15)
N–H4. . .O2 [5]	2.838(6)	N–H4. . .O3 [5]	2.886(6)
318 K		483 K	
N–H1. . .O3 [4]	2.850(4)	N–H1. . .O4 [4]	2.877(6)
N–H2. . .O4 [3]	2.867(4)	N–H2. . .O2 [3]	2.974(9)
N–H3. . .O1 [1]	3.149(7)	N–H2. . .O3 [5]	2.885(7)
N–H4. . .O1 [2]	3.196(7)	N–H3. . .O1 [1]	3.224(16)
N–H4. . .O2 [5]	2.962(5)	N–H3. . .O2 [1]	3.284(9)
		N–H4. . .O1 [2]	3.189(16)
383 K		N–H4. . .O3 [5]	2.885(7)
N–H1. . .O4 [4]	2.869(5)		
N–H2. . .O2 [3]	2.952(7)	523 K	
N–H2. . .O3 [5]	2.885(6)	N–H1. . .O3 [4]	2.900(13)
N–H3. . .O1 [1]	3.183(11)	N–H2. . .O4 [3]	2.899(14)
N–H4. . .O1 [2]	3.199(11)	N–H3. . .O1 [1]	3.28(2)
N–H4. . .O3 [5]	2.885(6)	N–H4. . .O1 [2]	3.15(2)
		N–H4. . .O2 [5]	2.984(17)

Symmetry code: [1] $= x-1/2, -y, 1-z$; [2] $= x+1/2, -y, 1-z$; [3] $= x-1/2, 1/2-y, 1/2+z$; [4] $= x, y-1/2, 3/2-z$; [5] $= 1/2+x, 1/2-y, 1/2+z$.

with weakest N . . . O hydrogen bond and the shortest Li–O length, which is in agreement with the assumption of higher electron localization in O1. This has also been observed in $(NH_4)_{2-x}K_xSO_4$ mixed crystals [12] and $(NH_4)_{2-x}K_xSeO_4$ [13, 14].

Table 7. Spontaneous polarization versus the temperature, which has been computed from the atomic coordinates by using an ionic model.

$T(K)$	$P \times 10^6$ (C cm^{-2})
293	0.26(4)
423	0.42(4)
483	0.03(4)
523	0.04(6)

The SO_4 tetrahedron shared all of its corners with LiO_4 tetrahedra and vice versa, giving a tetrahedral framework. The NH_4 ions lay approximately in the centre of the large asymmetric cavities in the framework, giving single or bifurcated hydrogen bonds with the oxygen atoms. At 298 K the hydrogen bonds with H1 and H3 were weak (average N . . . O bond length 3.21 Å), while those with H2 and H4 were stronger (2.84 Å). As the temperature increased N stretched to produce three strong hydrogen bonds and only one weak bond. This meant that the average N . . . O bond length was 3.03 Å at 298 K becoming 2.96–2.97 Å in the crystal structures at 318, 383 and 423 K. This average value however returned to growth in the transition from phase II or II′ to I or I′ (average values 3.02 Å at 483 K and 3.04 Å at 523 K).

We used an ionic model to compute the spontaneous polarization in each structure; the

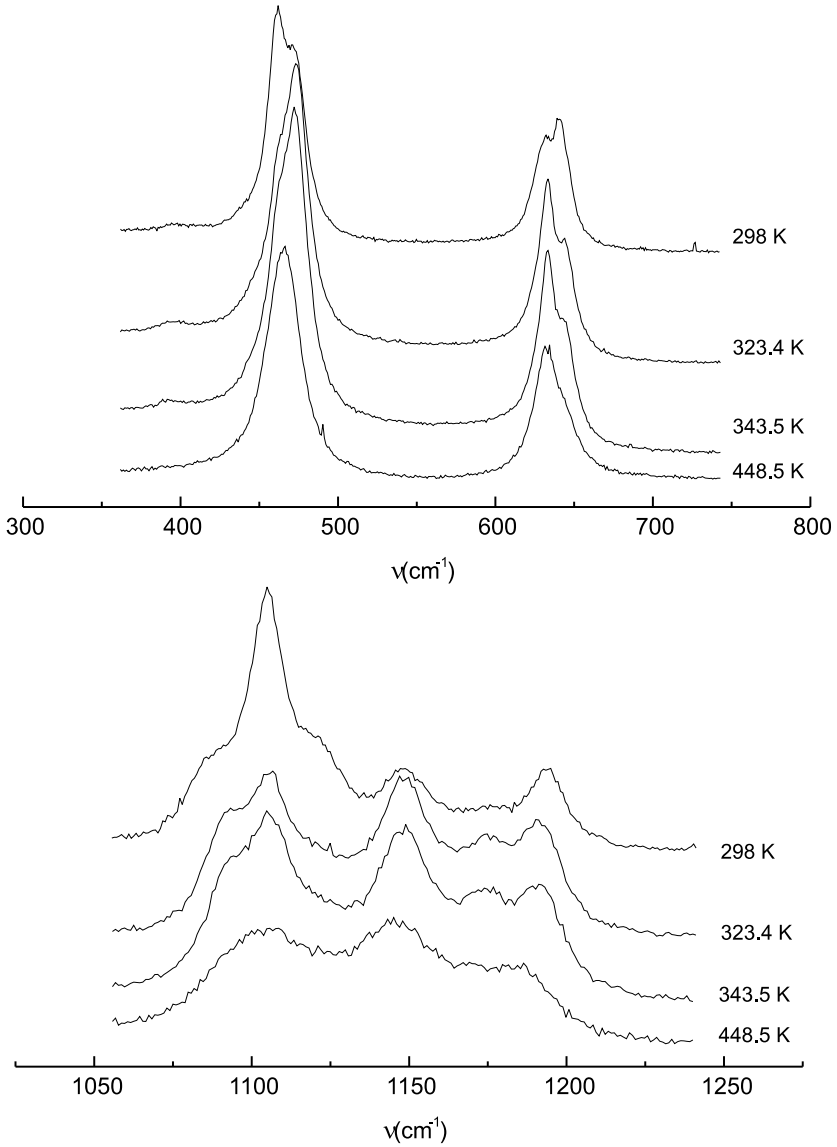

Figure 4. $\nu_2^{SO_4}$, $\nu_3^{SO_4}$ and $\nu_4^{SO_4}$ modes of LAS at different temperatures.

values obtained are shown in table 7. The spontaneous polarization along the x-axis was equal to:

$$\boldsymbol{P} = \Sigma \boldsymbol{x}_i q_i$$

where q_i is the charge of the ion i and $\boldsymbol{x}_i$ is the atomic displacement of the atom along the polarization axis. The solution of equation $0 = \Sigma \boldsymbol{x}_i q_i$ with the neutrality condition $0 = \Sigma q_i$ offers a trivial solution: for each value $\boldsymbol{x}_i$ there exists a j coordinate with $q_i = q_j$ where $\boldsymbol{x}_i = -\boldsymbol{x}_j$. This solution gives a non-polar space group of symmetry, but other combinations of $\boldsymbol{x}_i$ values lead to the removal of the spontaneous polarization depending on the number of terms in the equation.

4. Conclusions

We structurally characterized the phases of $LiNH_4SO_4$ in the temperature range 298–600 K. The framework of corner-shared LiO_4 and SO_4 tetrahedra is relatively flexible, producing large asymmetric cavities, in which the ammonium ions are located. The number of phases was dependent on the rate of the warming process. If a warming rate of 5 K min^{-1} is used, from the $P2_1nb$ structure (phase II), stable at room temperature, is obtained a new phase above 335 K (phase II′), which is close to the enantiomeric form of phase II and a paraelectric (with spontaneous polarization equal to 0) phase I′ above 461 K, which shows the non-polar $P2_1nb$ space group. A warming rate of 20 K min^{-1} gave directly the paraelectric phase I above 461 K. Phase I is close to the enantiomeric form of phase I′.

Acknowledgment

The authors thank the Comisión Interministerial de Ciencia y Tecnología for financial support through grant MAT97-0371.

References

[1] Kruglik I, Simonov M A and Aleksandrov K S 1978 *Kristallografiya* **23** 494
[2] Itoh K, Ishikura H and Nakamura E 1981 *Acta Crystallogr.* B **37** 664
[3] Lukaszewicz K and Pietraszko A 1992 *Pol. J. Chem.* **66** 2057
[4] Dollase A 1969 *Acta Crystallogr.* B **25** 2298
[5] Mashiyama H and Kasano H 1993 *J. Phys. Soc. Japan* **62** 155
[6] Polomska M, Hilezer B and Baran J 1994 *J. Mol. Struct.* **325** 105
[7] Torgashev V I, Yuzyuk Yu I, Smutny F and Polomska M 1988 *Sov. Phys. Crystallogr.* **33** 700
[8] Sheldrick G M 1997 *SHELXS. A Computer Program for Crystal Structure Determination* University of Göttingen
[9] Sheldrick G M 1997 *SHELXL, A Computer Program for Crystal Structure Determination* University of Göttingen
[10] Flack H D 1983 *Acta Crystallogr.* A **39** 867
[11] Rodríguez-Carvajal J 1996 *FULLPROF* version 3.1c, Laboratoire Leon Brillouin, Paris
[12] González-Silgo C, Solans X, Ruiz-Pérez C, Martínez-Sarrión M L, Mestres L and Bocanegra E 1997 *J. Phys.: Condens. Matter* **9** 2657
[13] González-Silgo C, Solans X, Ruiz-Pérez C, Martínez-Sarrión M L and Mestres L 1996 *Ferroelectrics* **177** 191
[14] Solans X, Ruiz-Pérez C, González-Silgo C, Mestres L, Martínez-Sarrión M L and Bocanegra E 1998 *J. Phys.: Condens. Matter* **10** 5245

INSTITUTE OF PHYSICS PUBLISHING JOURNAL OF PHYSICS: CONDENSED MATTER

J. Phys.: Condens. Matter **14** (2002) 5211–5220 PII: S0953-8984(02)33222-3

X-ray structural characterization, Raman and thermal analysis of $LiNaSO_4$. The phase diagram of the Li_2SO_4–Na_2SO_4 system

Jorge Mata, Xavier Solans, M Teresa Calvet, Judit Molera and Mercè Font-Bardia

Departament de Cristallografia, Universitat de Barcelona, E-08028 Barcelona, Spain

Received 30 January 2002
Published 9 May 2002
Online at stacks.iop.org/JPhysCM/14/5211

Abstract

An accurate structural study on the β-phase of $LiNaSO_4$ was carried out. This study shows that twin crystals are usually obtained when crystallization takes place from solution, which explains the observed low spontaneous polarization. Raman scattering of Li_2SO_4, Na_2SO_4 and $LiNaSO_4$ is explained from the structural data. The phase diagram of the binary system Li_2SO_4–Na_2SO_4 was determined by x-ray diffraction and the DTA method. Mixed crystals of the low-temperature phase of $Li_{2-x}Na_xSO_4$ with $1 \leqslant x \leqslant 1.22$ were observed for the first time. The temperatures of the process in this diagram are high, depending on the cooling rate. A more congruent diagram was obtained working at a lower cooling rate.

1. Introduction

The system Li_2SO_4–Na_2SO_4 has been widely studied because of the fast-ionic conductivity of the observed phases at high temperature. The first phase diagram of this system was determined by Nacken [1] and later revised in [2, 3]. An intermediate compound is observed in this phase diagram, $LiNaSO_4$. In [1] and [2] the decomposition of the α-$LiNaSO_4$ to give α-Li_2SO_4 + α-Na_2SO_4 during a cooling process it is considered, while in [3] a phase transition between the α- and β-phase is considered.

Li_2SO_4 undergoes a phase transition at 851 K [4]. The structure of high-temperature phase (α-phase) was determined at 908 [5], 883 [6] and 873 K [7], while the low-temperature phase (β-phase) was determined at room temperature [8]. From thermal [4] and electrical conductivity [9] and from ion diffusion [4, 10] studies of Li_2SO_4 it is concluded that the α-phase is a fast-ionic conductor. From the previously mentioned structural studies it is concluded that the conduction mechanism is a mixture of the paddle wheel model and the percolation model.

Na_2SO_4 undergoes four phase transitions in the range 700–293 K. The phases in order of decreasing temperature are named I, II, III, IV and V. The transition temperatures are 506, 498, 493 and 483 K in a cooling process according to the results from thermal analyses and electrical

conductivity [11–15]. Phase IV (range 493–483 K) is not observed by x-ray diffraction. The structure of phase I was determined at 693 [16] and 543 K [17, 18], phases II and III at 493 and 463 K [17], respectively, and phase V at 293 K [17, 19]. The discrepancies between the phase temperature transition and the temperature of crystal structure determination are due to the fact that the transition temperature depends on the cooling rate.

The structure of α-$LiNaSO_4$ was determined at 823 K [4]. Ion diffusion [10] and conductivity studies [20] show that this phase is also a fast-ionic conductor. The structure of the β-phase was determined by Morosin and Smith [21], but NMR results [22] seem to contradict this structure. Raman scattering of $LiNaSO_4$ has been widely studied [23–25]. Recently, the pressure-induced phase transition has also been studied [26].

Attempts to prepare $LiNaSO_4$ from melt and from solution gave results which did not agree with the phase diagram, so we decide to review the phase diagram and the structure of β-phase of $LiNaSO_4$.

2. Experimental details

2.1. Synthesis

The lithium sulfate and sodium sulfate were Aldrich and Fluka products, respectively (purity = 99.99%). The lithium sodium sulfate was obtained via the reaction of Na_2SO_4 with Li_2SO_4 in aqueous solution and via the melting of Na_2SO_4 and Li_2SO_4 at 913 K and posterior quenching or cooling process (1 day). The molar ratio between the sodium and lithium sulfates was 1:1. The obtained compound was analysed by ICP (induced condensed plasma) with a Jobin–Yvon analyser. Crystals were obtained by slow evaporation at 313 K.

2.2. Raman scattering

Raman spectra were excited on the powder sample using a Jobin–Yvon T64000 spectrometer, and an argon-ion laser excitation. The detector used was a Control Data CDC. The spectra were recorded with the 514.5 nm line and a light power equal to 1.05 W. All spectra were calibrated against selected neon lines. The position, half-width and relative intensity of each peak was determined, assuming it to be a Lorentzian function (the Gaussian contribution is negligible).

2.3. X-ray structure determination

Diffraction data were collected on a MAR345 automated diffractometer equipped with a graphite monochromator and image plate detector. The ϕ scan technique was used to record the intensities. Details of the structure determination are listed in table 1. The unit-cell parameters were obtained by a least-squares fit to the automatically centred settings from 1173 reflections ($3^\circ < \theta < 33^\circ$).

The structures were solved by direct methods using the SHELXS-97 computer program [27], and refined by the full-matrix least-squares method using the SHELXL-93 computer program [28]. The function minimized was $w||\mathrm{Fo}|^2 - |\mathrm{Fc}|^2|^2$, where the weighting scheme was $w = [\sigma^2(I) + (0.032P)^2 + 0.0928P]^{-1}$ and $P = (|\mathrm{Fo}|^2 + 2|\mathrm{Fc}|^2)/3$. Final refinement gave an $R1$ factor equal to 0.018, but the Flack coefficient [29] was 0.38(8), which indicated a chiral twin in the sample. Attempts using the enantiomorph coordinates or different twin laws failed, except when the twin law (1,0, 0/0, 1, 0/0, 0, −1) was used, which led to a final Flack coefficient equal to zero and a relative batch scale factor equal to 0.586 for the atomic coordinates listed in table 2 and 0.414 for the twinned coordinates.

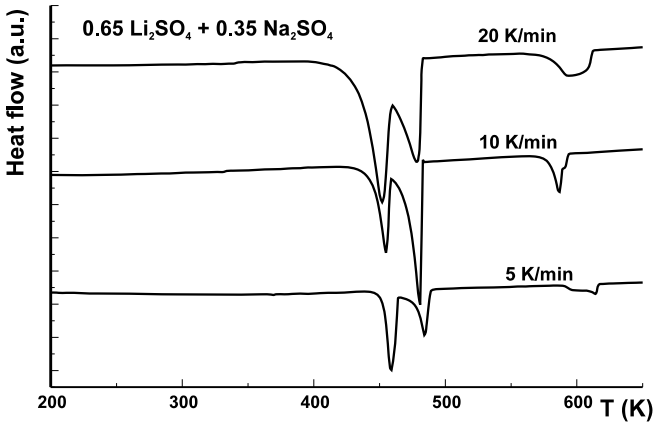

Figure 1. DTA results obtained at different cooling rates.

Table 1. Crystal data and structure refinement for $LiNaSO_4$.

Empirical formula	$LiNaSO_4$
Formula weight	125.99
Temperature (K)	293(2)
Wavelength (Å)	0.710 69
Crystal system, space group	Trigonal, $P31c$
a (Å)	7.6190(10)
c (Å)	9.8490(10)
Volume (Å^3)	495.13(10)
Z, ρ_c (mg m^{-3})	6, 2.535
μ (mm^{-1})	0.946
$F(000)$	372
Crystal size (mm^3)	$0.3 \times 0.2 \times 0.2$
Θ range for data collection (°)	3.09–33.13
Index ranges	$0 \leqslant h \leqslant 11$, $-9 \leqslant k \leqslant 0$, $-14 \leqslant l \leqslant 15$
Reflections collected/unique (R(int) = 0.0139)	1173/728
Data/parameters	701/66
Goodness of fit on F^2	1.161
R indices (all data)	$R1 = 0.018$, $wR2 = 0.053$
Absolute structure parameter	0.0(5)
Extinction coefficient	0.017(9)
Largest diff. peak and hole (e Å^{-3})	0.385 and −0.336

2.4. Phase diagram

The phase diagram of the Li_2SO_4–Na_2SO_4 system was based on the results of phase analysis and differential thermal analysis (DTA) and thermogravimetry (TG) measurements. The thermal analysis for the temperature range 298–1175 K was carried out in a Netzsch 409 DTA and TG. The sample was a mixture of $Li_2SO_4 \cdot H_2O$ and Na_2SO_4. The measured water loss by TG was used as an analysis of the composition of the mixture. Different warming and cooling rates were used (figure 1). The best-defined peaks were obtained at 10 K min^{-1} during the cooling process, so the phase diagram was elaborated at this rate. The weights of samples were about 80 mg and the reference material was alumina. The phase analyses were made with a Siemens D500 at different temperatures, using Cu Kα radiation and a secondary monochromator.

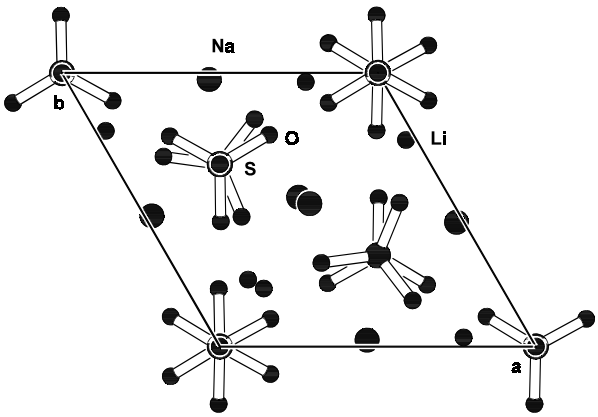

Figure 2. Projection of the unit-cell content of β-$LiNaSO_4$ down the c-axis.

Table 2. Atomic coordinates ($\times 10^4$) and equivalent isotropic displacement parameters ($Å^2 \times 10^3$) for $LiNaSO_4$. $U(eq)$ is defined as one-third of the trace of the orthogonalized U_{ij} tensor.

	x	y	z	$U(eq)$
Na	9 766(1)	4 543(1)	4 881(1)	20(1)
S(1)	10 000	10 000	17(1)	8(1)
S(2)	6 667	3 333	1 967(1)	8(1)
S(3)	3 333	6 667	2 629(1)	8(1)
O(1)	10 000	10 000	1 544(2)	10(1)
O(2)	6 667	3 333	3 451(2)	17(1)
O(3)	3 333	6 667	1 143(2)	18(1)
O(4)	7 898(2)	8 909(2)	−478(1)	14(1)
O(5)	7 742(2)	5 427(2)	1 450(1)	19(1)
O(6)	5 256(2)	8 313(3)	3 145(2)	28(1)
Li	9 670(5)	7 552(5)	2 605(3)	18(1)

The experiment was a warming process from 298 to 1175 K. The samples were left for 10 min at the melt point, followed by a cooling process with a cooling rate of 10 K min^{-1} between the same temperatures. The patterns were measured at different temperatures and the samples were left for 10 min at measuring temperature in order to stabilize the equipment and the sample. The step size was 0.025°, the time of each step 10 s and the 2θ range 10°–60°. Cell parameters from powder diffraction were refined with the FULLPROF computer program [30] using as structural model the structures obtained by single-crystal diffraction.

3. Results and discussion

Figures 2 and 3 show two projections of the cell content. The present atomic coordinates can be obtained from those of Morosin and Smith [21] by rotation about a twofold axis parallel to the $\boldsymbol{c}$-axis ($x = 1 - x_M$; $y = 1 - y_M$; $z = z_M$). From this is deduced that the two structures have the same chirality, but this twofold axis is not a crystallographic symmetry. Two hypotheses can be derived from this result: (I) the two phases are different or (II) the chirality of the structure of Morosin was not solved and was erroneous. (The $R1$ agreement coefficient of Morosin is higher and the thermal factors for S(1) and O(2) are nonpositive definite.) From the second hypothesis and as the product of the twofold axis parallel to $\boldsymbol{c}$ and the inversion

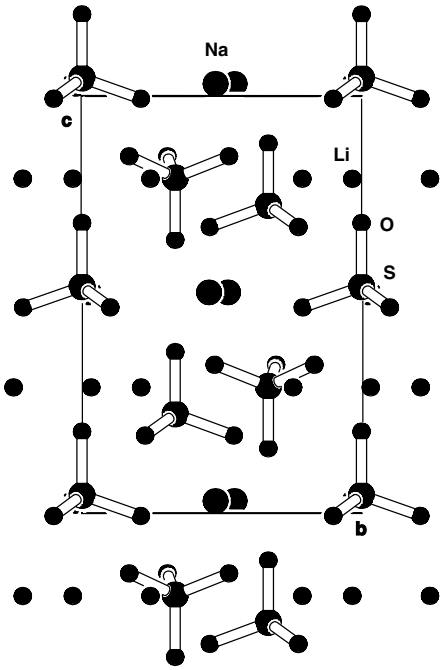

Figure 3. Projection of the unit-cell content of β-$LiNaSO_4$ down the a-axis.

centre gives a mirror plane perpendicular to $\boldsymbol{c}$ (the obtained twin law), we conclude that the enantiomorphic coordinates of Morosin correspond to the twin crystal observed in the present crystal structure determination. The results shown here then become the best determination of the crystal structure of $LiNaSO_4$. The problem of obtaining twinned crystals has already been observed in $LiKSO_4$, but in that case is possible to obtain untwinned crystals [31–33], although we have not been able to do this in $LiNaSO_4$.

The observation of the twinned crystal is in agreement with the results obtained by Junke *et al* [22] by NMR, where 12 rather than six different EFG tensors fall into two sets with six tensors each. The two sets transform into each other by a mirror plane perpendicular to the trigonal axis, which is the twin law obtained in the present crystal structure determination. The crystal structure of $LiNaSO_4$ at room temperature can be described as a framework of corner-shared LiO_4 and SO_4 tetrahedra with Na filling the cavities within the framework. The Na ion displays distorted bicapped trigonal prism coordination with respect to oxygen atoms, while this ion displays an octahedron in Na_2SO_4.

If the structures at room temperature of $LiKSO_4$ [31], $LiNH_4SO_4$ [34] and $LiNaSO_4$ are compared, all the unit-cell SO_4 tetrahedra are observed to have the same orientation in $LiKSO_4$; the relationship between up and down is 2:1 in $LiNaSO_4$ and 1:1 in $LiNH_4SO_4$. This explains the different spontaneous polarizations of the three compounds at room temperature. Spontaneous polarization is highest in $LiKSO_4$; it is poor in $LiNaSO_4$, where, moreover, the twin law reduces it, and it is low in $LiNH_4SO_4$, where the polarization axis is normal to the pseudo-trigonal axes and the polarization is more dipolar than charge polarization type [34].

Table 3 shows the observed frequencies in Raman scattering. The crystal structure of Li_2SO_4 [8] shows two lithium atoms, which are not equivalent by a symmetry operation, one with a range of O–Li–O angles 106.3°–115.7° and the second between 89.8° and 124.8°. This explains the shift of external mode t^{Li} (421.3(2) and 438.22(7) cm^{-1}), while the $LiNaSO_4$ only

Table 3. The observed frequencies (cm^{-1}) in Raman scattering of $LiNaSO_4$, Na_2SO_4 and Li_2SO_4. Values without e.s.d were not analytically fitted. The given value is the position of the peak maximum.

External modes			Internal modes		
$LiNaSO_4$	Na_2SO_4	Li_2SO_4	$LiNaSO_4$	Na_2SO_4	Li_2SO_4
55	54.8(4)	51.68(8)		446.9(4)	520.3(2)
80	75.44(6)	73.60(7)	475.29(9)	462.3(5)	609.75(4)
		86.91(11)	621.39(12)	617.3(2)	617.74(12)
		93			648.02(4)
103.1(7)	101		640.80(7)	628.9(4)	665.83(12)
114.7(7)		112.59(12)	656.6(2)	642.8(8)	
	131.45(8)	132.9(2)	970.05(8)		
		146.4(7)	991.15(17)		1005.14(2)
150.7(6)	155.47(14)	158	996.98(7)	990.12(2)	
	248.4(9)		1023.78(17)		
		352.5(5)	1066.8(3)		
		394.4(4)	1078.2(8)		
401.62(11)		421.3(2)	1099.3(6)	1098.9(3)	1120.54(4)
		438.22(7)	1121.09(16)	1129.2(3)	1145.0(2)
			1136.27(10)		1165.8(2)
			1150.9(3)	1150.00(19)	1184.9(2)
			1171.56(6)		1193.74(8)

Table 4. Bond lengths (Å) and angles (°) for $LiNaSO_4$. Symmetry transformations used to generate equivalent atoms: (i) $= -y+2, x-y+1, z$ (ii) $= y, x, z+1/2$ (iii)$x-y+1, -y+1, z+1/2$ (iv) $= -x+y+1, -x+1, z$ (v) $= -x+y+1, -x+2, z$ (vi) $= -y+1, x-y, z$ (vii) $= -y+1, x-y+1, z$ (viii) $= -x+y, -x+1, z$.

Na–O(6)(i)	2.394(2)	Na–O(3)	2.4069(14)
Na–O(4)(ii)	2.4156(14)	Na–O(5)(iii)	2.473(2)
Na–O(2)	2.4964(15)	Na–O(5)(iv)	2.679(2)
Na–O(4)(ii)	2.9593(14)	Na–O(6)(iv)	2.975(2)
S(1)–O(4)	1.4704(10)	S(1)–O(4)(v)	1.4704(10)
S(1)–O(4)(i)	1.4704(10)	S(1)–O(1)	1.504(2)
S(2)–O(2)	1.462(2)	S(2)–O(5)(vi)	1.4724(12)
S(2)–O(5)	1.4724(12)	S(2)–O(5)(iv)	1.4724(12)
S(3)–O(3)	1.463(2)	S(3)–O(6)(vii)	1.4632(13)
S(3)–O(6)	1.4632(13)	S(3)–O(6)(viii)	1.4632(13)
Li–O(4)(ii)	2.031(3)	Li–O(5)	1.922(3)
Li–O(6)(i)	1.891(3)	Li–O(1)	2.040(3)
O(4)–S(1)–O(4)(v)	109.56(5)	O(4)–S(1)–O(4)(i)	109.56(5)
O(4)(v)–S(1)–O(4)(i)	109.56(5)	O(4)–S(1)–O(1)	109.38(5)
O(4)(v)–S(1)–O(1)	109.38(5)	O(4)(i)–S(1)–O(1)	109.38(5)
O(2)–S(2)–O(5)(iv)	110.24(6)	O(2)–S(2)–O(5)	110.24(6)
O(5)(iv)–S(2)–O(5)	108.69(6)	O(2)–S(2)–O(5)(vi)	110.24(6)
O(5)(iv)–S(2)–O(5)(vi)	108.69(6)	O(5)-S(2)-O(5)(vi)	108.69(6)
O(3)–S(3)–O(6)(vii)	110.35(7)	O(3)–S(3)–O(6)	110.35(7)
O(6)(vii)–S(3)–O(6)	108.58(7)	O(3)–S(3)–O(6)(viii)	110.35(7)
O(6)(vii)–S(3)–O(6)(viii)	108.58(7)	O(6)–S(3)–O(6)(viii)	108.58(7)

shows a lithium atom in the asymmetric unit and one translational mode at 401.62(11) cm^{-1}. The role of oxygen atoms in the $LiNaSO_4$ structure is different (table 4), thus O(1) links with three Li ions, O(2) and O(3) with three Na atoms and the remaining oxygen atoms O(4),

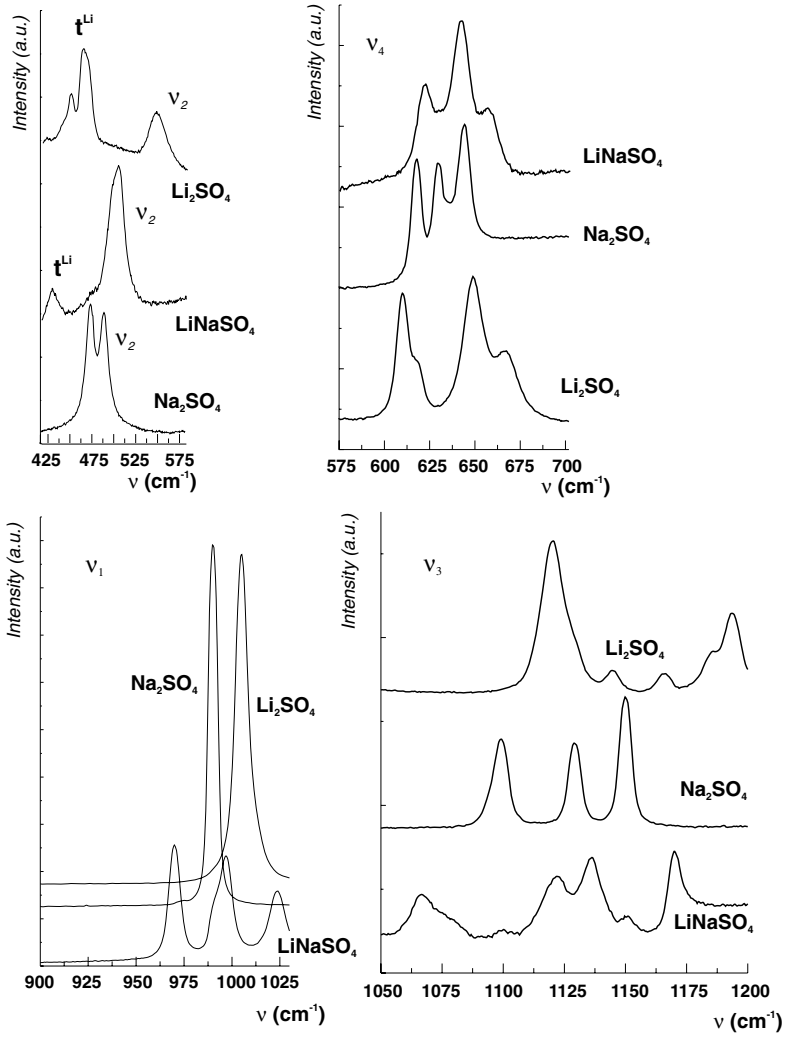

Figure 4. Different zones of Raman scattering of Li_2SO_4, Na_2SO_4 and $LiNaSO_4$.

O(5) and O(6) with two Na ions and one Li ion. This makes the S–O(1) bond length the longest (1.504(2) Å), while the S–O(2) and S–O(3) bonds are the shortest (average value 1.462(1) Å). This explains the three different internal $\nu_1(SO_4)$ modes in $LiNaSO_4$ Raman spectra (970.05(8), 996.98(7) and 1023.78(17) cm^{-1}), while the $\nu_1(SO_4)$ mode is at 990.12(2) in Na_2SO_4 and 1005.14(2) in Li_2SO_4. The splitting of the 996.98(7) mode in $LiNaSO_4$ to 991.15(17) and 996.98(7) (figure 4) is related to the two types of S–O(4), S–O(5) and S–O(6) length, the first close to 1.47 Å and the second close to 1.46 Å. The sulfate ion has a site symmetry C_3 in $LiNaSO_4$ and shows one $\nu_2(SO_4)$ mode at 475.29(9) cm^{-1}. This ion has a pseudo-C_3 symmetry in Li_2SO_4 and the $\nu_2(SO_4)$ mode appears at 520.3(2) cm^{-1} (the width of the peak in the second compound is larger than the first case). Finally the SO_4 ion has the site group D_2 symmetry in Na_2SO_4, so two $\nu_2(SO_4)$ modes at 446.9(4) and 462.3(5) cm^{-1} (figure 4).

The determination of the binary phase diagram Li_2SO_4–Na_2SO_4 is not easy. The different ATD analyses make it possible to deduce that the transition temperatures depend on the type

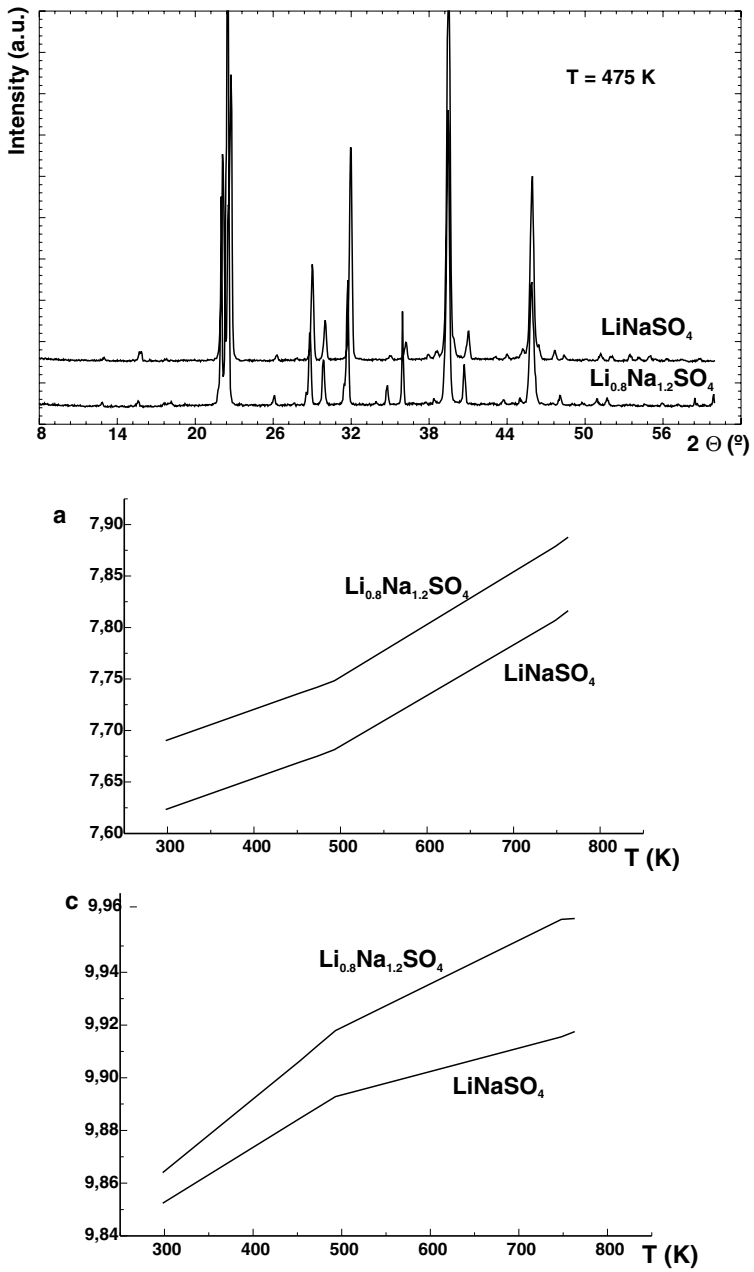

Figure 5. X-ray powder pattern of $LiNaSO_4$ and $Li_{0.8}Na_{1.2}SO_4$ at 475 K. Pt peaks at 39 and 45.5° are used as the standard reference. Bottom, variation of the cell parameters of $LiNaSO_4$ and $Li_{0.8}Na_{1.2}SO_4$ versus temperature.

of process (warming or cooling) and the cooling or warming rates. Moreover, it is not possible to analyse the high-temperature phases at room temperature, because they are not stable at this temperature when they are obtained by quenching.

From the x-ray powder analysis, we observe the formation of the mixed crystal $Li_{2-x}Na_xSO_4$ phase at low temperature in the compositional range $1 \leqslant x \leqslant 1.22$ (figure 5).

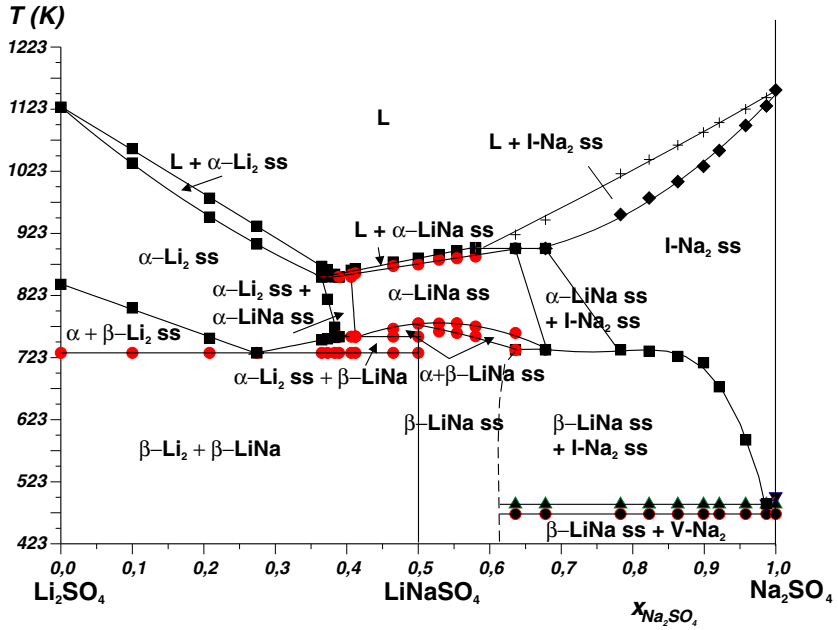

Figure 6. Phase diagram of the binary system Li_2SO_4– Na_2SO_4.
(This figure is in colour only in the electronic version)

The cell parameters increase in this compositional range; the influence of the temperature in the values of these parameters is shown in figure 5. The slope change in the variation of the cell parameters of the $Li_{2-x}Na_xSO_4$ at about 500 K suggests the possibility of phase transition at this temperature, but this has not been confirmed by x-ray diffraction. The phase diagram is shown in figure 6. The points of the diagram are from DTA data. The composition of each zone is from x-ray data. The curve of the diagram has been obtained by polynomial fitting of the different experimental points.

A eutectic reaction L $\leftrightarrow$ α-Li_2SO_4 (ss) + α-$LiNaSO_4$ (ss) takes place at 852.9 K. The composition at the eutectic point is a molar fraction of Na_2SO_4 equal to 0.389 mole. There are two eutectoid reactions: α-Li_2SO_4 (ss) $\leftrightarrow$ β-Li_2SO_4 + β-$LiNaSO_4$ at 730.6 K with molar fraction of the eutectoid point 0.274 and α-$LiNaSO_4$ (ss) $\leftrightarrow$ I-Na_2SO_4 (ss) + β-$LiNaSO_4$ (ss) at 735.5 K with composition 0.678. A peritectoid reaction L + I-Na_2SO_4 (ss) $\leftrightarrow$ α-$LiNaSO_4$ (ss) occurs at 900.2 K. We have observed that an increase of the cooling rate produces an enlargement of the I-Na_2SO_4 domain and a displacement of the α-$LiNaSO_4$ (ss) + I-Na_2SO_4 (ss) zone to richer compositions in lithium.

4. Conclusions

The structure of $LiNaSO_4$ has been correctly determined. This result and the crystal structures of Li_2SO_4 and Na_2SO_4 explain the NMR spectrum and the low spontaneous polarization of $LiNaSO_4$ as well as the Raman scattering of Li_2SO_4, $LiNaSO_4$ and Na_2SO_4. A new phase diagram of the binary system Li_2SO_4–Na_2SO_4 is deduced using a lower cooling rate. From this diagram the mixed crystals of $Li_{2-x}Na_xSO_4$ with $1 \leqslant x \leqslant 1.22$ are observed for the first time.

References

[1] Nacken R 1907 *Neues Jahrb. Mineral. Geol. Beilageband* **24** 42
[2] Schroeder K and Kvist A 1968 *Z. Naturf.* **23** 773
[3] Schroeder K, Kvist A and Ljungmark H 1972 *Z. Naturf.* **27** 1252
[4] Suleiman B M, Gustavsson M, Karawacki E and Lundén A 1997 *J. Phys. D: Appl. Phys.* **30** 2553
[5] Nilsson L, Thomas J O and Tofield B C 1980 *J. Phys. C: Solid State Phys.* **13** 6441
[6] Karlsson L and McGreevy R L 1995 *Solid State Ion.* **76** 301
[7] Forland T and Krogh-Moe J 1957 *Acta Chem. Scand.* **11** 565
[8] Alcock N W, Evans D A and Jenkins H D B 1973 *Acta Crystallogr.* B **29** 360
[9] Mellander B E and Lazarus D 1985 *Phys. Rev.* B **31** 6801
[10] Tärneberg R and Lundén A 1996 *Solid State Ion.* **90** 209
[11] Kracek F C 1929 *J. Phys. Chem.* **33** 1281
[12] Eysel W 1973 *Am. Mineral.* **58** 736
[13] Murray R M and Secco E A 1978 *Can. J. Chem.* **56** 2616
[14] Davies J E D and Sandford E F 1975 *J. Chem. Soc. Dalton Trans.* **19** 1912
[15] Cody C A, Dicario L and Darlington R K 1981 *J. Inorg. Nucl. Chem.* **43** 398
[16] Naruse H, Tanaka K, Morikawa H, Marumo F and Mehrotra B N 1987 *Acta Crystallogr.* B **43** 143
[17] Rasmussen S E, Jorgensen J E and Lundtoft B 1996 *J. Appl. Crystallogr.* **29** 42
[18] Eysel W, Höfer H H, Keester K L and Hahn Th 1985 *Acta Crystallogr.* B **41** 5
[19] Nord A G 1973 *Acta Chem. Scand.* **27** 814
[20] Mellander B E, Granéli B and Roos J 1990 *Solid State Ion.* **40–1** 162
[21] Morosin B and Smith D L 1967 *Acta Crystallogr.* **22** 906
[22] Junke K D, Mali M, Roos J and Brinkmann D 1988 *Solid State Ion.* **28/30** 1329
[23] Teeters D and Frech R 1982 *Phys. Rev.* B **26** 4132
[24] Teeters D and Frech R 1982 *J. Chem. Phys.* **76** 799
[25] Dharmasena G and Frech R 1995 *J. Chem. Phys.* **102** 6941
[26] Sakuntala T and Arora A K 2000 *J. Phys. Chem. Solids* **61** 103
[27] Sheldrick G M 1997 *SHELXS A Computer Program for Crystal Structure Determination* Univ. Göttingen
[28] Sheldrick G M 1993 *SHELXL A Computer Program for Crystal Structure Determination* Univ. Göttingen
[29] Flack H D 1983 *Acta Crystallogr.* A **39** 867
[30] Rodríguez-Carvajal J 1996 *FULLPROF* version 3.1c, Laboratoire Leon Brillouin, Paris
[31] Solans X, Calvet M T, Martínez-Sarrión M L, Mestres L, Bakkali A, Bocanegra E, Mata J and Herraiz M 1999 *J. Solid State Chem.* **148** 316
[32] Ortega J, Extxebarría J and Breczewski T 1993 *J. Appl Crystallogr.* **26** 549
[33] Solans X, Calvet M T, Martínez-Sarrión M L, Mestres L, Bakkali A, Bocanegra E, Mata J and Herraiz M 2001 *J. Solid State Chem.* **156** 251
[34] Solans X, Mata J, Calvet M T and Font-Bardia M 1999 *J. Phys.: Condens. Matter* **11** 8995

Journal of Solid State Chemistry **156,** 251–252 (2001)
doi:10.1006/jssc.2000.8988, available online at http://www.idealibrary.com on IDEAL®

RAPID COMMUNICATION

Comment on "Thermal Analysis and X-Ray Diffraction Study on $LiKSO_4$: A New Phase Transition"

Xavier Solans,* M. Teresa Calvet,* M. Luisa Martínez-Sarrión,† Lourdes Mestres,† Aniss Bakkali,† Eduardo Bocanegra,‡ Jorge Mata,* and Marta Herraiz†

* *Departament Cristallografia, Mineralogia i Dipòsits Minerals, Universitat de Barcelona, E-08028 Barcelona, Spain;* † *Departament de Química Inorgànica, and* ‡ *Departamento de Física Aplicada II, Universidad del Pais Vasco, E-48080 Bilbao, Spain*

Received July 19, 2000; in revised form September 4, 2000; accepted October 6, 2000; published online December 21, 2000

In the preceding manuscript, Tomaszewski comments on our previous paper, X. Solans *et al.*, *J. Solid State Chem.* 148, 316 (1999). These comments can be summarized in two points: (a) The influence of the domain or/and twinning on the obtained results and (b) the poor data obtained in the mentioned paper. An answer is given. © 2001 Academic Press

1. THE DOMAIN/TWINNING STRUCTURE

There is great confusion between twinning and domain formation in the Comment of Tomaszewski. We think that it is necessary to differentiate between the twin crystal obtained from a crystallization process and domain formation (or could be accepted twin formation) due to phase transition. Reference (1) is not the first manuscript on $LiKSO_4$ that deals with an untwinned crystal. An example is reported in (2), and we think that Tomaszewski accepts it, because he states in his introduction "the data obtained below the room temperature are controversial," so as a minimum he accepts the results at room temperature or above room temperature. The phase at room temperature is $P6_3$ (ordered structure), while a twin crystal at room temperature gives a $P6_3$ (disordered structure) or $P2_1$ (3). We remark that the same untwinned crystal was used in all processes on the single-crystal diffractometer in (1). The second point is the domain formation. Here there are two possibilities: These domains can be randomly distributed or ordered. Randomly distributed could produce double or broad peaks in the X-ray diffraction pattern and a high standard deviation in the obtained cell parameters. In the structure determination process a high Flack coefficient for the refined structural model would be obtained, an example of which and how it is solved can be found in (4). An ordered distribution of the domains will give good cell parameters with good standard deviations; surely, a disordered atomic structure and (if the disorder model is correct) will give a correct Flack coefficient. We remark that the authors of (1) are in this second possibility and we state in our results and discussion and in our conclusions that the phase $P6_3mc$ and $Cmc2_1$ "have multiple domains of $P6_3$ and Cc symmetry," which agrees with the comments of Tomaszewski in the preceding manuscript and with the results of (5) and (6). The lack of observation of domains in the phase $P31c$ agrees with the results of (6), of which Tomaszewski is an author. In (6), p. 916, section 3, line 17, the authors state (during a heating process) "Above 194 K the domains disappear ...." Above 194 K corresponds in (1) to the phase $P31c$, which is assumed by Solans *et al.*, to be without domain structure. Could Tomaszewski explain the contradiction between his present comment and that in his paper (6)?

2. THE POOR DATA OF (1)

Tomaszewski states that the cell parameters obtained by X-ray Bond method (7) have an accuracy of 10^{-5}. He confuses the equipment accuracy of 2θ with the accuracy of the cell parameters. An example of our comment is the paper (8) where the Bond method is used. In Table 1 of this manuscript the accuracy of the obtained cell parameters is 2×10^{-4} for a and b parameters and 10^{-4} for c parameter for a crystal of cell volume equal to 400 Å^3. An accuracy of 10^{-4} was obtained in (1).

In Table 1 the measurements of cell parameters of Desert *et al.* (9) and Solans *et al.* (1) are compared. The two measurements are different and give different results because

(a) The higher cooling and heating rates in Solans *et al.* measurements facilitate the kinetics of phase transitions,

0022-4596/01 $35.00

TABLE 1
Comparison of the Method Used to Determined the Cell Parameters at Different Temperatures in Refs. (1) and (9)

	Desert *et al.* (9)	Solans *et al.* (1)
Geometry	Reflection	Transmission
Beam	Divergent	Parallel
Sample	Single crystal	Powder
Scan	Missing ($\omega/2\theta$ from Figs. 1 and 4?)	Detector: fixed Sample: Phi rotation
Wavelength	Missing	Cu$K\alpha$
Primary monochromator	Missing (None from figures)	Quartz monochromator
Exposure time for each value	Scan speed is missing	>1 h
Temperature range	100–298 K	163–298 K
Cooling and heating rate	0.43 K/min	10 K/min
No. of reflections used to determine cell parameters	2 (0 0 8 and 0 4 0)	All between 2 and 120°

while the lower rate in Desert *et al.* measurements facilitates the observation of metastable phases.

(b) The number of reflections used to determine the cell parameters by Solans *et al.* give an average information for the entire sample. The use of one reflection to determine each cell parameter in Desert *et al.* implies that systematic errors in the measurements of this peak will be reflected in the obtained cell parameter.

(c) The phi scan used by Solans *et al.* diminishes the domain effects on the determination of cell parameters. In the Desert *et al.* study a phi scan is not used in order to study the domain effects, as is stated in (9).

(d) The shortest temperature range in (1) does not allow the study of the $Cmc2_1$ phase.

The results of Desert *et al.* are different because

(a) Desert *et al.* use reflection geometry and divergent beam, so the width and the asymmetry effects of the peak are higher than those obtained by Solans *et al.* The overlapping of $K\alpha_1$ and $K\alpha_2$ in the 0 4 0 reflection is important and the number of counts per peak is different in the two measurements because different type of sample and exposure time are used. All that produces less accuracy in the determination of the peak position in the measurements of Desert *et al.* than that obtained by Solans *et al.*

(b) The main problem in the measurements reported in (7) and (9) is the tilt angle between the crystal face and the goniometer plane, a test of which is not stated in either manuscript.

Despite all that, it is well known that all phase transition processes depend on their history, so the two measurements are not readily comparable.

The enthalpies of the phases transitions in (1) were measured during the heating process. The peak overlap of phase transitions II and III was solved by a multipeak computer fit, using an asymmetric pseudo-Voight function. The onset temperatures were determined using the maximum slope method.

As a last remark, we agree with Tomaszewski's comment concerning the phase at 189 K. The space group is $P31c$.

REFERENCES

1. X. Solans, M. T. Calvet, M. L. Martínez-Sarrión, L. Mestres, A. Bakkali, E. Bocanegra, J. Mata, and M. Herraiz, *J. Solid State Chem.* **148,** 316 (1999).
2. J. Ortega, J. Etxebarria, and T. Breczewski, *J. Appl. Cryst.* **26,** 549 (1993).
3. S. Bhakay-Tamhane, A. Sequeira, and R. Chidambaram, *Acta Crystallogr. Sect. C* **40,** 1648 (1984).
4. X. Solans, J. Mata, M. T. Calvet, and M. Font-Bardia, *J. Phys.: Condens. Matter* **11,** 8995 (1999).
5. W. Kleemann, F. J. Schaefer, and A. S. Chaves, *Solid State Commun.* **64,** 1001 (1987).
6. R. Cach, P. E. Tomaszewski, and J. Bornarel, *J. Phys. C: Sol. State Phys.* **18,** 915 (1985).
7. P. E. Tomaszewski and K. Lukaszewicz, *Phase Transit.* **4,** 37 (1983).
8. P. E. Tomaszewski and A. Pietraszko, *Phys. State Sol. (a)* **56,** 467 (1979).
9. A. Desert, A. Gibaut, A. Righi, U. A. Leitao, and R. L. Moreira, *J. Phys.: Condens Matter* **7,** 8445 (1995).

3B2v7.51c GML4.3.1 YJSSC : 32 Prod.Type:COM pp.1–9(col.fig.:NIL) ED:Gayathri PAGN: vs SCAN: VijayaKumar

ARTICLE IN PRESS

Available online at www.sciencedirect.com

SCIENCE DIRECT®

ACADEMIC PRESS

Journal of Solid State Chemistry ▮ (▮▮▮▮) ▮▮▮–▮▮▮

JOURNAL OF SOLID STATE CHEMISTRY

http://elsevier.com/locate/jssc

Structural and vibrational studies of $Li[K_x(NH_4)_{1-x}]SO_4$ and $Li_2KNH_4(SO_4)_2$ mixed crystals

Jorge Mata, Xavier Solans,* and Judit Molera

Departament de Cristal·lografia, Universitat de Barcelona, Martin i Franquès s/n, E-08028 Barcelona, Spain

Received 8 October 2002; received in revised form 13 January 2003; accepted 20 January 2003

Abstract

Mixed crystals of $Li[K_x(NH_4)_{1-x}]SO_4$ have been obtained by evaporation from aqueous solution at 313 K using different molar ratios of mixtures of $LiKSO_4$ and $LiNH_4SO_4$. The crystals were characterized by Raman scattering and single-crystal and powder X-ray diffraction. Two types of compound were obtained: $Li[K_x(NH_4)_{1-x}]SO_4$ with $x \geqslant 0.94$ and $Li_2KNH_4(SO_4)_2$. Different phases of $Li[K_x(NH_4)_{1-x}]SO_4$ were yielded according to the molar ratio used in the preparation. The first phase is isostructural to the room-temperature phase of $LiKSO_4$. The second phase is the enantiomorph of the first, which is not observed in pure $LiKSO_4$, and the last is a disordered phase, which was also observed in $LiKSO_4$, and can be assumed as a mixture of domains of two preceding phases. In the second type of compound with formula $Li_2KNH_4(SO_4)_2$, the room-temperature phase is hexagonal, symmetry space group $P6_3$ with cell-volume nine times that of $LiKSO_4$. In this phase, some cavities are occupied by K^+ ions only, and others are occupied by either K^+ or NH_4^+ at random. Thermal analyses of both types of compounds were performed by DSC, ATD, TG and powder X-ray diffraction. The phase transition temperatures for $Li[K_x(NH_4)_{1-x}]SO_4$ $x \geqslant 0.94$ were affected by the random presence of the ammonium ion in this disordered system. The high-temperature phase of $Li_2KNH_4(SO_4)_2$ is also hexagonal, space group $P6_3/mmc$ with the cell a-parameter double that of $LiKSO_4$. The phase transition is at 471.9 K.

Keywords: Phase transition; Ferroelectric material; X-ray diffraction; Raman scattering; Thermal analysis; Crystal structure; Mixed crystals; Lithium sulfate compounds; Ammonium; Potassium

1. Introduction

A great number of studies have examined the physical properties of, and phase transitions in, lithium potassium sulfate [1–4], $LiKSO_4$, and lithium ammonium sulfate [5,6], $LiNH_4SO_4$. Interest in the former is due to its pyroelectric, ionic conductivity, ferroelastic and ferroelectric properties, while interest in the latter is due to its ferroelastic and ferroelectric properties.

$LiKSO_4$ has a hexagonal structure derived from tridymite. The framework of corner-sharing LiO_4 and SO_4 tetrahedra forms cavities which are filled by K^+ ions. The framework is relatively flexible, as shown by the large number of phases in the range 123–1000 K. $LiNH_4SO_4$ is pseudo-isostructural to $LiKSO_4$ and also shows several phases. The main difference between the two structures is in the orientation of LiO_4 and SO_4 tetrahedra. All SO_4 tetrahedra have the same orientation in $LiKSO_4$. The relationship between up and down along the pseudo-trigonal axis is 1:1 in $LiNH_4SO_4$. This explains the different spontaneous polarization of the two compounds at room temperature, which is parallel to the trigonal axis in the $LiKSO_4$ and normal to the pseudo-trigonal axis in $LiNH_4SO_4$.

The S–O bond lengths are in the range 1.467(4)–1.519(4) Å in the structure of $LiNH_4SO_4$ [5] at room temperature. This is due to NH_4–O hydrogen bonds. In the structure of the $LiKSO_4$ at room temperature, the four S–O distances are equal (range: 1.464(3)–1.465(6) Å). We conclude that the dipolar contribution to the spontaneous polarization is higher in $LiNH_4SO_4$ than in $LiKSO_4$. In $LiKSO_4$ the spontaneous polarization disappears when the temperature rises and a mirror plane then appears perpendicular to the polarization axis. At room temperature the highest deviation of the ionic centers from this mirror plane is 0.30 Å (in the Li atom) in $LiNH_4SO_4$ and 2.53 Å (in K) in $LiKSO_4$. We

*Corresponding author. Fax: +34-934021340.
E-mail address: xavier@geo.ub.es (X. Solans).

0022-4596/03/$ - see front matter © 2003 Elsevier Science (USA). All rights reserved.
doi:10.1016/S0022-4596(03)00092-6

conclude that the ionic contribution to the polarization is higher in $LiKSO_4$ than in $LiNH_4SO_4$. These differences in the structural behavior of NH_4^+ and K^+, which modified the results of spontaneous polarization, also altered the results of no-lineal optics (NLO) [7,8].

The main purposes of this study are: (a) to examine the effect of the random presence of electronically different cations of similar size on the phase transition sequence of the pure compounds. (b) To study the influence of this random presence of cations on the compounds' physical properties and to search for new phases produced by new arrangements of the various cations.

A Raman scattering study of $LiK_{0.96}(NH_4)_{0.04}SO_4$ [9] and Raman and birefringence studies of $LiK_{1-x}Rb_xSO_4$ [10] preceded the work described here.

2. Experimental section

2.1. Synthesis

Lithium potassium sulfate and lithium ammonium sulfate were prepared as indicated elsewhere [1,5]. Mixtures of these compounds in several molar ratios were dissolved in water. Crystals were obtained by slow evaporation at constant temperature of 313 K. The compounds obtained were analyzed by induced condensed plasma (ICP) with a Jobin-Yvon analyzer, powder and single-crystal diffraction.

2.2. Raman scattering

Polarized Raman spectra were excited on the powder sample using a Jobin-Yvon T64000 spectrometer and argon-ion laser excitation. The detector was a Control Data CDC. The spectra were recorded with three monochromator gratings and the 514.5 nm line was used with a light power of 1.05 W. The range measured was 40–2000 cm^{-1}. All spectra were calibrated against selected neon lines. A Mettler FP84 sample warming cell was used in order to measure the spectra at 298, 423, 473, 513, 473, 423 and 298 K. The position, half-width and relative intensity of each peak were determined, assuming a Lorentzian function (the Gaussian contribution was negligible).

2.3. X-ray structure determination

The same method was followed in all single-crystal structure determinations. The intensities were collected at 298 K on an Enraf-Nonius CAD4 automated diffractometer equipped with a graphite monochromator. The $\omega - 2\theta$ scan technique was used to record the intensities. Scan widths were calculated as $A + B\tan\theta$, where A is estimated from the mosaicity of the crystal and B allows for the increase in peak width due to Mo$K\alpha_1$–$K\alpha_2$ splitting.

Table 1
Crystal data and structure refinement for different phases of $LiK_x(NH_4)_{1-x}SO_4$ measured at 298 K

	Phase III	Phase III′	Phase IV	Phase II
Formulae	$LiK_{0.97}(NH_4)_{0.03}SO_4$	$LiK_{0.97}(NH_4)_{0.03}SO_4$	$LiK_{0.93}(NH_4)_{0.07}SO_4$	$Li_2KNH_4(SO_4)_2$
Wavelength (Å)	0.71069	0.71069	0.71069	0.71069
Crystal system	Hexagonal	Hexagonal	Hexagonal	Hexagonal
Space group	$P6_3$	$P6_3$	$P6_3mc$	$P6_3$
a (Å)	5.1370(8)	5.1412(13)	5.152(2)	18.1780(14)
c	8.638(7)	8.644(8)	8.642(3)	8.595(15)
Volume (Å^3)	197.41(17)	197.9(2)	198.65(13)	2460(5)
Z, calculated density (Mg/m^3)	2, 2.368	2, 2.387	2, 2.340	12, 2.088
μ (mm^{-1})	1.669	1.687	1.622	1.142
Crystal size (mm)	$0.1\times0.1\times0.1$	$0.20.2\times0.2$	$0.1\times0.1\times0.1$	$0.1\times0.1\times0.3$
Θ range for data collection (°)	4.58–29.96	4.58–29.94	4.57–29.99	2.24–29.98
Index ranges	$-7\leqslant h\leqslant6$	$-7\leqslant h\leqslant6$	$-7\leqslant h\leqslant7$	$-21\leqslant h\leqslant0$
	$0\leqslant k\leqslant7$	$-2\leqslant k\leqslant7$	$-7\leqslant k\leqslant7$	$0\leqslant k\leqslant25$
	$-3\leqslant l\leqslant12$	$0\leqslant l\leqslant12$	$-2\leqslant l\leqslant12$	$0\leqslant l\leqslant12$
Reflections collected/unique	660/208	661/207	1026/131	2567/2421
R(int)	0.0256	0.0329	0.0153	0.0246
Completeness to $2\Theta=29.96°$	100.0%	100.0%	94.9%	95.2%
Data/parameters	208/24	207/24	131/24	2421/256
Goodness-of-fit on F^2	1.119	1.102	1.131	1.043
R_1 index (all data)	0.0271	0.0221	0.0170	0.0407
wR_2 index (all data)	0.0657	0.0498	0.0417	0.1115
Absolute structure parameter	0.12(10)	0.08(7)	0.09(16)	0.00(9)
Largest diffraction peak (e Å^{-3})	0.358	0.377	0.177	0.763
Largest diffraction hole (e Å^{-3})	−0.655	−0.280	−0.216	−0.368

Table 2
Majority phase obtained from the crystallization in water solution vs. the starting molar ratio of $LiKSO_4$ and $LiNH_4SO_4$

Molar ratio $LiKSO_4$:$LiNH_4SO_4$	Obtained phase	
Pure $LiKSO_4$		
9:1	III–$LiK_x(NH_4)_{1-x}SO_4$	$x \geqslant 0.94$
7:3	III′—$LiK_x(NH_4)_{1-x}SO_4$	$x \geqslant 0.94$
1:1	IV—$LiK_x(NH_4)_{1-x}SO_4$	$x \geqslant 0.94$
3:7	III—$LiK_x(NH_4)_{1-x}SO_4$	$x \geqslant 0.94$
1:9	$Li_2KNH_4(SO_4)_2$	
1:18	$LiNH_4SO_4$	
Pure $LiNH_4SO_4$		

Details of structure determination are listed in Table 1. The unit-cell parameters were obtained by a least-squares fit to the automatically centered settings from 25 reflections ($12^\circ < 2\theta < 21^\circ$). The intensities from three control reflections for each measurement showed no significant fluctuation during data collection.

The structures were solved by direct methods, using the SHELXS-97 computer program [11] and refined by the full-matrix least-squares method, using the SHELXL-97 computer program [12]. The function minimized was $w||F_o|^2 - |F_c|^2|^2$, where the weighting scheme was $w = [\sigma^2(I) + (k_1P)^2 + k_2P]^{-1}$ and $P = (|F_o|^2 + 2|F_c|^2)/3$. The values of k_1 and k_2 were also refined. The chirality of the structure was defined from the Flack coefficient [13].

2.4. X-ray powder diffraction

Powder-diffraction data were collected with a Siemens D500 at different temperature, using Cu$K\alpha$ radiation and a secondary monochromator. The experiments were: warming from 298 to 950 K followed by cooling between the same temperatures, using an HTK Aaton Par Camera for $LiK_x(NH_4)_{1-x}SO_4$. Cooling from 298 to 150 K followed by warming between the same temperatures, using a TTK Aaton Camera for the same compound and warming from 298 to 523 K followed by cooling for $Li_2KNH_4(SO_4)_2$. The cooling and warming rates were 5 K/min and the sample was left for 10 min at measuring temperature in order to stabilize the equipment and the sample. The step size was 0.05°, the time of each step 10 s and the 2θ range was 10–80°. Cell parameters from powder diffraction were determined using 25 peaks with the TREOR97 program and refined with the WINPLOTR program [14].

2.5. Thermal analysis

The thermal analyses above room temperature were carried out in a differential thermal analysis (DTA) and thermogravimetry (TG) NETZSCH STA409. Loss of mass was not observed in the analysis of the phase transitions. The thermal analyses for temperatures below room temperature were carried out in a differential scanning calorimeter (DSC) Perkin-Elmer DSC-7. Different warming and cooling rates were used, but the results are given at 5 K/min. The weight of samples was about 80 mg and the reference material was alumina.

Table 3
Atomic coordinates ($\times 10^4$) and equivalent isotropic displacement parameters ($Å^2 \times 10^3$) for $LiK_x(NH_4)_{1-x}SO_4$. U(eq) is defined as one-third of the trace of the orthogonalized U_{ij} tensor

	x	y	z	U(eq)
Phase III				
S	6667	3333	4239(2)	14(1)
X	10,000	0	6297(1)	23(1)
O(1)	6667	3333	5942(10)	47(2)
O(2)	9418(6)	5977(6)	3706(5)	32(1)
Li	6667	3333	8152(13)	14(2)
Phase III′				
S	6667	3333	4242(1)	14(1)
X	10,000	0	6299(1)	23(1)
O(1)	6667	3333	5937(6)	46(1)
O(2)	9419(5)	3442(5)	3712(4)	33(1)
Li	6667	3333	8137(10)	16(2)
Phase IV				
S	6667	3333	4251(3)	14(1)
X	10,000	0	6316(3)	23(1)
O(1)	6667	3333	5957(15)	47(3)
O(2)	9430(16)	5979(18)	3701(9)	32(2)
Li	6667	3333	8160(2)	21(4)

$X = K$ and (NH_4). Occupancy factor for K in X site is 0.972(4) for Phase III, 0.972(3) for Phase III′ and 0.9329(13) for Phase IV.

Table 4
Bond lengths (Å) and angles (deg) for $LiK_x(NH_4)_{1-x}SO_4$

	Phase III	Phase III′	Phase IV
S–O(2) ($\times 3$)	1.471(9)	1.462(2)	1.453(6)
S–O(1)	1.461(3)	1.465(6)	1.472(4)
K–O(2) ($\times 3$)	2.842(4)	2.846(3)	2.841(4)
K–O(2) ($\times 3$)	2.958(4)	2.958(3)	2.969(4)
K–O(1) ($\times 3$)	2.9817(10)	2.9847(9)	2.9929(13)
Li–O(1)	1.910(12)	1.901(9)	1.917(9)
Li–O(2) ($\times 3$)	1.920(4)	1.926(3)	1.919(4)
O(2)–S–O(2) ($\times 3$)	110.58(17)	110.65(13)	110.60(14)
O(2)–S–O(1) ($\times 3$)	108.34(18)	108.26(14)	108.32(15)
O(1)–Li–O(2) ($\times 3$)	104.4(4)	105.0(3)	104.7(3)
O(2)–Li–O(2) ($\times 3$)	114.0(3)	113.6(2)	113.8(2)

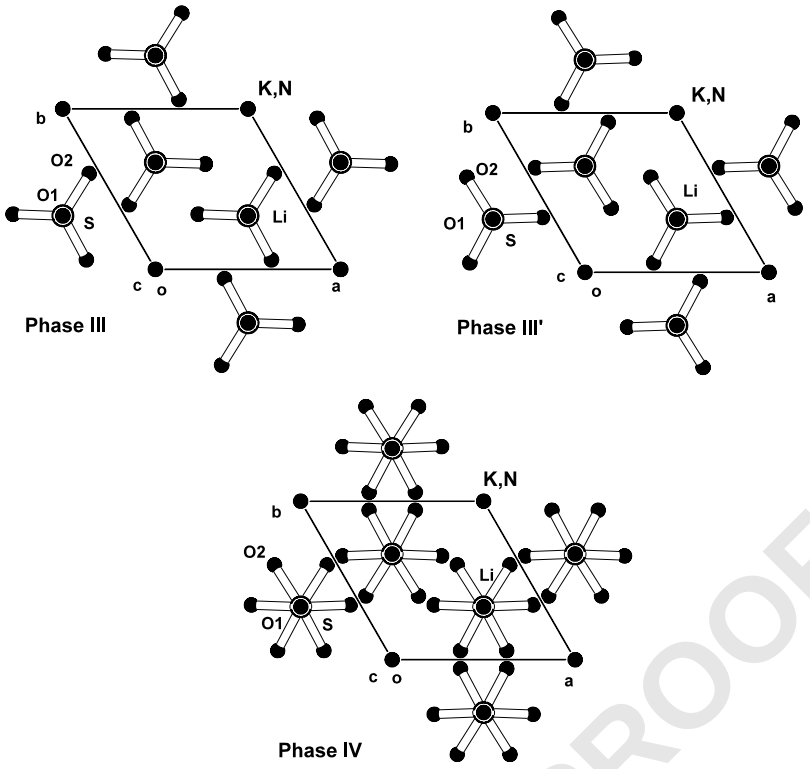

Fig. 1. Projection of the structure of the three obtained phases of $Li[K_{0.94}(NH_4)_{0.06}]SO_4$ down the *c*-axis.

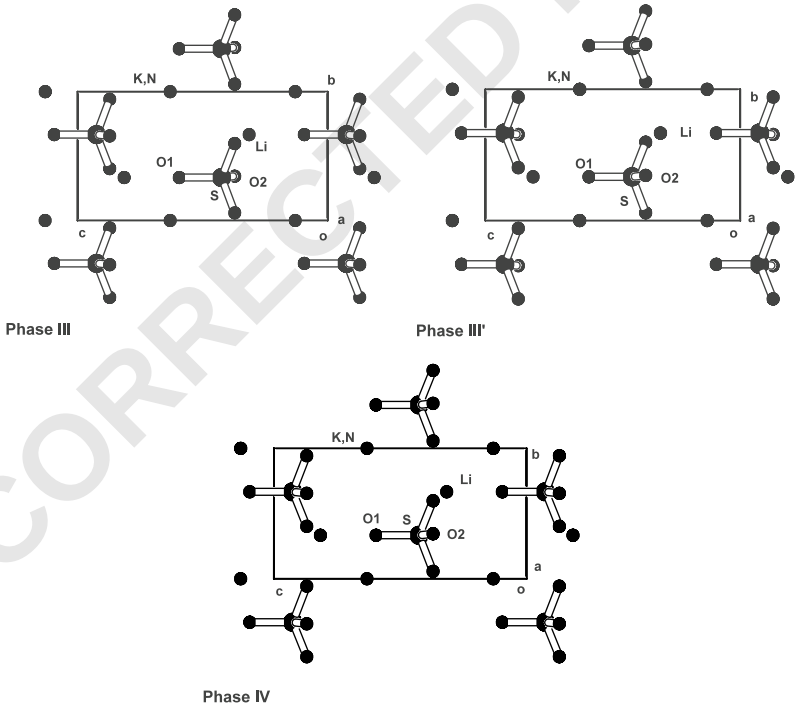

Fig. 2. Projection of the structure of the three obtained phases of $Li[K_{0.94}(NH_4)_{0.06}]SO_4$ down the *a*-axis.

3. Results and discussion

The phase diagram of the binary system $LiKSO_4$–$LiNH_4SO_4$ cannot be determined from liquidus because $LiNH_4SO_4$ decomposes at 601 K. [5] The results, obtained from the 32 crystallization using different molar ratios of mixtures of $LiKSO_4$ and $LiNH_4SO_4$, are summarized in Table 2. The *x* values obtained for

$LiK_x(NH_4)_{1-x}SO_4$ were in the range $1 > x \geqslant 0.94$. From Table 2 it is deduced that the crystals obtained are rich in potassium. This is because the solubility of the $LiKSO_4$ in water is lower than that of $LiNH_4SO_4$. The $LiK_x(NH_4)_{1-x}SO_4$ ($x \geqslant 0.94$) and $Li_2KNH_4(SO_4)_2$ crystals were easy to distinguish optically since the former are equidimensional, showing the crystal forms {001} and {101} and the latter are prisms with the forms {011} and {110}. The largest crystals obtained were $2 \times 2 \times 2$ cm for $LiK_x(NH_4)_{1-x}SO_4$ ($x \geqslant 0.94$) and $4 \times 1 \times 1$ cm for $Li_2KNH_4(SO_4)_2$.

3.1. The $LiK_x(NH_4)_{1-x}SO_4$ mixed crystals

The different phases of the mixed crystals $LiK_x(NH_4)_{1-x}SO_4$ were characterized by single-crystal X-ray diffraction. Atomic coordinates and selected bond lengths and angles are listed in Tables 3 and 4, respectively. Figs. 1 and 2 show the structure down the *c*- and *a*-axis, respectively. Phases III and IV are isostructural to Phases III and IV, respectively, of $LiKSO_4$ [1]. The difference between Phases III and III′ is the rotation of 60° around the *c*-axis of the sulfate ion, which causes Phase III′ to be the enantiomorph of Phase III. The existence of Phase III′ was suggested more than 100 years ago by Traube [15,16]. The crystal structure has now been solved. The identification of a phase whose chirality depends on the preparation had already been observed in $LiNH_4SO_4$ [5]. Klapper et al. [17] studied the twin domains and twin boundaries in $LiKSO_4$, which suggest that Phase IV is a twinned Phase III. We consider that the X-ray intensity measured in a twin crystal is equal to $Iobs[hkl] = x\,I[hkl] + (1-x)\,I[S(hkl)]$, where S is the twin law as, for example, happens in [5,18]. On the other hand if $Iobs(hkl) = I(hkl)$ we consider that the structural model corresponds to a phase [19]. For this reason we consider the existence of a Phase IV which is a disordered phase. However, the disordered phase is at low temperature, which suggests that the disorder is static and is formed by multiple domains of Phase III and III′. This conclusion agrees with the equivalent thermal coefficients obtained. From this result and Table 2 we conclude that two processes lead to the crystallization. The increase of the NH_4^+ concentration diminishes the crystallization rate because the mixture is more soluble in water, which leads to the formation of stable phases and, on the other hand, the NH_4^+ acts as a poisoned site, producing the enantiomorph form of Phase III.

Two different processes were followed in the thermal analysis of $LiK_x(NH_4)_{1-x}SO_4$: a warming process followed by a cooling process in the range 298–950 K, using the ATD; and a cooling process, followed by a warming process in the range 298–150 K, using the DSC. In Table 5, the transition temperatures for $LiKSO_4$ and $LiK_{0.94}(NH_4)_{0.06}SO_4$ are compared. The transition between Phases III and IV was not observed by Raman scattering [9] because the site symmetry is the same in the two phases. The results obtained for the other two-phase transitions at low temperature agree with the results of Freire et al. [9].

From these results we conclude that the metastable Phase IV at room temperature and the new Phase III′ can be obtained by varying the NH_4^+ concentration in the solution, while the same phases that in $LiKSO_4$ are obtained by varying the temperature. The phase transition temperatures are affected by the random

Table 5
Comparison between the phase transition temperature (in K) during the cooling process of $LiKSO_4$ and $LiK_{0.94}(NH_4)_{0.06}SO_4$. Values for $LiKSO_4$ are from [1]

Phase	I	II	III	IV	V	VI
$LiKSO_4$	937	707	226	200	186	T (K)
$LiK_{0.94}(NH_4)_{0.06}SO_4$	923	746	225	212	183	T (K)

Table 6
Atomic coordinates ($\times 10^4$) and equivalent isotropic displacement parameters ($Å^2 \times 10^3$) for $Li_2KNH_4(SO_4)_2$ at room temperature

	x	y	z	U(eq)
K(1)	3333	−3333	2208(3)	53(1)
K(2)	0	0	2417(2)	40(1)
K(3)	6667	3333	2206(3)	51(1)
S(1)	3342(1)	6(1)	4382(1)	24(1)
S(2)	3278(1)	−1722(1)	307(1)	23(1)
S(3)	5041(1)	1667(1)	313(1)	21(1)
S(4)	1596(1)	−76(1)	297(1)	18(1)
K(1N)	1823(1)	−1502(1)	7314(2)	44(1)
K(2N)	4819(1)	34(1)	7345(2)	40(1)
K(3N)	3354(1)	1438(1)	7406(2)	42(1)
Li(1)	3292(2)	3(2)	456(10)	30(2)
Li(2)	3365(3)	−1719(3)	4106(7)	25(1)
Li(3)	5083(3)	1674(2)	4142(6)	21(1)
Li(4)	1611(2)	−99(3)	4105(6)	22(1)
O(11)	3341(1)	25(2)	2662(4)	46(1)
O(12)	3596(3)	−614(2)	4920(4)	66(1)
O(13)	2490(2)	−196(3)	5012(4)	65(1)
O(14)	4018(2)	831(2)	5030(4)	56(1)
O(21)	2777(2)	−2574(2)	−496(4)	47(1)
O(22)	3001(2)	−1896(2)	1979(3)	44(1)
O(23)	3025(2)	−1095(2)	−230(3)	51(1)
O(24)	4175(2)	−1328(2)	159(4)	57(1)
O(31)	5825(2)	1933(2)	−577(4)	53(1)
O(32)	5230(2)	1572(2)	2010(3)	47(1)
O(33)	4384(2)	815(2)	−246(3)	53(1)
O(34)	4679(2)	2212(2)	200(4)	60(1)
O(41)	1301(2)	593(2)	124(3)	51(1)
O(42)	1436(1)	−349(1)	1954(3)	30(1)
O(43)	2500(2)	289(2)	−71(3)	44(1)
O(44)	1104(2)	−829(2)	−707(4)	62(1)

U(eq) is defined as one-third of the trace of the orthogonalized U_{ij} tensor. Occupancy factor for $K(1N)$, $K(2N)$ and $K(3N)$: $K = 0.333$, $N = 0.667$.

Table 7
Selected bond lengths (Å) and angles (deg)for $Li_2KNH_4(SO_4)_2$

K(1)–O(31) × 3	2.924(4)	K(2)–O(41) × 3	2.844(4)	K(3)–O(21) × 3	2.868(4)
K(1)–O(22) × 3	2.969(3)	K(2)–O(42) × 3	3.005(3)	K(3)–O(32) × 3	2.956(3)
K(1)–O(21) × 3	3.119(5)	K(2)–O(41) × 3	3.102(4)	K(3)–O(31) × 3	3.263(5)
K(1N)–O(44)	2.774(4)	K(2N)–O(12)	2.837(5)	K(3N)–O(22)	2.847(4)
K(1N)–O(34)	2.850(4)	K(2N)–O(33)	2.837(5)	K(3N)–O(14)	2.859(5)
K(1N)–O(23)	2.857(5)	K(2N)–O(24)	2.847(4)	K(3N)–O(43)	2.870(4)
K(1N)–O(13)	2.854(5)	K(2N)–O(32)	2.892(3)	K(3N)–O(42)	2.877(4)
K(1N)–O(43)	3.170(5)	K(2N)–O(14)	3.207(5)	K(3N)–O(34)	3.188(6)
K(1N)–O(11)	3.298(4)	K(2N)–O(24)	3.233(5)	K(3N)–O(13)	3.294(6)
		K(2N)–O(12)	3.359(6)	K(3N)–O(33)	3.314(5)
S(1)–O(11)	1.479(5)	S(2)–O(21)	1.514(3)	S(3)–O(31)	1.469(3)
S(1)–O(12)	1.489(3)	S(2)–O(22)	1.503(4)	S(3)–O(32)	1.528(4)
S(1)–O(13)	1.503(3)	S(2)–O(23)	1.500(3)	S(3)–O(33)	1.485(3)
S(1)–O(14)	1.492(3)	S(2)–O(24)	1.420(3)	S(3)–O(34)	1.441(2)
S(4)–O(41)	1.561(3)	Li(1)–O(43)	1.815(7)	Li(2)–O(31)	1.723(6)
S(4)–O(42)	1.488(4)	Li(1)–O(33)	1.885(5)	Li(2)–O(22)	1.916(8)
S(4)–O(43)	1.467(3)	Li(1)–O(23)	1.896(4)	Li(2)–O(12)	1.964(6)
S(4)–O(44)	1.481(4)	Li(1)–O(11)	1.897(10)	Li(2)–O(34)	2.069(6)
Li(3)–O(21)	1.838(5)	Li(4)–O(41)	1.836(6)		
Li(3)–O(32)	1.874(7)	Li(4)–O(13)	1.863(6)		
Li(3)–O(14)	1.927(5)	Li(4)–O(42)	1.892(7)		
Li(3)–O(24)	1.956(6)	Li(4)–O(44)	1.968(6)		
O(11)–S(1)–O(12)	109.4(2)	O(24)–S(2)–O(23)	107.4(2)		
O(11)–S(1)–O(14)	111.08(19)	O(24)–S(2)–O(22)	111.8(2)		
O(12)–S(1)–O(14)	103.54(19)	O(23)–S(2)–O(22)	104.78(17)		
O(11)–S(1)–O(13)	110.63(19)	O(24)–S(2)–O(21)	115.31(18)		
O(12)–S(1)–O(13)	112.0(2)	O(23)–S(2)–O(21)	112.36(19)		
O(14)–S(1)–O(13)	109.9(2)	O(22)–S(2)–O(21)	104.72(18)		
O(34)–S(3)–O(31)	116.07(19)	O(43)–S(4)–O(44)	108.29(17)		
O(34)–S(3)–O(33)	106.8(2)	O(43)–S(4)–O(42)	110.13(15)		
O(31)–S(3)–O(33)	108.5(2)	O(44)–S(4)–O(42)	108.82(18)		
O(34)–S(3)–O(32)	110.3(2)	O(43)–S(4)–O(41)	111.80(17)		
O(31)–S(3)–O(32)	107.4(2)	O(44)–S(4)–O(41)	112.4(2)		
O(33)–S(3)–O(32)	107.50(16)	O(42)–S(4)–O(41)	105.38(15)		
O(43)–Li(1)–O(33)	111.8(4)	O(31)–Li(2)–O(22)	112.1(3)		
O(43)–Li(1)–O(23)	113.7(3)	O(31)–Li(2)–O(12)	113.9(3)		
O(33)–Li(1)–O(23)	109.8(2)	O(22)–Li(2)–O(12)	113.0(3)		
O(43)–Li(1)–O(11)	106.2(3)	O(31)–Li(2)–O(34)	118.6(3)		
O(33)–Li(1)–O(11)	106.4(3)	O(22)–Li(2)–O(34)	99.9(3)		
O(23)–Li(1)–O(11)	108.5(4)	O(12)–Li(2)–O(34)	98.0(3)		
O(21)–Li(3)–O(32)	107.4(3)	O(41)–Li(4)–O(13)	113.4(4)		
O(21)–Li(3)–O(14)	114.4(2)	O(41)–Li(4)–O(42)	108.9(3)		
O(32)–Li(3)–O(14)	116.4(3)	O(13)–Li(4)–O(42)	115.8(3)		
O(21)–Li(3)–O(24)	115.2(3)	O(41)–Li(4)–O(44)	106.3(2)		
O(32)–Li(3)–O(24)	104.4(2)	O(13)–Li(4)–O(44)	106.2(3)		
O(14)–Li(3)–O(24)	98.5(3)	O(42)–Li(4)–O(44)	105.5(3)		

presence of the ammonium ion in this disordered system. The transition between the Phase IV and III could be of order–disorder or displacive. However, the disordered phase is at low temperature, so thermodynamic considerations suggest that the Phase IV has multiple domains of $P6_3$ symmetry and the phase transition is displacive. The conclusion that Phase IV has multiple domains agrees with the finding that Phase III′ was obtained by varying the ammonium concentration in the solution and with the optical observations of $LiKSO_4$ [20].

3.2. The $Li_2KNH_4(SO_4)_2$

$Li_2KNH_4(SO_4)_2$ was characterized by single-crystal X-ray diffraction. Atomic coordinates and selected bond length and angles are listed in Tables 6 and 7, respectively. Projection of the structure are shown in Fig. 3. The crystal structure can be described as a framework of corner-sharing LiO_4 and SO_4 tetrahedra with K^+ and NH_4^+ filling the cavities in the framework. Three symmetrically non-equivalent cavities are occupied by K^+ ions and the other three are randomly

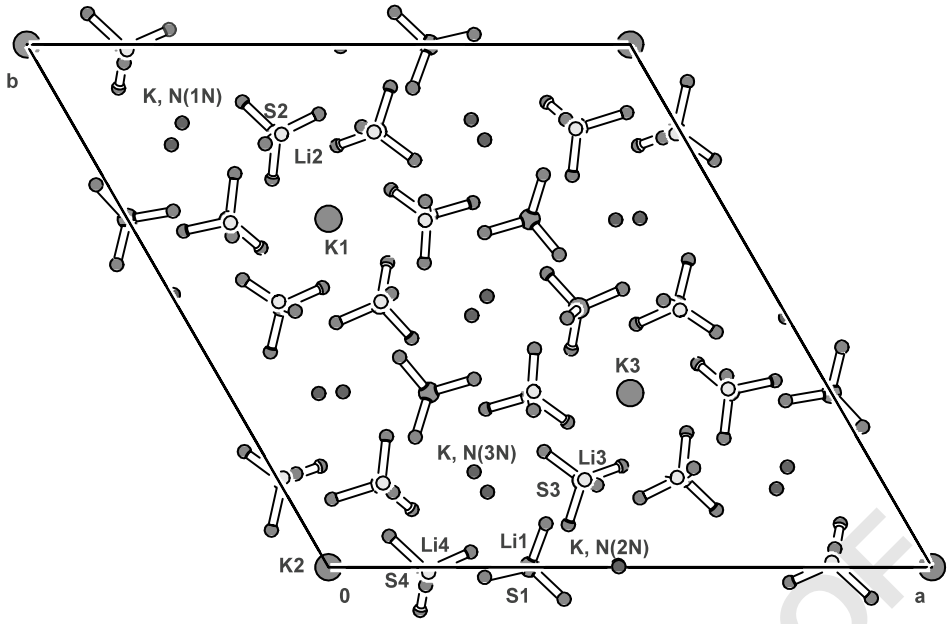

Fig. 3. Projection of the structure of the $Li_2KNH_4(SO_4)_2$ down the c-axis.

occupied by ammonium and potassium ions. The former displays nine-coordination while the latter displays six or seven-coordination. The S(1) sulfate ion acts as the bridge between four lithium ions and five cavities occupied randomly by potassium and ammonium. The remaining sulfate ions in the asymmetric unit act as the bridge between four lithium ions, two potassium ions and four cavities occupied randomly by ammonium and potassium. The structure has the same space group as Phase III of $LiKSO_4$ and a subunit of type of unit cell of $LiKSO_4$ can be defined. The subunit is defined by the vectors $a_{su} = -a/6 - b/3$; $b_{su} = a/3 + b/6$, $c_{su} = c$. The SO_4 ions are not oriented in parallel alignment as in $LiKSO_4$. If the structures at room temperature of $LiKSO_4$ [1], $LiNH_4SO_4$ [5], $LiNaSO_4$ [18,21] and $Li_2KNH_4(SO_4)_2$ are compared, all the unit-cell SO_4 tetrahedra are observed to have the same orientation in $LiKSO_4$, which is parallel to three-fold axes, the relationship between up and down is 3:1 in $Li_2KNH_4(SO_4)_2$, 2:1 in $LiNaSO_4$ and 1:1 in $LiNH_4SO_4$. The total spontaneous polarization for $Li_2KNH_4(SO_4)_2$ has been computed using the observed atomic coordinates and using an ionic model. The value obtained is 9.4×10^{-8} C/cm^2.

Table 8 shows the observed frequencies in Raman scattering of $Li_2KNH_4(SO_4)_2$. The vibration mode assignments in Raman spectra are easily obtained from the vibrational spectra studies for $LiNH_4SO_4$ [5] and $LiKSO_4$ [22–26].

The fitting in ν_2 (SO_4) spectral range was obtained if two peaks were assumed (Fig. 4). Only one mode is observed in this zone in $P6_3$ symmetry, while two modes are observed in $LiNH_4SO_4$ by the site group D_2

Table 8
The observed frequencies (cm^{-1}) in Raman scattering of $Li_2KNH_4(SO_4)_2$ which are compared with the Raman modes of $LiNH_4SO_4$ (5) and $LiKSO_4$ (18,19)

	$Li_2KNH_4(SO_4)_2$	$LiNH_4SO_4$(5)	$LiKSO_4$(18)	$LiKSO_4$(19)
t^{SO_4}	46.4(4)	41.14		
t^{SO_4}	58.3(3)			
t^{SO_4}	77.92(9)	76.5		
t^{K}	81.47(7)			
t^{K}	83.16(7)			
t^{NH_4}	197	195.2		
t^{Li}	404	394.6	405	
t^{Li}			411	
$\nu_2^{SO_4}$	458.3(2)	463.9	467	463
$\nu_2^{SO_4}$	474.91(17)	475.1		
$\nu_4^{SO_4}$	625.78(5)	633.2	623	623
$\nu_4^{SO_4}$	641.14(12)	642.3	635	635
$\nu_4^{SO_4}$	657.4(2)		647	
$\nu_1^{SO_4}$	1007.01(3)	1007.83	1012	1013
$\nu_3^{SO_4}$	1100.7(3)	1086.6		1118
$\nu_3^{SO_4}$	1116.4(4)	1104.86	1120	1119
$\nu_3^{SO_4}$		1121.6		
$\nu_3^{SO_4}$	1157.3(3)	1149.9		
$\nu_3^{SO_4}$	1177.3(13)	1175.0		
$\nu_3^{SO_4}$	1252.3(10)	1192.7	1204	
$\nu_3^{SO_4}$	1295.1(4)			
$\nu_4^{NH_4}$		1408.70		
$\nu_4^{NH_4}$	1422.0(5)	1441.5		
$\nu_2^{NH_4}$		1646		
$\nu_2^{NH_4}$	1684.2(11)	1680.55		

Values without e.s.d were not analytically fitted. The given value is the position of peak maximum.

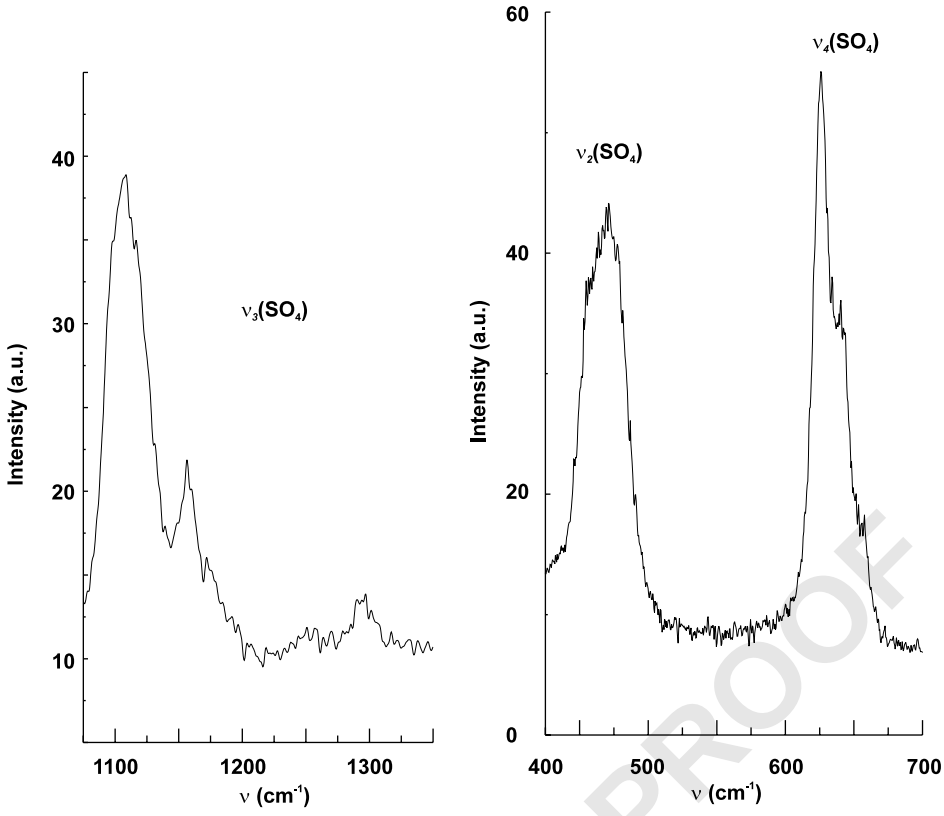

Fig. 4. Selected frequency ranges of Raman scattering of $Li_2KNH_4(SO_4)_2$ at room temperature.

symmetry of the SO_4. The shift of v_2 (SO_4) mode is explained by the different roles of SO_4 in the structure. The fitting in v_4 (SO_4) zone was obtained using three peaks (Fig. 4), which is similar to the result of Hiraishi et al. [22] for the $LiKSO_4$. The shift of the 1101–1116 v_3 (SO_4) mode was also observed by Frech et al. [23] in $LiKSO_4$ and Solans et al. [5] in $LiNH_4SO_4$. The remaining weaker peaks in the v_3 (SO_4) zone are more similar to those observed in $LiNH_4SO_4$. The v_4 (NH_4) and v_2 (NH_4) peaks are broader than those observed in $LiNH_4SO_4$, which indicates the disorder in this ion (Fig. 5).

Thermal analyses of $Li_2KNH_4(SO_4)_2$ were made using ATD, TG and powder X-ray diffraction. A phase transition is observed at 471.9 K. The high-temperature Phase is hexagonal, space group $P6_3/mmc$. The cell parameters at 483 K are $a = 10.5569(6)$ and $c = 8.7128(7)$ Å. During cooling (8 h), the transition is not reversible. The cell a parameter of the high-temperature phase is double the value of $LiKSO_4$, so the transition produces ion diffusion. The Raman scattering at different temperatures shows the phase transition of $Li_2KNH_4(SO_4)_2$ and the non-reversibility of the process after 2 h. The frequencies decrease with temperature. This agrees with the results obtained by Frech et al. [23] in $LiKSO_4$. The frequencies tend to overlap and the intensity decreases in inverse proportion to the temperature.

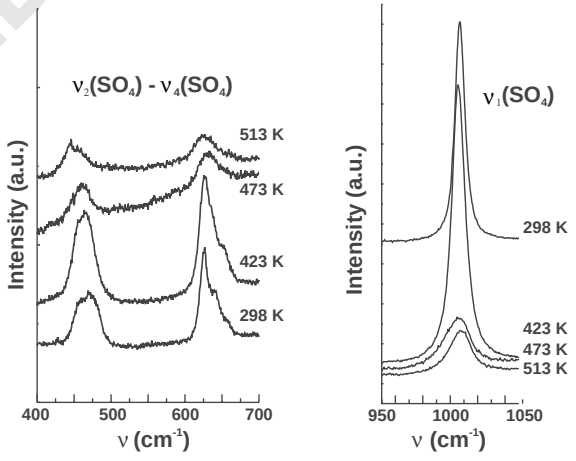

Fig. 5. Selected frequency ranges of Raman scattering of $Li_2KNH_4(SO_4)_2$ at different temperatures. The frequencies were measured in a warming process.

4. Conclusions

The results indicate that two processes lead to crystallization: the increase of the NH_4^+ concentration diminishes the crystallization rate because the mixture is more soluble in water and the NH_4^+ facilitates the formation of the enantiomorph form of Phase III. The use of single-crystal X-ray diffraction has allowed

determination of the enantiomorph of the phases obtained. From this, the new Phase III′ was determined and the observation of Phase IV confirms the existence of the same Phase in $LiKSO_4$, determined for the first time in [1]. The framework of corner-sharing LiO_4 and SO_4 tetrahedra is, then, relatively flexible. The phase transition temperatures for $Li[K_x(NH_4)_{1-x}]SO_4$ $x \geqslant 0.94$ are shown to be affected by the random presence of the ammonium ion in this disordered system.

A new phase $Li_2KNH_4(SO_4)_2$ has been obtained where the SO_4^{2-} ions are not oriented in parallel arrangement as in $LiKSO_4$. Moreover, the relationship between up and down SO_4^{2-} tetrahedra is 3:1. This relationship is higher than the value observed in other similar structures such as $LiNH_4SO_4$ and $LiNaSO_4$ and lower than $LiKSO_4$. The high-temperature Phase is hexagonal, space group $P6_3/mmc$, as in $LiKSO_4$, but the cell a-parameter is double that observed at high-temperature in $LiKSO_4$. The intermediate orthorhombic phase of $LiKSO_4$ is not observed in $Li_2KNH_4(SO_4)_2$. The phase transition is at 471.9 K, showing the high-temperature Phase in greater disorder as indicated by the Raman scattering results.

References

[1] X. Solans, M.T. Calvet, M.L. Martínez-Sarrión, L. Mestres, A. Bakkali, E. Bocanegra, J. Mata, M. Herraiz, J. Solid State Chem. 148 (1999) 316 (and references therein).
[2] M.A. Pimenta, P. Echegut, Y. Luspin, G. Hauret, F. Gervais, P. Abélard, Phys. Rev. B 39 (1989) 3361.
[3] U.A. Leitao, A. Righi, P. Bourson, M.A. Pimenta, Phys. Rev. B 50 (1994) 2754.
[4] C.B. Pinheiro, M.A. Pimenta, G. Chapuis, N.L. Speziali, Acta Crystallogr. B 56 (2000) 607.
[5] X. Solans, J. Mata, M.T. Calvet, M. Font-Bardia, J. Phys.: Condens. Matter 11 (1999) 8995 (and references therein).
[6] V. Lemos, R. Centoducatte, F.E.A. Melo, J. Mendes-Filho, J.E. Moreira, A.R.M. Martins, Phys. Rev. B 37 (1988) 2262.
[7] X. Dongfeng, Z. Siyuan, J. Phys. Chem. Solids 57 (1996) 1321.
[8] X. Dongfeng, Z. Siyuan, Chem. Phys. Lett. 301 (1999) 449.
[9] P.T.C. Freire, W. Paraguassu, A.P. Silva, O. Pilla, A.M.R. Teixeira, J.M. Sasaki, J. Mendes-Filho, I. Guedes, F.E.A. Melo, Solid State Commun. 109 (1999) 507.
[10] R.L. Moreira, P. Bourson, U.A. Leitao, A. Righi, L.C.M. Belo, M.A. Pimenta, Phys. Rev. B 52 (1995) 12591.
[11] G.M. Sheldrick, SHELXS A Computer Program for Crystal Structure Solution, University of Göttingen, 1997.
[12] G.M. Sheldrick, SHELXL A Computer Program for Crystal Structure Determination, University of Göttingen, 1997.
[13] H.D. Flack, Acta Crystallogr. A 39 (1983) 867.
[14] J. Rodríguez-Carvajal, WINPLOTR Laboratoire Léon Brillouin, Paris, France, 2000.
[15] H. Traube, N. Jahrbuch, Mineralogie Bd II (1892) 57.
[16] H. Traube, N. Jahrbuch, Mineralogie Bd I (1894) 171.
[17] H. Klapper, Th. Hahn, S.J. Chung, Acta Crystallogr. B 43 (1987) 147.
[18] J. Mata, X. Solans, M.T. Calvet, J. Molera, M. Font-Bardia, J. Phys.: Condens. Matter 14 (2002) 5211.
[19] W. Clegg, A.J. Blake, R.O. Gould, P. Main, in: Crystal Structure Analysis Principles and Practice, Vol. 144, Oxford Science Publishers, Oxford, 2002.
[20] R. Cach, P.E. Tomaszewski, J. Bornarel, J. Phys. C: Sol. State Phys. 18 (1985) 915.
[21] B. Morosin, D.L. Smith, Acta Crystallogr. 22 (1967) 906.
[22] J. Hirashi, N. Taniguchi, H. Takahashi, J. Chem. Phys. 65 (1976) 3821.
[23] R. Frech, D. Teeters, J. Phys. Chem. 88 (1984) 417.
[24] D. Teeters, R. Frech, Phys. Rev. B 26 (1982) 4132.
[25] S.L. Chaplot, K.R. Rao, A.P. Roy, Phys. Rev. B 29 (1984) 4747.
[26] N. Choudhury, S.L. Chaplot, K.R. Rao, Phys. Rev. B 33 (1986) 8607.

BOLETIN DE LA SOCIEDAD ESPAÑOLA DE
Cerámica y Vidrio
A R T I C U L O

Caracterización por difracción de rayos-X, análisis térmico y espectroscopía Raman de los cristales mixtos $Li(NH_4)_{1-x}K_xSO_4$

J. MATA, X. SOLANS Y T. CALVET
Departament de Cristal·lografia, Universitat de Barcelona, 08028-Barcelona, España.

En este trabajo se estudia la preparación y caracterización de las fases de los cristales mixtos de fórmula $Li(NH_4)_{1-x}K_xSO_4$. La caracterización se ha efectuado por análisis térmico con DSC y ATD, difracción de rayos-X sobre polvo cristalino con temperatura variable, difracción de rayos-X sobre muestra monocristalina a temperatura variable a fin de determina su estructura cristalina y por espectroscopía Raman a temperatura variable. Se han obtenido dos tipos de fases. Una solución sólida con $0.94 < x < 1$ que presenta los mismos tipos estructurales que el $LiKSO_4$, pero según el método de cristalización pueden aparecer nuevas fases que no presenta el $LiKSO_4$. El segundo tipo de compuesto tiene por fórmula $Li(NH_4)_{0.53}K_{0.47}SO_4$, el cual presenta una estructura hexagonal con parámetro $a \approx 3\ a_{LiKSO4}$. Este compuesto tiene por encima de la temperatura ambiente una sola transición a 463K.

Palabras clave: Cerámicas ferroeléctricas. Caracterización estructural. Espectroscopia Raman. Difracción de Rayos-X.

X-ray diffraction, thermal analysis and raman spectroscopy characterization of $Li(NH_4)_{1-x}K_xSO_4$ mixex crystals.

The preparation and characterization of mixed crystals with formula $Li(NH_4)_{1-x}K_xSO_4$ has been carried out. The characterization was by thermal analysis (DSC and ATD), X-ray diffraction on powder and single crystal samples at variable temperature and Raman spectroscopy at variable temperature. Two type of phases have been obtained: A solid solution with $0.94 < x < 1$, with the same phases to those observed in the $LiKSO_4$, but new phases, which are not shown by the $LiKSO_4$, can be obtained according to the crystallization process. The second type of compounds have the formula $Li(NH_4)_{0.53}K_{0.47}SO_4$, with an hexagonal structure ($a \approx 3\ a_{LiKSO4}$). This compound have a phase transition at 463K.

Key words: Ferroelectric ceramics. Structural characterization. Raman spectroscopy. X-Ray diffraction.

1. INTRODUCCIÓN

El $LiKSO_4$ presenta una estructura cristalina hexagonal, derivada de la tridimita, con los tetraedros SO_4 y LiO_4 orientados en la dirección [001] y todos ellos en el mismo sentido. El compuesto presenta numerosas transiciones de fases, con algunas de ellas con propiedades ferroeléctricas. Una revisión de la caracterización de este compuesto ha sido efectuada por Solans, Calvet, Martínez-Sarrión, Mestres, Bakkali, Bocanegra, Mata y Herraiz (1) a fin de dilucidar las numerosas contradicciones que se encuentran en la bibliografía. La polarización espontánea de este compuesto es paralela al eje [001] y del tipo iónico.

El $LiNH_4SO_4$ presenta una estructura rómbica derivada de la tridimita, es pseudo-isoestructural a la del $LiKSO_4$ con los tetraedros SO_4 y LiO_4 orientados en la dirección [001] de la celda hexagonal, que deriva de la celda rómbica que presenta la estructura, pero difiere del $LiKSO_4$ en que los tetraedros están orientados en los dos sentidos de la dirección $[001]_{hex}$. El compuesto presenta también numerosas transiciones de fases y una caracterización de las diferentes fases en el intervalo 298-700K ha sido efectuada por Solans, Mata, Calvet y Font-Bardia (2). La polarización espontánea de este compuesto es perpendicular al eje $[001]_{hex}$ y del tipo dipolar.

El estudio de soluciones sólidas entre compuestos que presentan diferentes tipos de transiciones ha sido utilizado para determinar la competitividad entre diferentes iones y caracterizar mas claramente las causas que provocan éstas. Ello, por ejemplo, ha sido efectuado en los compuestos del tipo A_2BX_4 (3) con estructura del tipo β-K_2SO_4. Siguiendo esta línea se ha efectuado este trabajo.

2. EXPERIMENTAL

2.1 Síntesis y cristalización. $LiMSO_4$ (M = K, NH_4) se obtuvo por reacción del M_2SO_4 con Li_2SO_4. H_2O en una solución acuosa a 333K. Detalles de su síntesis y cristalización fueron descritos en (1 y 2). Los cristales mixtos se obtuvieron por reacción en solución acuosa de $LiNH_4SO_4$ y $LiKSO_4$ a diferentes proporciones. (Se ha trabajado con 9:1, 7:3, 1:1, 3:7 y 1:9). La cristalización fue por evaporación lenta a 333K. Todos los cristales obtenidos fueron analizados por ICP (Induced Condensed Plasma) con un analizador Jobin-Yvon y por difracción de rayos-X sobre polvo cristalino con un equipo Siemens D500.

2.2 Análisis térmico. Los análisis térmicos fueron realizados con un Calorímetro Diferencial de Barrido (DSC) Perkin-Elmer DSC-7 para procesos de temperaturas inferiores a la temperatura ambiental y con un Análisis Térmico Diferencial (DTA) Netzsch, el cual lleva incorporado una balanza térmica (TG), para procesos a temperaturas superiores a la ambiental. La velocidad de calentamiento fue, usualmente, de 5 K/min.

2.3 Determinación de estructuras cristalinas. El mismo método fue seguido en todas las determinaciones estructurales. Las intensidades fueron recogidas en un difractómetro Enraf-Nonius CAD4 equipado con un monocromador de grafito. Se utilizó la técnica de rastreo ω-2Θ scan. La anchura del scan fue calculada por la expresión A + B tan Θ, en donde A se define a partir de la mosaicidad que presenta la muestra y B es definido por el tipo de radiación utilizada y se aplica para incrementar la anchura de medida para incorporar la separación producida por el Mo $K\alpha_1$-$K\alpha_2$ splitting.

Los parámetros de la celda se obtuvieron por mínimos cuadrados a partir del centraje automático de 25 reflexiones en el intervalo $12° < \Theta < 21°$. Tres intensidades se midieron cada dos horas como control de intensidad y de la orientación del cristal. Una caída de intensidad no fue observada en ninguna muestra.

Las estructuras fueron resueltas por métodos directos utilizando el programa SHELXS (4) y refinadas por mínimos cuadrados, utilizando la matriz completa, con el programa SHELXL (5). La función minimizada fue $w \, ||Fo|^2 - |Fc|^2|^2$, en donde el método de pesaje fue $w = [\sigma^2(I) + (k_1 P)^2 + k_2 P]^{-1}$ y $P = (|Fo|^2 + 2|Fc|^2)/3$. Los valores de k_1 y k_2 fueron también afinados. La quiralidad de la estructura fue definida por el coeficiente de Flack.

2.4 Difracción de polvo cristalino. La difracción de polvo cristalino fue realizada en un equipo Siemens D500, con una cámara Aaton-Par HTK, que permitía variar la temperatura de la muestra. Se utilizó la radiación Cu Kα y un monocromador secundario. La velocidad de calentamiento o enfriamiento fue de 5 K/min y la muestra fue dejada 10 min a la temperatura de medida a fin de estabilizar el equipo y la muestra. La anchura de paso fue 0.025°, el tiempo de paso fueron 10 seg y los intervalos de 2 Θ de medida fueron 10 - 80°. Los parámetros de celda se afinaron con el programa FULLPROF (6).

2.5 Espectroscopia Raman. Espectros de Raman fueron excitados sobre muestras pulvurentas utilizando un espectrómetro Jobin Yvon T64000 y una excitación por medio de un láser de argón. El detector fue un Control Data CDC. Se trabajó con la línea 514.5 nm y la potencia fue seleccionada según la respuesta de cada muestra. Una celda calentadora Mettler FP84 se utilizó para medir el espectro a diferentes temperaturas. La posición, la amplitud a media altura y la intensidad relativa de cada pico fue calculada considerando los picos como una función Lorentziana (La contribución Gaussiana es despreciable).

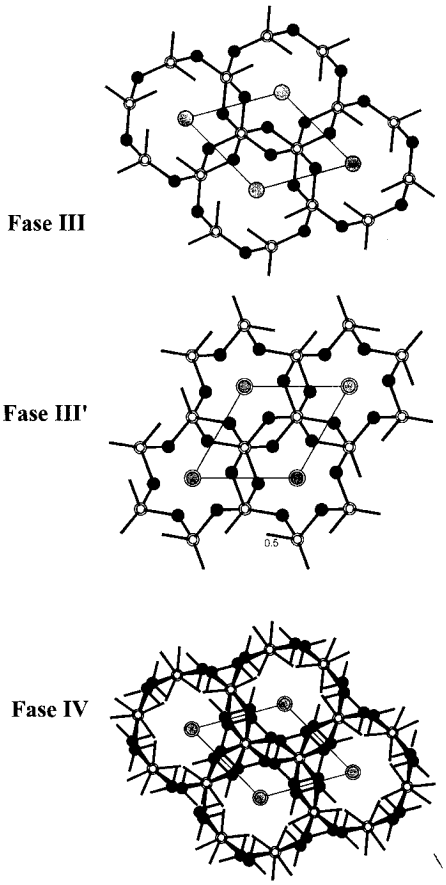

Figura 1 Las diferentes estructuras cristalinas del $Li(NH_4)_{0.06}K_{0.94}SO_4$

3. RESULTADOS Y DISCUSIÓN

La preparación de los cristales mixtos presenta varias dificultades: El $LiNH_4SO_4$ por encima de los 601 K descompone en el momento que funde, ello impide la obtención de los cristales mixtos por fusión. Si se preparan a partir de disolución acuosa, la dificultad está en la diferente solubilidad del $LIKSO_4$ y del $LiNH_4SO_4$, siendo menos soluble el primero. La tercera dificultad son aquellas típicas del método de disolu-

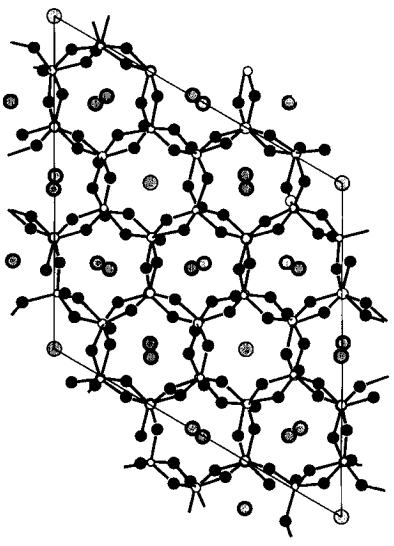

Figura 2 Estructura cristalina a temperatura ambiente del $Li(NH_4)_{0.53}K_{0.47}SO_4$

TABLA I. DATOS CRISTALINOS Y DEL REFINAMIENTO DE LA ESTRUCTURA $Li(NH_4)_{0.06}K_{0.94}SO_4$

	Fase III	Fase III'	Fase IV
Peso de la fórmula	140.73	140.94	139.99
Temperatura (K)	293(1)	293(1)	293(1)
Longitud de onda (Å)	0.71069	0.71069	0.71069
Sistema cristalino	hexagonal	hexagonal	hexagonal
Grupo espacial	$P6_3$	$P6_3$	$P6_3mc$
a(Å)	5.1370(8)	5.1467(7)	5.152(2)
c(Å)	8.638(7)	8.666(3)	8.642(3)
Volumen($Å^3$)	197.41(17)	198.80(8)	198.65(13)
Z, Densidad calculada (Mg/m^3)	2, 2.368	2, 2.355	2, 2.340
Coeficiente de Absorción (mm^{-1})	1.669	1.668	1.622
F(000)	139	139	139
Dimensiones del cristal (mm)	0.2 x 0.2 x 0.3	0.1 x 0.1 x 0.2	0.1 x 0.1 x 0.3
Intervalo de 2Q en I_{hkl} medidos (°)	4.58 - 29.96	4.57 - 30.02	4.57 - 29.99
Intensidades medidas / únicas	660 / 208		
[R(int) = 0.0256]	1155 / 211		
[R(int) = 0.0758]	1026 / 131		
[R(int) = 0.0153]			
Porcentaje de medidas para 2Q = 29.98	100%	99.5%	
	94.9%		
Datos/parámetros	208 / 24	211 / 24	131 / 24
Goodness-of-fit on F^2	1.319	1.363	1.285
Final R [I>2sigma(I)]	R1 = 0.0366		
	R1 = 0.0380		
wR2 = 0.0926	R1 = 0.0344		
wR2 = 0.1034			
wR2 = 0.0980			
R índices (Todos los datos)	R1 = 0.0366		
wR2 = 0.0926	R1 = 0.0380		
wR2 = 0.1034	R1 = 0.0344		
wR2 = 0.0980			
Parámetro de estructura absoluta	0.2(2)	-0.1(4)	-0.1(3)
Máximo y min. pico en síntesis de diferencia (e. $Å^{-3}$)	0.502 y -1.110	0.696 y -0.579	0.494 y -0.481

TABLA II. TEMPERATURAS DE TRANSICIÓN DEL $Li(NH_4)_{0.06}K_{0.94}SO_4$ Y COMPARACIÓN CON LAS TEMPERATURAS DEL $LIKS0_4$

$LiKS0_4$	$LI(NH_4)_{0.06}K_{0.94}SO_4$
937	923
707	746
226	225
200	212
186	183

TABLA III. DATOS CRISTALINOS Y DEL REFINAMIENTO DE LA ESTRUCTURA $Li(NH_4)_{0.53}K_{0.47}SO_4$

Peso de la fórmula	128.85
Temperatura (K)	293(1)
Longitud de onda (Å)	0.71069
Sistema cristalino	hexagonal
Grupo espacial	$P6_3$
a(Å)	18.188(2)
c(Å)	8.595(15)
Volumen($Å^3$)	2460(5)
Z, Densidad calculada (Mg/m^3)	24, 2.088
Coeficiente de Absorción (mm^{-1})	1.142
F(000)	1528
Dimensiones del cristal (mm)	0.2 x 0.2 x 0.3
Intervalo de 2Θ en I_{hkl} medidos (°)	2.24 - 29.98
Intensidades medidas / únicas	7543 / 2472 [R(int) = 0.0152]
Porcentaje de medidas para 2Θ = 29.98	97.2%
Datos/parámetros	2421 / 256
Goodness-of-fit on F^2	1.042
Final R [I>2sigma(I)]	R1 = 0.0389, wR2 = 0.1043
R índices (Todos los datos)	R1 = 0.0391, wR2 = 0.1045
Parámetro de estructura absoluta	0.00(9)
Máximo y min. Pico en síntesis de diferencia (e. $Å^{-3}$)	0.778 y -0.378

ción, especialmente los gradientes de concentración en la solución. Todo ello provoca las dificultades de la elaboración del diagrama de fases y a partir de los resultados obtenidos se observa cierta tendencia a cristalizar compuestos con mayor riqueza de K a causa de su menor solubilidad.

3.1 Solución sólida $Li(NH_4)_{1-x}\ K_xSO_4$ para $x > 0.94$. Siempre que se cristaliza con relaciones de $LIKSO_4$: $LINH_4SO_4$ igual a 9:1 en la primera cristalización se obtiene esta solución sólida, y las siguientes recristalizaciones de las aguas madres se obtiene directamente el $LIKSO_4$. Si la relación es 7:3 se obtiene en todas las recristalizaciones la solución sólida descrita, pero en la primera cristalización se obtiene la fase III´ que no se observa en el $LIKSO_4$ (Figura 1 y Tabla I), en la segunda se obtiene como metastable la fase IV del $LIKSO_4$ y en las posteriores la fase III del mismo compuesto. Con la relación 5:5 y 3:7 se obtiene como primera cristalización esta solución sólida, mientras que aparecen otras fases en las posteriores recristalizaciones. Para el elemento obtenido más rico en NH_4 se ha efectuado la caracterización térmica del compuesto, presentando las mismas transiciones que el $LIKSO_4$ (Tabla II).

3.2 La fase $Li(NH_4)_{1-x}\ K_xSO_4$ para $x < 0.94$. Se ha determinado la estructura cristalina a temperatura ambiente para $x = 0.47$. Ésta es hexagonal como el $LIKSO_4$ (Figura 4 y Tabla III). Sus parámetros de celda son $a = 18.178 \approx 3\ .\ a_{LiKSO4}$ mientras que el parámetro $c = 8.5949$ Å $\approx c_{LiKSO4}$. Al ser la estructura hexagonal indica que los tetraedros SO_4 y LiO_4 no sólo están orientados en la dirección [001] si no también están todos en la misma dirección. El potasio y el amonio ocupan las cavidades dejadas por la red tridimensional de tetraedros, existiendo cavidades exclusivamente ocupadas por el ion K^+ y otras ocupadas aleatoriamente por los iones potasio y amonio.

Si se compara el Raman a temperatura ambiente de esta fase y aquel medido para el $LINH_4SO_4$ (Figura 5) se observa que las diferencias más importantes se produce en los modos externos de vibración y en los modos internos ν_4^{SO4} y ν_3^{SO4}.

Por análisis térmico y por Raman se ha estudiado el comportamiento térmico del compuesto. Éste presenta una transición a 463 K. La figura 6 muestra los resultados obtenidos a diferentes temperaturas. Se observa que la fase de alta temperatura permanece estable al enfriar la muestra, lo cual sugiere que la transición es de primer orden. Estudios exhaustivos sobre el tiempo de permanencia de la metastabilidad no se han efectuado. El límite que en estos momentos se dispone de información es de permanencia de la metastabilidad durante 3 horas. La interpretación de los Raman a elevada temperatura presenta la dificultad del incremento del fondo producido por la fluorescencia que da la muestra. A pesar de ello se observa un descenso de los modos externos lo que sugiere una estructura mas abierta y menos compacta. Ello viene confirmado por la variación de los modos de vibración del amonio y la aparición de amplios máximos que representan nuevos modos de ν^{SO4}.

4. CONCLUSIONES

Se han observado dos tipos estructurales de cristales mixtos de fórmula $Li(NH_4)_{1-x}\ K_xSO_4$: El primero presenta la misma estructura que el $LiKSO_4$ a temperatura ambiente, observándose las mismas transiciones estructurales que este. La composición de estos cristales mixtos queda reducida al intervalo $0.94 \leq x \leq 1$. Se pueden presentar algunas fases metastables que no se observan en el $LiKSO_4$ según las condiciones de crecimiento de los cristales. El segundo presenta una composición entorno $K{:}NH_4 = 1{:}1$, con una estructura de la misma simetría que el $LiKSO_4$, pero con un parámetro a triplicado. El estudio debe de continuar ensayando cristalizaciones con proporciones de $LiKSO_4$:$LiNH_4SO_4$ inferiores a 1:9 a fin de determinar si existen cristales mixtos más ricos en amonio. La proporción viene definida por la mayor solubilidad del $LiNH_4SO_4$ con respecto al $LiKSO_4$.

BIBLIOGRAFÍA

1. X. Solans, T. Calvet, M.L. Martínez-Sarrión, L. Mestres, A. Bakkali, E. Bocanegra, J. Mata y M. Herraiz. "Thermal Analysis and X-Ray Diffraction Study on $LiKSO_4$: A New Phase Transition". J. of Solid State Chem., **147**, in press, 1999.
2. X. Solans, J. Mata, T. Calvet y M. Font-Bardia. "X-Ray Structural Characterization", Raman and Thermal Analysis of $LiNH_4SO_4$ Above Room Temperature. J. of Physics: Condensed Matter, **11**, 8995-9007, (1999).
3. C. González-Silgo, X. Solans, y C. Ruiz´-Pérez. "Stability of b-K_2SO_4 Type Structures with Paraelectric-Ferroelectric Transition". Acta Cryst., B, in press, 1999 (y referencias en este trabajo).
4. G.M. Sheldrick. SHELS 97. "A computer program for crystal structure determination", University of Göttingen, Alemania, 1997.
5. G.M. Sheldrick. SHELL 97. "A computer program for crystal structure determination" University of Göttingen, Alemania, 1997.
6. J. Rodríguez-Carvajal. FULLPROF, version 3.1c, Laboratoire Leon Brioullin, Paris, Francia, 1996.

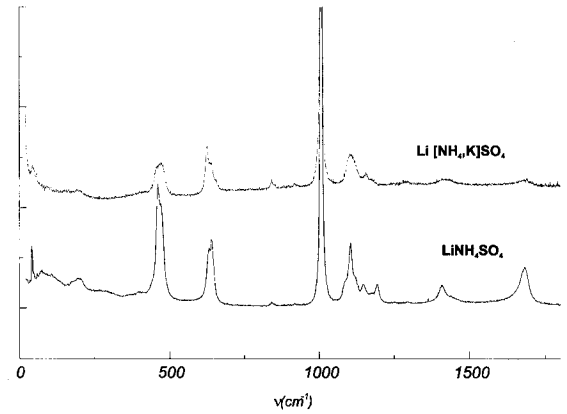

Figura 3 Comparación de los espectros Raman del $Li(NH_4)_{0.53}\ K_{0.47}SO_4$ y $LiNH_4SO_4$

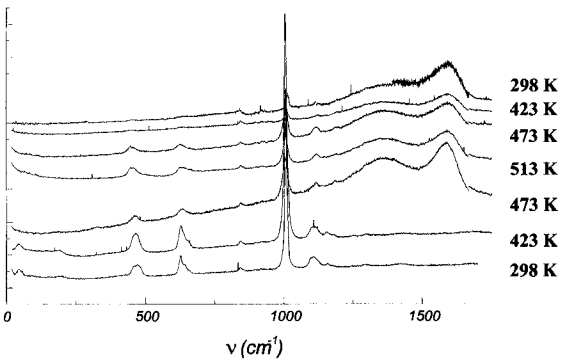

Figura 4 Espectros Raman a diferentes temperaturas del $Li(NH_4)_{0.53}\ K_{0.47}SO_4$

International Centre for Diffraction Data
12 Campus Boulevard
Newtown Square, Pennsylvania 19073-3273 U.S.A.
Technical: 610.325.9814 • Sales: 610.325.9810
Fax: 610.325.9823 • info@icdd.com • www.icdd.com

ICDD®
ISO 9001:1994 Certified

23 August 2002

Dr. Xavier Solans
Departament Cristallografia
Mineralogia i Dipòsits Minerals,
Universitat de Barcelona
E-08028-Barcelona
Spain

Dear Dr. Solans:

Enclosed is a copy of your submitted powder pattern as it will appear in Release 2002 of the **Powder Diffraction File**. Also enclosed is a certificate which is being awarded to you in recognition of your significant contribution to the File.

Again, the ICDD appreciates your cooperation and interest in the **Powder Diffraction File**.

Yours truly,

W. Frank McClune

W. Frank McClune
Editor-in-Chief

WFM:jah
enclosures

52-1600

C

$LiNH_4SO_4$

Lithium Ammonium Sulfate

Rad. CuKα **λ** 1.5418 **Filter** Mono **d-sp** Calculated
Cut off **Int.** Calculated **$I/I_{cor.}$**
Ref. Solans, X., Dept. Cristallografia, Univ. de Barcelona, Spain, *Private Communication*, (2000)

Sys. Orthorhombic **S.G.** $P2_1nb$ (33)
a 5.3105(7) **b** 8.7612(8) **c** 9.2114(7) **A** **C**
α **β** **γ** **Z** 4 **mp**
Ref. Solans, X. et al., *J. Phys.: Condens. Matter*, **11** 8995 (1999)

D_x 1.876 D_m **SS/FOM** F_{30}=1000(.000,44)

Pattern taken at 468 K. Phase I'. C.D. Cell: a=8.761, b=9.211, c=5.311. a/b=0.9511, c/b=0.5765. S.G.=$Pna2_1$ (33). PSC: oP44.

Plus 2 reflections to 1.5650.

dÅ	Int	hkℓ	dÅ	Int	hkℓ
6.3483	293	011	2.2047	20	221
4.6057	293	002	2.1903	163	040
4.6007	118	101	1.9214	49	231
4.3806	408	020	1.9030	12	124
4.0767	999	012	1.8257	32	223
4.0732	445	111	1.8029	335	015
3.9560	22	021	1.7831	11	043
3.3792	86	120	1.7405	28	105
3.2337	412	112	1.7397	30	204
3.1741	445	022	1.7384	19	301
3.1725	468	121	1.7214	37	051
2.8977	42	013	1.7118	88	134
2.7838	55	031	1.7072	36	115
2.7246	40	122	1.7064	25	214
2.6581	158	103	1.7051	13	311
2.6552	317	200	1.6904	13	143
2.5436	12	113	1.6896	21	240
2.5143	100	023	1.6549	10	233
2.4664	26	032	1.6412	12	320
2.4656	71	131	1.6377	23	052
2.4496	81	211	1.6375	33	151
2.3028	28	004	1.6237	45	312
2.3003	43	202	1.6175	64	125
2.2272	18	014	1.6169	32	224
2.2249	156	212	1.5871	12	044

Journal of Solid State Chemistry **156,** 251–252 (2001)
doi:10.1006/jssc.2000.8988, available online at http://www.idealibrary.com on IDEAL®

RAPID COMMUNICATION

Comment on "Thermal Analysis and X-Ray Diffraction Study on $LiKSO_4$: A New Phase Transition"

Xavier Solans,* M. Teresa Calvet,* M. Luisa Martínez-Sarrión,† Lourdes Mestres,† Aniss Bakkali,† Eduardo Bocanegra,‡ Jorge Mata,* and Marta Herraiz†

* *Departament Cristallografia, Mineralogia i Dipòsits Minerals, Universitat de Barcelona, E-08028 Barcelona, Spain;* † *Departament de Química Inorgànica, and* ‡ *Departamento de Física Aplicada II, Universidad del Pais Vasco, E-48080 Bilbao, Spain*

Received July 19, 2000; in revised form September 4, 2000; accepted October 6, 2000; published online December 21, 2000

In the preceding manuscript, Tomaszewski comments on our previous paper, X. Solans *et al.*, *J. Solid State Chem.* 148, 316 (1999). These comments can be summarized in two points: (a) The influence of the domain or/and twinning on the obtained results and (b) the poor data obtained in the mentioned paper. An answer is given. © 2001 Academic Press

1. THE DOMAIN/TWINNING STRUCTURE

There is great confusion between twinning and domain formation in the Comment of Tomaszewski. We think that it is necessary to differentiate between the twin crystal obtained from a crystallization process and domain formation (or could be accepted twin formation) due to phase transition. Reference (1) is not the first manuscript on $LiKSO_4$ that deals with an untwinned crystal. An example is reported in (2), and we think that Tomaszewski accepts it, because he states in his introduction "the data obtained below the room temperature are controversial," so as a minimum he accepts the results at room temperature or above room temperature. The phase at room temperature is $P6_3$ (ordered structure), while a twin crystal at room temperature gives a $P6_3$ (disordered structure) or $P2_1$ (3). We remark that the same untwinned crystal was used in all processes on the single-crystal diffractometer in (1). The second point is the domain formation. Here there are two possibilities: These domains can be randomly distributed or ordered. Randomly distributed could produce double or broad peaks in the X-ray diffraction pattern and a high standard deviation in the obtained cell parameters. In the structure determination process a high Flack coefficient for the refined structural model would be obtained, an example of which and how it is solved can be found in (4). An ordered distribution of the domains will give good cell parameters with good standard deviations; surely, a disordered atomic structure and (if the disorder model is correct) will give a correct Flack coefficient. We remark that the authors of (1) are in this second possibility and we state in our results and discussion and in our conclusions that the phase $P6_3mc$ and $Cmc2_1$ "have multiple domains of $P6_3$ and Cc symmetry," which agrees with the comments of Tomaszewski in the preceding manuscript and with the results of (5) and (6). The lack of observation of domains in the phase $P31c$ agrees with the results of (6), of which Tomaszewski is an author. In (6), p. 916, section 3, line 17, the authors state (during a heating process) "Above 194 K the domains disappear ...." Above 194 K corresponds in (1) to the phase $P31c$, which is assumed by Solans *et al.*, to be without domain structure. Could Tomaszewski explain the contradiction between his present comment and that in his paper (6)?

2. THE POOR DATA OF (1)

Tomaszewski states that the cell parameters obtained by X-ray Bond method (7) have an accuracy of 10^{-5}. He confuses the equipment accuracy of 2θ with the accuracy of the cell parameters. An example of our comment is the paper (8) where the Bond method is used. In Table 1 of this manuscript the accuracy of the obtained cell parameters is 2×10^{-4} for a and b parameters and 10^{-4} for c parameter for a crystal of cell volume equal to 400 Å^3. An accuracy of 10^{-4} was obtained in (1).

In Table 1 the measurements of cell parameters of Desert *et al.* (9) and Solans *et al.* (1) are compared. The two measurements are different and give different results because

(a) The higher cooling and heating rates in Solans *et al.* measurements facilitate the kinetics of phase transitions,

0022-4596/01 $35.00

TABLE 1
Comparison of the Method Used to Determined the Cell Parameters at Different Temperatures in Refs. (1) and (9)

	Desert *et al.* (9)	Solans *et al.* (1)
Geometry	Reflection	Transmission
Beam	Divergent	Parallel
Sample	Single crystal	Powder
Scan	Missing ($\omega/2\theta$ from Figs. 1 and 4?)	Detector: fixed Sample: Phi rotation
Wavelength	Missing	Cu$K\alpha$
Primary monochromator	Missing (None from figures)	Quartz monochromator
Exposure time for each value	Scan speed is missing	>1 h
Temperature range	100–298 K	163–298 K
Cooling and heating rate	0.43 K/min	10 K/min
No. of reflections used to determine cell parameters	2 (0 0 8 and 0 4 0)	All between 2 and 120°

while the lower rate in Desert *et al.* measurements facilitates the observation of metastable phases.

(b) The number of reflections used to determine the cell parameters by Solans *et al.* give an average information for the entire sample. The use of one reflection to determine each cell parameter in Desert *et al.* implies that systematic errors in the measurements of this peak will be reflected in the obtained cell parameter.

(c) The phi scan used by Solans *et al.* diminishes the domain effects on the determination of cell parameters. In the Desert *et al.* study a phi scan is not used in order to study the domain effects, as is stated in (9).

(d) The shortest temperature range in (1) does not allow the study of the $Cmc2_1$ phase.

The results of Desert *et al.* are different because

(a) Desert *et al.* use reflection geometry and divergent beam, so the width and the asymmetry effects of the peak are higher than those obtained by Solans *et al.* The overlapping of $K\alpha_1$ and $K\alpha_2$ in the 0 4 0 reflection is important and the number of counts per peak is different in the two measurements because different type of sample and exposure time are used. All that produces less accuracy in the determination of the peak position in the measurements of Desert *et al.* than that obtained by Solans *et al.*

(b) The main problem in the measurements reported in (7) and (9) is the tilt angle between the crystal face and the goniometer plane, a test of which is not stated in either manuscript.

Despite all that, it is well known that all phase transition processes depend on their history, so the two measurements are not readily comparable.

The enthalpies of the phases transitions in (1) were measured during the heating process. The peak overlap of phase transitions II and III was solved by a multipeak computer fit, using an asymmetric pseudo-Voight function. The onset temperatures were determined using the maximum slope method.

As a last remark, we agree with Tomaszewski's comment concerning the phase at 189 K. The space group is $P31c$.

REFERENCES

1. X. Solans, M. T. Calvet, M. L. Martínez-Sarrión, L. Mestres, A. Bakkali, E. Bocanegra, J. Mata, and M. Herraiz, *J. Solid State Chem.* **148,** 316 (1999).
2. J. Ortega, J. Etxebarria, and T. Breczewski, *J. Appl. Cryst.* **26,** 549 (1993).
3. S. Bhakay-Tamhane, A. Sequeira, and R. Chidambaram, *Acta Crystallogr. Sect. C* **40,** 1648 (1984).
4. X. Solans, J. Mata, M. T. Calvet, and M. Font-Bardia, *J. Phys.: Condens. Matter* **11,** 8995 (1999).
5. W. Kleemann, F. J. Schaefer, and A. S. Chaves, *Solid State Commun.* **64,** 1001 (1987).
6. R. Cach, P. E. Tomaszewski, and J. Bornarel, *J. Phys. C: Sol. State Phys.* **18,** 915 (1985).
7. P. E. Tomaszewski and K. Lukaszewicz, *Phase Transit.* **4,** 37 (1983).
8. P. E. Tomaszewski and A. Pietraszko, *Phys. State Sol. (a)* **56,** 467 (1979).
9. A. Desert, A. Gibaut, A. Righi, U. A. Leitao, and R. L. Moreira, *J. Phys.: Condens Matter* **7,** 8445 (1995).

J. Phys.: Condens. Matter **12** (2000) 8933–8936. Printed in the UK PII: S0953-8984(00)12363-X

COMMENT

Comment on 'X-ray structural characterization, Raman and thermal analysis of $LiNH_4SO_4$ above room temperature'

Paweł E Tomaszewski

Institute of Low Temperature and Structure Research, Polish Academy of Sciences, 50–950 Wrocław 2, Poland

Received 29 February 2000, in final form 27 July 2000

Abstract. In a recent paper (1999 *J. Phys.: Condens. Matter* **11** 8995) Solans *et al* observed a new phase transition and solved the structure of high-temperature phases. We believe that the results commented on can be explained by the mixture of two different components (α and β modifications or ferroic domains) in the sample and not by introducing the two new intermediate phases supposed by Solans *et al*.

In a recent publication Solans *et al* [1] present results of their x-ray and Raman studies of $LiNH_4SO_4$ above room temperature. This crystal has been well known since 1868 [2, 3]. Its structure and physical properties were extensively studied by various methods especially in the period 1974–1983. Now, the $LiNH_4SO_4$ bibliography contains about 200 papers. Thus, it seems that each new paper about this compound should present better and more reliable data than the previously published ones. Unfortunately, the paper commented on here does not present such a case. The authors published the rather poor data obtained, as it seems, on mixed and/or multidomain samples and presented in a unconventional manner, and without critical review of the main previously published results. Below some of the questioned statements will be discussed. The results of the Raman studies are out of the scope of this comment.

1. Phase situation

The phase situation in the title crystal is clearly indicated in the corresponding entry of the phase transition database [4]. The main result is that $LiNH_4SO_4$ exists in *two* different polymorphic modifications called α and β [2, 5]. Each of them has its *own* phase diagram. The first modification (α) has a phase transition at about 255 K [6] from $Pmc2_1$ symmetry at room temperature to unknown symmetry below. The second modification (β) has phase transitions at about 285 K and 460 K [7–9]. The symmetry changes from $Pmcn$ for the high-temperature phase, to $P2_1cn$ for the room-temperature phase to $P2_1/c$ for the low-temperature phase. Below 27 K another phase exists with Cc symmetry. The α modification can be transformed to the β modification by using temperature. This transition occurs at about 350 K [8, 9] and has an irreversible character. Thus, the reverse transition is impossible and, when lowering the temperature, the β modification is the only stable phase in the whole temperature region in the subsequent temperature cycling; the phase transitions observed are from the β modification only. Furthermore, depending on the growth conditions (mainly of temperature), both modifications could *coexist* in the same sample [2, 8, 9]. Next, only one of these phases (β) has a *ferroelectric* behaviour (which involves the existence of ferroelectric *domains*) and

0953-8984/00/418933+04$30.00

a peak in the dielectric permittivity curve against temperature [10, 11]. Last, but not at least, the α modification may exist in three *polytypes* [5, 12].

Taking into account all the above properties, the analysis of all experimental data should be made very carefully. Without, at least, reference by the authors to the complicated situation described above, all their further statements may be without significant scientific value.

It is not sufficient to write the temperature of sample growth. The studied crystals were grown at 333 K, thus in the region where the phase transition from α to β modification occurs (the onset for this transition is about 325 K and the peak of DTA spectrum is at 350 K [8]). The pH of water solution was also unknown, thus we could not exclude the growth of the α modification as an intergrowth in the large crystals of β modification or as separate crystals. The well known latter possibility could affect the powder experiments when the sample was prepared by milling as-grown crystals. This needs detailed further studies or, at least, detailed author comment.

It should be noted that the cited paper by Połomska [9] is related to the phase transition from the α to β modification and not from phase I to II within the β modification, as wrongly stated in the paper commented on!

Nevertheless, the results presented in the paper commented on strongly indicate that the studied sample is a *mixture* of two different modifications (α and β). This leads to the experimental data showing a phase transition from both modifications as in the reported data. Moreover, the vanishing of the transition at about 335 K is a proof of the initial presence of the α modification in the sample [8, 9]; the subsequent thermal cycles do not show the existence of the α modification. The same results were observed by Chhor *et al* [13] but without satisfactory explanation. Now, it is well established that the α modification transforms *irreversibly* with slow kinetics to the β modification at this temperature [8, 9]. Samples believed to be pure single phase have turned out to be mixtures.

2. Lattice parameters

The authors published data of insufficient quality on the changes of the lattice parameters calculated from the powder diffraction data, and do not compare them with the precise results (of the accuracy of 10^{-5}) obtained by the x-ray Bond method [7]. Peculiarities in the thermal dependence of lattice parameters obtained from a single crystal experiment which could suggests supplementary phase transitions in $LiNH_4SO_4$ were not found. Similar good data were published several times [14–16].

3. Crystal structure analysis

The structure of both $LiNH_4SO_4$ modifications (α [5]) and β [17–19]) are totally different, thus it is not possible to make a common structure analysis by the only supposition about the twinning of β modification. It seems that the structure of all phases of β-$LiNH_4SO_4$ were solved and refined (with hydrogens; e.g. [6, 18–20]) with sufficiently high accuracy that new analysis is not needed, especially without finding the positions of hydrogen atoms. NB: the authors of [1] wrongly think that the paper by Pietraszko and Łukaszewicz [5] concerns the β modification while it reports the crystal structure of the α modification!

The x-ray measurements using automatic CAD diffractometer procedures (as used by the authors of the paper commented on) allow us to omit several Bragg reflections not corresponding to the cell chosen for measurements. Thus, the collected data corresponding to the one modification (i.e. β) might be affected in several reflections by the intensity from

another modification (i.e. α). The 'average' structure could be wrong!

A second source of errors could be related to the existence of domain structure in the β modification [10, 11, 21]. When solving the crystal structure of the ferroelectric phase (as in our case of the phase II and II′) it is necessary to take into account the obvious presence of ferroelectric domain structure, which disturbs the final results of studies leading to the 'average structure'. If the amount of both types of domain is not equal, the 'average structure' has a symmetry lower than the truly average structure observed as high-temperature phase I Misinterpretation of such data may occur in the case of the paper commented on.

4. New phase transition

The 'new' phase transition at 335 K introduced by Solans *et al* has a reasonable explanation by a mixture of two different components. Both types of such components, polymorphic modifications or ferroic domains, give a more significant description than the simple existence of a new phase transition.

(a) The first interpretation is based on the coexistence of α and β modifications within the studied sample. The phase transition in the smaller component α in the sample should affect the data by changing the intensity of some of the reflections. Such a change in the intensity distribution may be interpreted as a change due to the phase transition in the main component of the sample.

(b) The second possible interpretation is based on the domain structure of the β modification. The phase transition at about 335 K from phase II to new phase II′ seems to be an artefact due to the accidental change in domain structure at that temperature. The amount of 'right-oriented' domains contained in the sample investigated was changed with the temperature with respect to the amount of 'left-oriented' domains (like in $LiCsSO_4$ reported by Pietraszko *et al* [22]). When domains move in the sample the apparent 'switch' from 'left' to 'right' domain may occur at an arbitrary temperature, here it appears accidentally at about 335 K. This changes the intensities of some Bragg reflections and results in the 'average' structure of different degree of averaging of the 'left-' and 'right-oriented' domains. The search for the basic structure of one domain (single domain sample) is then difficult. The authors of [1] have seen this effect when they wrote that the new phase (phase II′ above 335 K) is close to the enantiomeric phase II.

5. Other remarks

In the paper commented on some other wrong or uncertain results should be noticed.

(a) The $P2_1nb$ space group is *polar* and not 'non-polar' as was wrongly stated by the authors! The high-temperature phase is non-polar as regards the physical properties (such as ferroelectricity or the existence of spontaneous polarization) and then centrosymmetric with regard to the symmetry of the structure and physical properties.

(b) The choice of polar space group $P2_1nb$ for the high-temperature phase is in contradiction with the physical properties of this phase. The vanishing of spontaneous polarization in the ferroelectric–paraelectric phase transition (on heating) indicates non-polar symmetry and the subsequent structure refinement should be made in the highest possible non-polar space group (in our case in $Pmcn$ like in [20, 23]).

(c) Several authors have stated that the decomposition of $LiNH_4SO_4$ occurs at a temperature well below those given in the paper commented on as a melting temperature [7, 16, 24, 25]. What then really happens at 601 K?

(d) The presentation of data is rather unconventional with the large empty space in figures 1(a) and 1(c). In this case the best solution is to show all data in the same diagram. All possible correlation will be then seen without any problems.

(e) There is a lack of error bars in the figure 1. One could suppose that the standard deviations for the presented data are at least about 10^{-3} A, thus 'hiding' all anomalies on the curves (see remark (b)).

(f) The authors of [1] present their data in an unconventional manner. What are the mean data for the multicomponent sample written in a single column in table 1 under the caption indicating both names of components (phase II + II′)? The presented data should correspond either to phase II or to phase II′. The average data are without any physical meaning.

(g) Finally, the assumption of non-disordered structure of high-temperature phase I leads to the wrong interpretation of the character of phase transition. The correct, and well described in the literature, mechanism is of order–disorder type (e.g. [16, 26–28]).

The situation in $LiNH_4SO_4$ is still far from being clear and the commented paper does not bring us closer to the desired understanding of the nature of structure and phase transitions.

References

[1] Solans X, Mata J, Calvet M T and Font-Bardia M 1999 *J. Phys.: Condens. Matter* **11** 8995
[2] Scacchi A 1868 *Atti R. Accad. Napoli, Sci. Fis. Mat.* **3** 1
[3] Wyrouboff G 1880 *Bull. Soc. Min. France* **3** 198
[4] Tomaszewski P E 1992 *Phase Transitions* **38** 127
[5] Pietraszko A and Łukaszewicz K 1992 *Pol. J. Chem.* **66** 2057
[6] Hildmann B O 1980 *PhD Thesis* Aachen
[7] Tomaszewski P E and Pietraszko A 1979 *Phys. Status Solidi* a **56** 467
[8] Sosnowska I, Hilczer B and Piskunowicz P 1990 *Solid State Commun.* **74** 1249
[9] Połomska M, Hilczer B and Baran J 1994 *J. Mol. Struct.* **325** 105
[10] Hilczer B, Meyer K-P and Szcześniak L 1984 *Ferroelectrics* **55** 201
[11] Połomska M, Wolak J and Szcześniak L 1994 *Ferroelectrics* **159** 179
[12] Tomaszewski P E 1992 *Solid State Commun.* **81** 333
[13] Chhor K, Abello L and Pommier C 1989 *J. Phys. Chem. Solids* **50** 423
[14] Gierlotka S, Przedmojski J and Pura B 1986 *Fiz. Dielektr. Radiospektroskop.* **12** 161
[15] Hirotsu S *et al* 1981 *J. Phys. Soc. Japan* **50** 3392
[16] Iskornev I M and Flerov I N 1977 *Fiz. Tverd. Tela* **19** 1040 (Engl. transl. *Sov. Phys. Solid State* **19** 605)
[17] Dollase A 1969 *Acta Crystallogr.* B **25** 2298
[18] Hildmann B O, Hahn Th, Heger G, Kurtz W and Arnold H 1978 *KfK-Bericht* **2719** 19
[19] Mashiyama H and Kasano H 1993 *J. Phys. Soc. Japan* **62** 155
[20] Hildmann B O, Hahn Th, Kurtz W and Heger G 1979 *KfK-Bericht* **2911** 17
[21] Połomska M and Tikhomirova N A 1982 *Ferroelectr. Lett.* **44** 205
[22] Pietraszko A, Tomaszewski P E and Łukaszewicz K 1981 *Phase Transitions* **2** 141
[23] Itoh K, Ishikura H and Nakamura E 1981 *Acta Crystallogr.* B **37** 664
[24] Loiacono G M *et al* 1980 *Ferroelectrics* **23** 89
[25] Mitsui T *et al* 1975 *J. Phys. Soc. Japan* **39** 845
[26] Aleksandrova I P, Blat D Kh, Zinenko V I and Kruglik A I 1981 *Kristallografiya* **26** 531 (Engl. transl. *Sov. Phys.–Crystallogr.* **26** 301)
[27] Rozanov O V, Aleksandrova I P and Rosenberger H 1982 *J. Mol. Struct.* **83** 399
[28] Yamamoto I, Hiroe A and Hirotsu S 1983 *J. Phys. Soc. Japan* **52** 920